HILO BAY
WATER CIRCULATION AND WATER QUALITY STUDY

DEPARTMENT OF THE ARMY

U.S. ARMY CORPS OF ENGINEERS

HONOLULU DISTRICT

for COUNTY OF HAWAII

January 2009

EXECUTIVE SUMMARY

By letter dated October 14, 2004, the County of Hawaii (County) requested planning assistance from the U.S. Army Corps of Engineers, Honolulu District (POH) to evaluate water circulation and apparent degraded water quality within Hilo Bay and identify potential solutions. In response to the County's request, this study was initiated under the authority of Section 22 of the Water Resources Development Act of 1974 (Public Law 93-251) as amended, through a cost-sharing partnership between POH and the County. Technical assistance was provided by the U.S. Army Engineer Research and Development Center's (ERDC) Coastal and Hydraulics Laboratory (CHL) and Field Research Facility (FRF), and the University of Hawaii at Hilo (UHH) to collect field data and implement numerical modeling of circulation, wave transformation, and identify alternatives to improve water quality in Hilo Bay.

The present study by POH investigates the feasibility of modifying the Hilo Harbor breakwater to increase water circulation within Hilo Harbor. Increased circulation could potentially provide corresponding improvements in water quality within the bay thereby providing a more suitable environment for recreation and a greater aesthetic enjoyment of the area. The resulting changes to wave energy within the harbor are also investigated to quantify the relative effects that breakwater modification may have on navigation. Model results and predictions for five alternative plans are documented in this technical report. This report does not provide a specific recommendation to address the water quality issue within Hilo Bay, but rather provides information to be used by Federal, State and County agencies and other stakeholders in determining an appropriate course of action.

The criteria for assessing alternative plans in this study were determined by examining changes in waves, current circulation, water quality, and residence time, as well as by determining areas subject to stagnant or weak circulation or focused wave energy resulting from proposed alternatives. The initial numerical modeling efforts concentrated on quantifying change in circulation and wave patterns with and without the alternatives in place for a range of forcing conditions.

All breakwater modifications considered in this report resulted in an increase in wave energy within the harbor and navigation channel, as evidenced by numerical wave modeling of each alternative. The increase in wave energy within the navigation channel varies greatly between alternatives, from a minimal increase that may be acceptable for safe navigation to a significant increase that would likely be considered unacceptable. Overall water quality model predictions indicated little difference in the results for any of the proposed harbor alternatives. At some locations there were differences in some constituent values such as particulate organic carbon. However, these differences appear to be due to phasing in the model response to the circulation and were relatively small and short lived. Further evaluation of these effects with input from all stakeholders will be required before initiating any breakwater modification to improve water quality within Hilo Bay.

Cost estimates for the conceptual alternatives were also prepared by POH to enable comparison between the various conceptual features. Other considerations that should be evaluated in future breakwater modification studies include the effects on the Hilo Bay shoreline, the changes to breakwater access, and the impacts to Blonde Reef. Evaluation of these additional impacts was not within the scope of this report.

Water quality in Hilo Harbor and Hilo Bay is dependent on several interrelated environmental processes which include the effects of the breakwater, as detailed in this report. Another major contributor to the water quality in Hilo Bay is the input of pollutants and organic materials from the Hilo Bay watershed via surface water, ground water, and storm water runoff. In order to comprehensively evaluate the bay's water quality and possible methods for improvement, these sources of contaminants must also be included in an overall watershed study that encompasses the ancient Hawaiian ahupua'a concept of "mountain to the sea" stewardship. This approach has been initiated and led by the Hilo Bay Watershed Advisory Group and Dr. Tracy Wiegner at the University of Hawaii at Hilo, and should be continued with a more detailed evaluation of breakwater modifications and their effect on water quality included as an integral component of the overall study.

HILO BAY
WATER CIRCULATION
AND
WATER QUALITY STUDY

TABLE OF CONTENTS

LIST OF FIGURES

LIST OF FIGURES
(continued)

LIST OF FIGURES
(continued)

LIST OF TABLES

HILO BAY
WATER CIRCULATION
AND
WATER QUALITY STUDY

1. INTRODUCTION

1.1. Authority

Federal funding for this study was provided through the Section 22 Planning Assistance to States (PAS) program. The PAS program was authorized by the Water Resources Development Act of 1974 (Public Law 93-251). It provides authority for cooperating with any state in preparation of comprehensive plans for water resources develop, utilization and conservation. Cost sharing for the PAS program is 50% federal and 50% non-federal. PAS program is applicable to coastal zone and lake shores as well as riverine and drainage areas. PAS studies may include collection of new data, but only in the context of a legitimate planning study (not for large data sets). Non-federal funding for 50% of the study cost was provided by the County of Hawaii.

1.2. Study Purpose

Hilo Harbor appears degraded to an undefined degree which does not provide a suitable environment for recreation and aesthetic enjoyment of the area. The objective of any conceptual alternative considered is to promote greater water circulation in the Hilo Harbor to improve its water quality. The present study by the US Army Corps of Engineers (USACE), Honolulu District investigates the feasibility of modifying the Hilo Harbor breakwater to increase water circulation within Hilo Harbor and potentially provide corresponding improvements in water quality within the bay. The resulting changes to wave energy within the harbor are also investigated to relatively quantify the effects that breakwater modification may have on navigation.

1.3. Project Background

1.3.1. <u>General Description</u>

Hilo Bay is located along the east (windward) coast of the island of Hawaii, extending south from Pepe'ekeo Point, and west from Leleiwi Point (Figure 1-1). Hilo Harbor encompasses an area approximately 3658 meters (12,000 feet) by 2134 meters (7,000 feet) in the bight of Hilo Bay. The 3072 meter-long (10,080-foot-long) Hilo breakwater, completed in 1929, extends across the northeastern half of the harbor, constructed on the relatively shallow Blonde Reef. The Hilo Harbor Federal navigation project consists of an entrance channel that is 2,200 feet long by 440 feet wide by 39 feet deep, a turning basin 1,800 feet long by 1,400 feet wide by 38 feet deep and the breakwater. The small boat harbor maintained by the State of Hawaii exists at the easternmost end of the harbor known as Radio Bay, near the root of the breakwater.

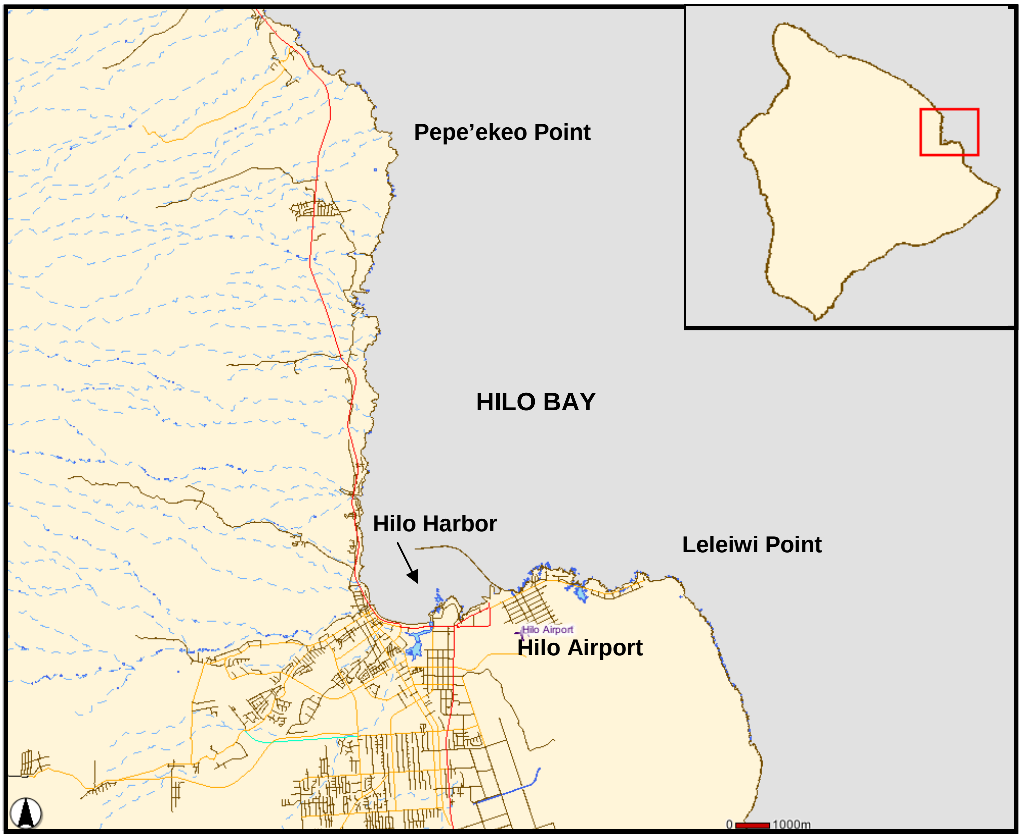

Figure 1-1. Vicinity Map of Hilo Bay and Hilo Harbor

1.3.2. Fresh Water Inflow to Hilo Bay

There are two major rivers that empty into Hilo Bay, see Figure 1-2. The larger is the Wailuku River which has a drainage area of 125 square miles. The average annual flow of water from the Wailuku River into Hilo Bay is one million cubic meters. The flow of the Wailuku can vary widely depending upon rainfall with a range of 40 thousand -7 billion cubic meters (M & E Pacific, 1980). The other tributary is the Wailoa River which connects Hilo Bay and Waiakea Pond. The main source of flow is a large basal compound spring, Waiakea Spring, which provides the single largest source of groundwater into Hilo Bay (M & E Pacific, 1980). It is estimated that 1.8 million cubic meters of groundwater enters the Bay annually in this area (M & E Pacific, 1980).

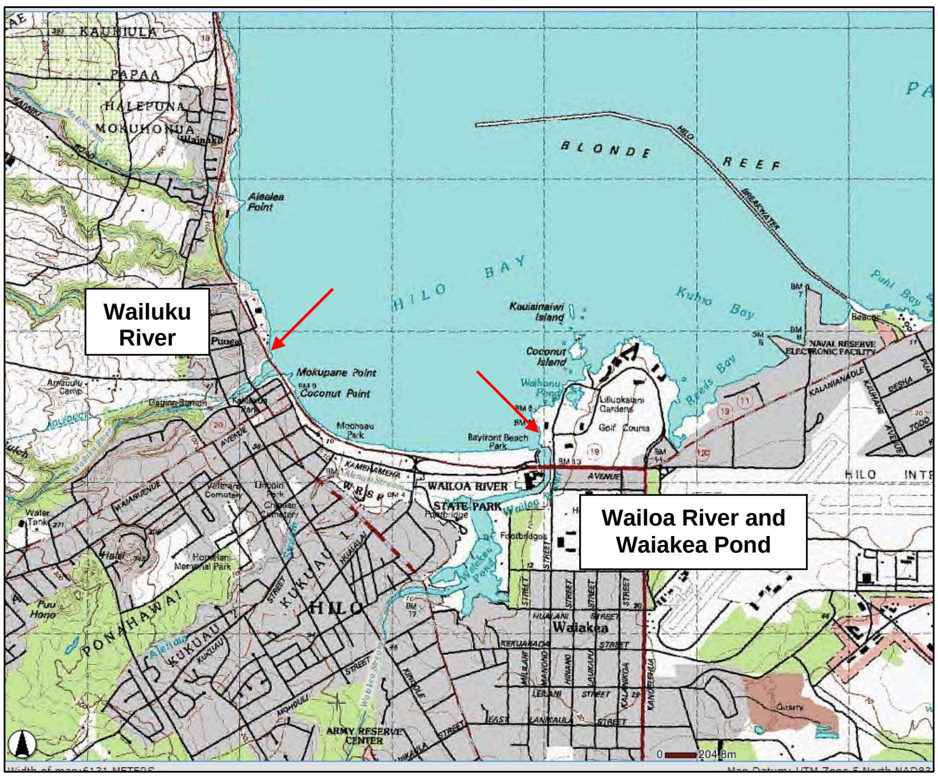

Figure 1-2. Major fresh water sources at Hilo Bay (Wailoa and Wailuku Rivers)

1.3.3. Wind and Tides

In the Hilo area, the tradewind flow is modified by the presence of Mauna Loa and Mauna Kea. During typical east-northeast tradewind conditions, the wind speeds off East Hawaii are relatively lighter than over the open ocean. This area of minimum wind speed is centered at Hilo. The temperature differential between land and sea results in the formation of a land and sea breeze system in the Hilo vicinity, which alternately reinforces and opposes the already weak underlying trade wind flow. During the day the onshore sea breeze reinforces the trade winds. At night, the offshore land breeze dominates, resulting in light southwest winds (Sea Engineering, 1981). Figure 1-3 shows a wind rose from the area offshore of Hilo Bay between the years 1981 – 2004.

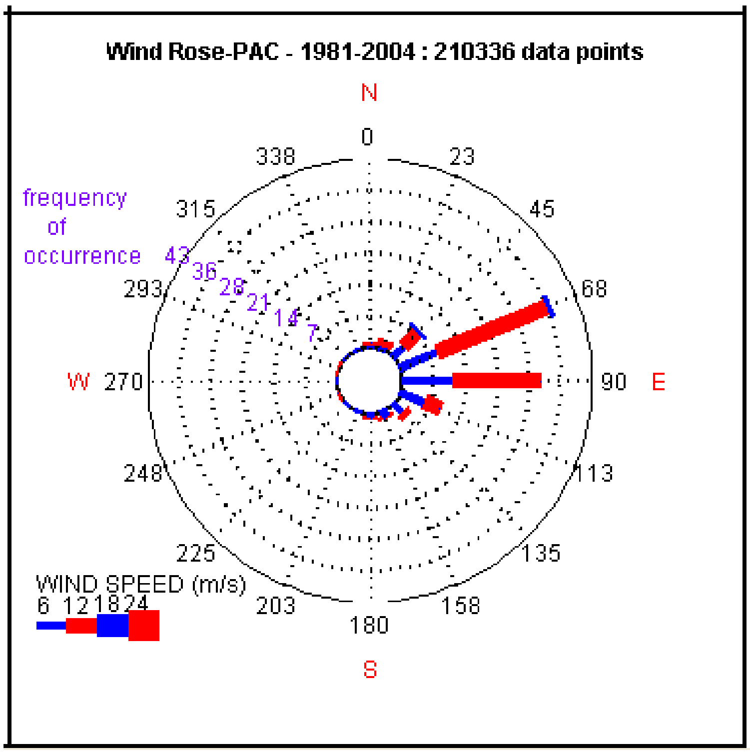

Figure 1-3. Wind rose for 1981 – 2004 (WIS Pacific Station 105)

The tides in Hilo Harbor are semi-diurnal (two high and two low tides per 25-hour period) with a pronounced diurnal inequality. The total tide range, or difference between Mean Lower Low Water (average of all lower low water heights of each tidal day) and Mean Higher High Water (average of all higher high water heights of each tidal day), is 0.731 meters (2.40 feet) during the most recent tidal epoch (1983-2001).

1.3.4. <u>Waves</u>

Hilo Bay is directly exposed to waves approaching from the sector north through east. Figure 1- 4 shows a wave rose from the area offshore of Hilo Bay between the years 1981 – 2004. Both tradewind waves and North Pacific swells may approach from this direction. Tradewind waves may approach from the sector north through southeast, with the predominant direction from the east-northeast. These waves are present 80 to 90 percent of the time during the summer; the frequency decreases to 60 to 70 percent during the winter. Tradewind waves have typical heights of 4 to 12 feet and periods of 7 to 10 seconds. Although Hilo Bay is exposed to tradewind wave approach, the breakwater shelters Hilo Harbor from direct approach of all but the most northerly tradewind waves (Sea Engineering, 1981).

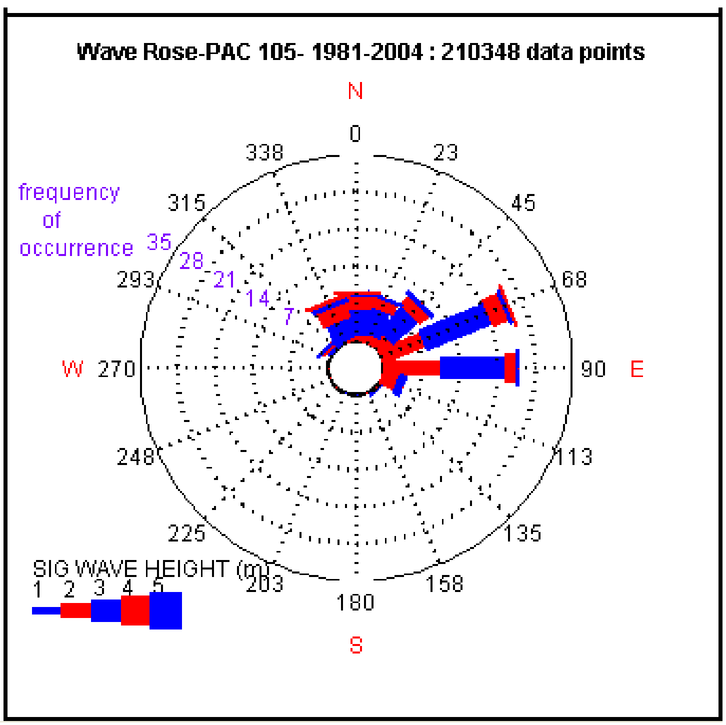

Figure 1-4. Wave rose for 1981 – 2004 (WIS Pacific Station 105)

North Pacific swell is generated by winter storms in the North Pacific and may approach from the sector west through northeast. The most common approach direction is from the northwest. This wave type is most frequent from October through April. The average wave period is 14 seconds and deepwater heights range up to 15 feet. Hilo Harbor is directly exposed to only the North Pacific swell approaching from the north and northeast. Total frequency of occurrence of all North Pacific swell is 75 percent; however, it approaches from the north and northeast only 12 percent of the time. Because of its large size and long period, though, even swells approaching from more westerly directions may refract and have some influence on the wave climate in the harbor (Sea Engineering, 1981).

1.3.5. Navigation and Recreational Use

Hilo Harbor is currently the primary location of commercial waterborne traffic for the Island of Hawaii. The harbor is used by commercial vessels (deep and shallow draft) that moor at Piers 1, 2, and 3 along the interior of the Federal Channel, as well as recreational vessels that occupy the small-boat harbor at Radio Bay, the mooring area at Reeds Bay and use the launch ramps at the Wailoa River. Canoe paddling, surfing, fishing and other water sports are also popular recreational uses of the harbor.

1.4. Previous Circulation Studies

The Public Health Service (1963) conducted a dye tracer study to determine flushing and mixing patterns in Hilo Bay. The PHS found the following:

"The forces influencing diffusion patterns in Hilo Bay are in some part attributable to littoral (shallow water) currents, tidal currents, currents due to fresh water runoff, and locally generated wind-driven currents. Littoral or alongshore currents resulting from the breaking of the distant generated sea swell at an angle with the coastline is probably a major force. This, together with land runoff from both surface streams and subsurface springs and seeps, is believed to predominate in producing net advective movement and turbulent diffusion of water masses in the area being considered. Hilo Bay is at the intersection of a north-south and east-west coastline resulting in a current somewhat analogous to a rip current moving seaward in a northeasterly direction in opposition to the incoming swell.

Though tidal currents most certainly add in some way to the dispersion process, they do not have the pronounced effect found in estuaries. Because of the high porosity of the breakwater, tidal flows undoubtedly pass through them quite readily and their effect, therefore, on tidal current patterns within the harbor is probably very minimal."

Neighbor Island Consultants (1973) collected data in Hilo Harbor between July 17 and August 21, 1972. The data indicated a two cell circulation pattern in the surface layers of the harbor. The eastern cell, in Kuhio Bay, circulated clockwise with the tide while the western cell, centered northwest of Coconut Island, circulated counterclockwise. Net transport of the entire system was seaward, due at least in part to fresh water runoff from the Wailoa and Wailuku Rivers and ground water inflow. Salinity of the deeper harbor waters indicated replenishment from the ocean.

M & E Pacific, Inc. (1977 and 1980) conducted an evaluation of circulation characteristics, water quality and geological definition of bottom types. The circulation measurements were concentrated in the main reaches of the harbor and the harbor entrance channel. A summary of the M & E findings is presented below (Sea Engineering, 1981):

- There is a two-layer salinity stratified pattern in Hilo Harbor. Vertical stratification of the water column is caused by the large amounts of fresh water entering the harbor from both ground water and surface flow. The salinity gradient is more pronounced during the wet season (winter).

- The net transport of the surface layer is out of the harbor at a rate dependent upon the quantity of freshwater input and wind speed and direction.

- The subsurface flows at the harbor mouth are influenced by the tide. During flood tide, subsurface flow was generally into the harbor and during ebb tide the flow generally reversed. During ebb tide, however, occasions were noted when an inward flow persisted along the western half of the harbor mouth. Similarly, there were times when the subsurface water along the eastern side of the channel moved continually seaward, even during flood tide. Flood and ebb tide current speeds in the harbor entrance area averaged approximately 4cm/second during the 1980 phase of the study. Current meter data at the harbor entrance showed a net transport into the harbor. The relatively small volume of tidal exchange (the tidal prism) relative to the large cross-section areas of the harbor entrance results in the very low tide-related currents.

- The two cell circulation in the upper layer described by Neighbor Island Consultants (1973) was not confirmed by the M & E Pacific findings. Variations between studies and even between drogues placed on the same day were thought to be due to eddies with higher speeds than those associated with the tidal flow.

- Drogues placed off the mouth of the Wailoa River on April 7, 1977 during an ebbing tide moved north and west, or in a seaward direction. Drogue depths were surface and 5 feet.

- The results indicated weak and variable currents in the study area. An ebb tide eddy is in the opposite direction of anticipated flow and may be a countercurrent formed in response to ebb flows in the main harbor channel. The flow reversals are apparently not wind related, as the easterly trades would have reinforced movement in the opposite direction.

M&E Pacific, Inc. (1980) determined that seasonal variations in circulation and exchange characteristics in Hilo Harbor are primarily a function of the amount of surface runoff which in turn is a function of rainfall. During the winter, the larger fresh water inflow results in a thicker surface layer of fresh water, a more pronounced stratification, and a stronger hydraulic gradient of seaward flow in the surface layer.

Current studies nearshore in the vicinity of the bayfront beach by Sea Engineering (1981) generally indicated weak and variable currents, with the presence of eddies and tidal reversals. The study showed that resultant wave approach at the bayfront beach is from north or northwest, and the breaking waves at the shoreline set up an alongshore current moving to the east.

Dudley & Hallacher (1991) found that Hilo Bay is a salt wedge estuary that is stratified with a freshwater surface layer existing up to a mile offshore. This stratification is most pronounced during the wet season when surface runoff to Hilo Bay is high. The dense saline layer moves offshore at depth with the tide and the upper freshwater layer is pushed shoreward by easterly and northeasterly trade winds. There is minimal mixing between freshwaters and saltwater layers inside the breakwater because baywide wind/tidal circulation and wave energy is low. Low wave energy also allows sediments carried by the rivers to settle out into the lower salty layer, where they may be transported back into the bay with the incoming tide. Wind generated tidal velocities are probably too low to re-suspend bottom sediments, but suspended sediments will move in and out of Hilo Bay with the wind and tide.

1.5. Study Method

This report was prepared under the authority of Section 22 by the USACE Honolulu District (POH) with assistance from the U.S. Army Engineer Research and Development Center's (ERDC) Coastal and Hydraulics Laboratory (CHL) and Field Research Facility (FRF), as well as the University of Hawaii at Hilo (UHH) to collect field data and to implement numerical modeling of circulation, wave transformation, and potential water quality improvement in Hilo Bay. The initial focus of the study was to apply appropriate numerical models to assess various project alternatives to promote greater water circulation in Hilo Bay in order to improve water quality. Model results and predictions for five alternative plans are documented in this technical report to facilitate selection of an appropriate course of action. The criteria for assessing alternative plans in this study were determined by examining changes in waves, current circulation, water quality, and residence time, as well as by determining areas subject to stagnant or weak circulation or focused wave energy resulting from proposed alternatives. The initial numerical modeling efforts concentrated on quantifying change in circulation and wave patterns with and without the alternatives in place for a range of forcing conditions.

The modeling of hydrodynamic and water quality conditions within Hilo Bay was conducted utilizing a suite of linked models. An example of a previous application of this linked modeling methodology is found in Bunch et al (2003). Specific to Hilo Bay, regional and nested grid wave model STeady-state spectral WAVE model (STWAVE, Smith et al., 1999) simulations were performed to generate wave climate information and more specifically radiation stress gradient fields used as wave forcing within water circulation models ADvanced CIRCulation (ADCIRC, Luettich et al., 1992) and CH3D-WES (Chapman et al., 1996). Regional scale ADCIRC simulations were performed to provide water surface elevation boundary conditions for the near-field CH3D-WES circulation model. Lastly, CH3D-WES simulations were performed to supply hydrodynamic transport input for the CE-QUAL-ICM, (Cerco and Cole, 1994) bay flushing and water quality simulations. Descriptions of the individual models and their respective linkage components within the overall model linkage and simulation system is provided in Sections 4 and 5 of this report.

2. HARBOR ALTERNATIVES CONSIDERED

2.1. Existing Conditions and Additional Dredging

The Hilo Harbor Federal navigation project consists of an entrance channel that is 2,200 feet long by 440 feet wide by 39 feet deep, a turning basin 1,800 feet long by 1,400 feet wide by 38 feet deep and a 10,080-foot long continuous breakwater. Figure 2-1 displays the existing conditions within Hilo Bay and Hilo Harbor. Dredging of approximately 780,000 cubic yards of silty material from the interior of the bay is assumed to be required for all alternatives to provide initial water quality improvements within the bay.

2.2. Alternative 1

This alternative considers deauthorization and removal of the outer 7,500 feet of the existing Hilo Harbor breakwater, construction of a new 2,000-foot long breakwater and dredging within Hilo Bay (see Figure 2-2). In order to increase wave induced circulation within Hilo Bay, the outer 7,500 feet of the existing breakwater would be completely removed down to pre-construction depths. A new 1,500-foot long breakwater would be constructed along the seaward extent of the Hilo Harbor turning basin and a portion of the entrance channel to provide safe navigation and mooring.

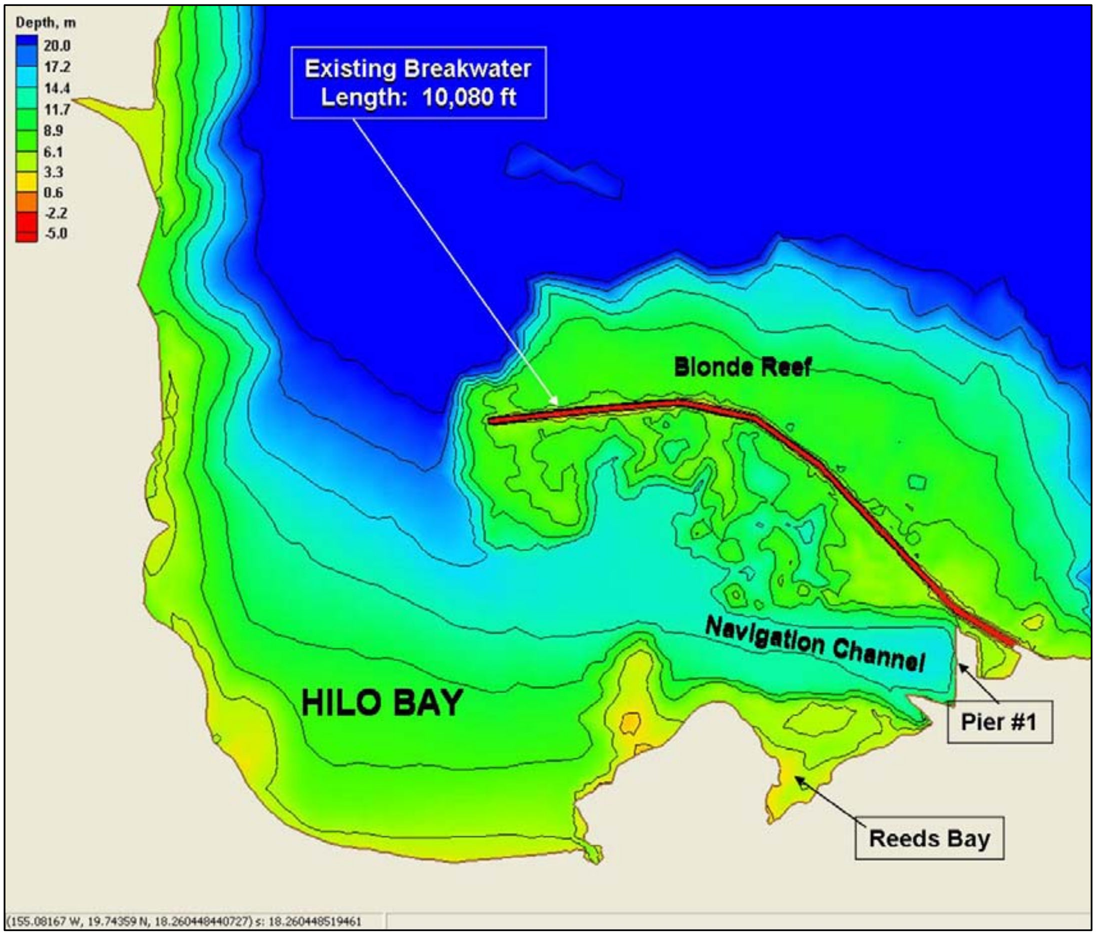

Figure 2-1. Existing conditions within Hilo Harbor

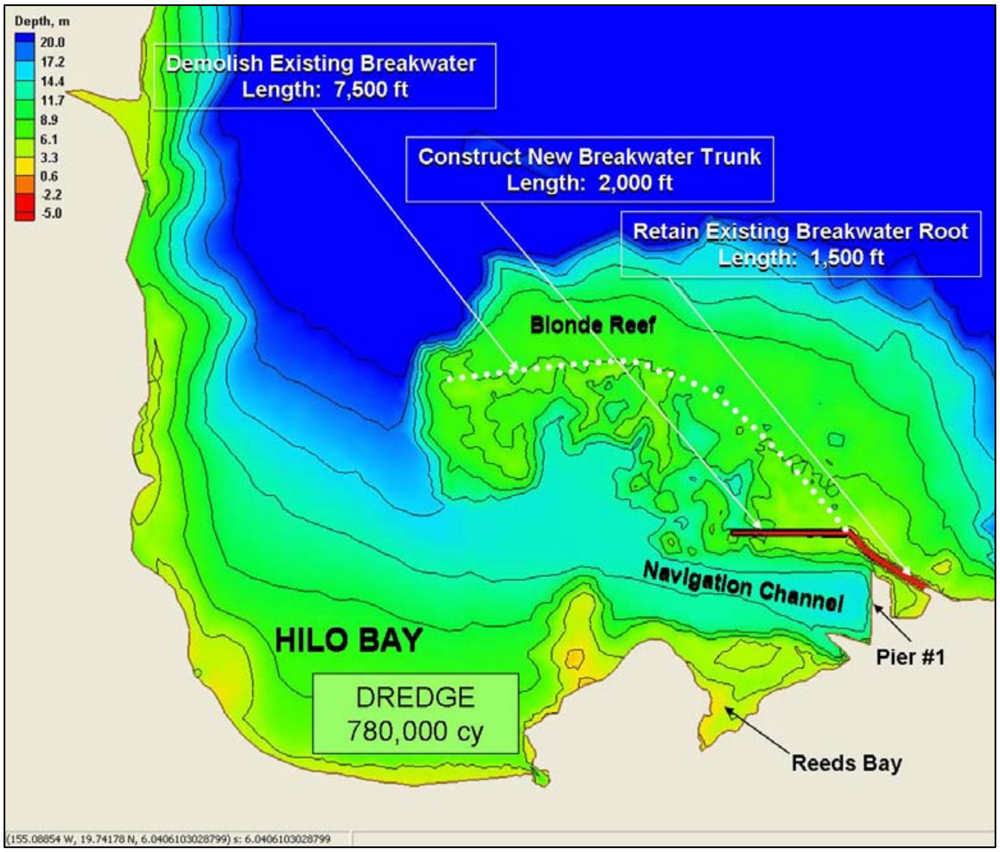

Figure 2-2. Alternative 1

2.3. Alternative 2

This alternative considers notching six gaps into the existing Hilo Harbor breakwater and dredging within Hilo Bay (see Figure 2-3). In order to increase wave induced circulation within Hilo Bay, six 250-foot long gaps would be notched into the outer portion of the existing breakwater at 750-foot intervals

2.4. Alternative 3

Similar to Alternative 2, this alternative (see Figure 2-4) also includes six detached breakwaters segments on the harborside of the existing breakwater. The offset segmented breakwaters would be constructed to reduce direct wave transmission into the bay.

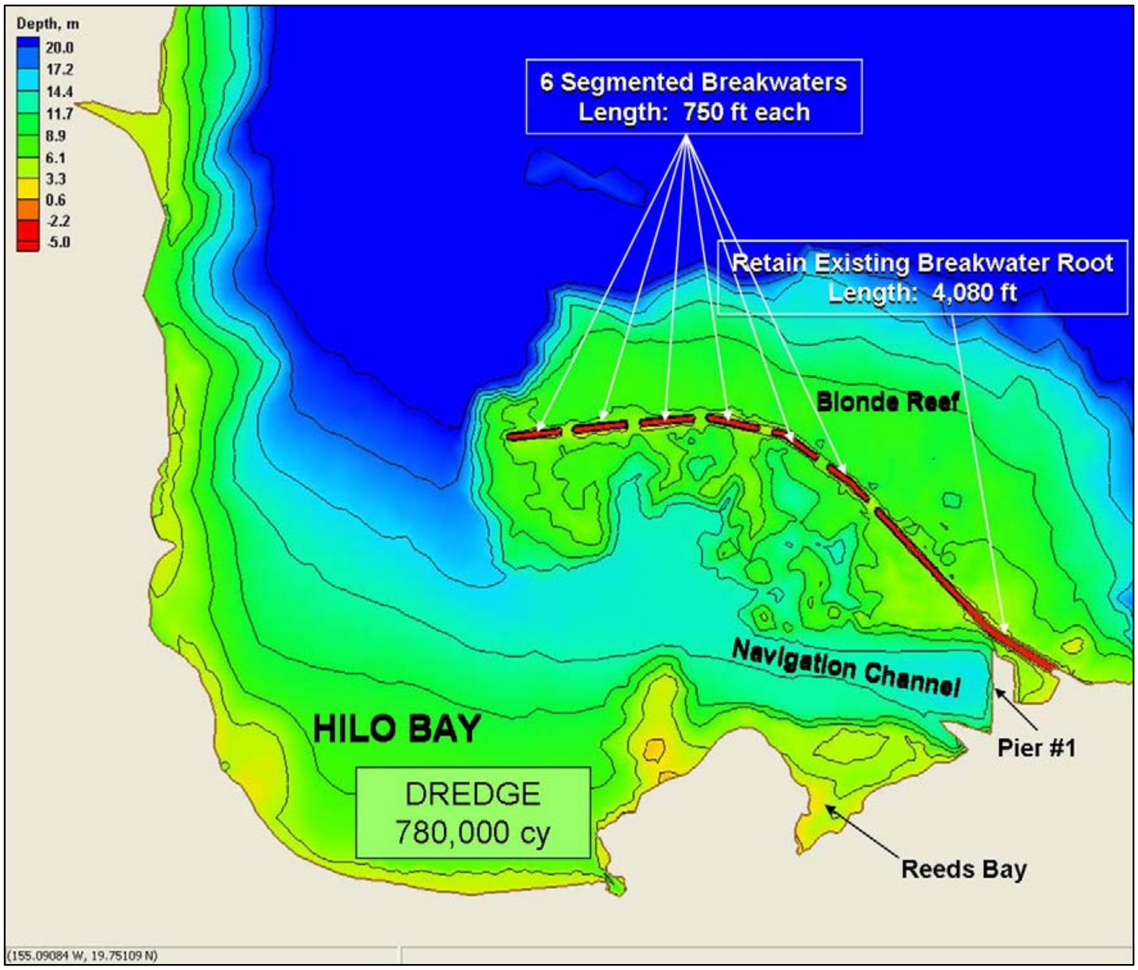

Figure 2-3. Alternative 2

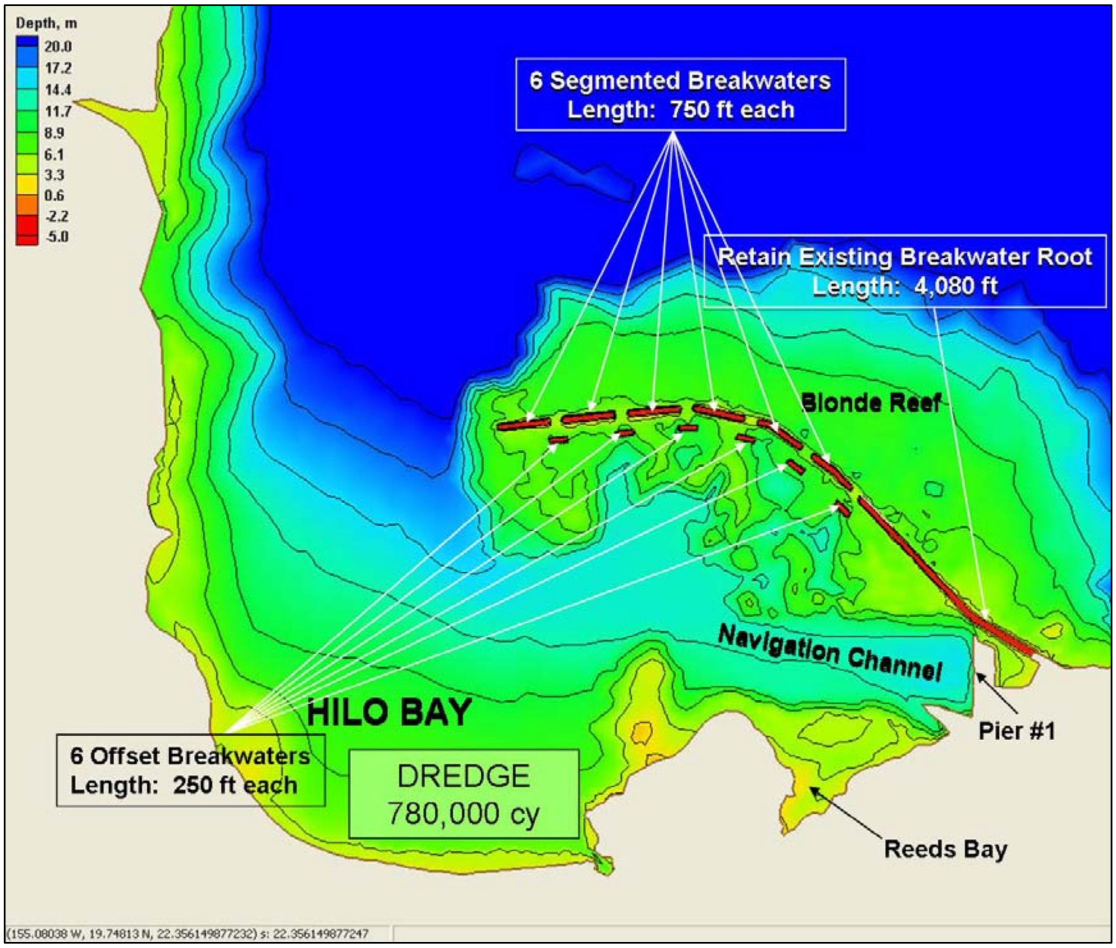

Figure 2-4. Alternative 3

2.5. Alternative 4

Alternative 4 (as shown in Figure 2-5) consists of notching the existing breakwater to provide one gap in the structure's root. The 500-foot gap in the breakwater would provide increased water exchange between Hilo Bay and the ocean.

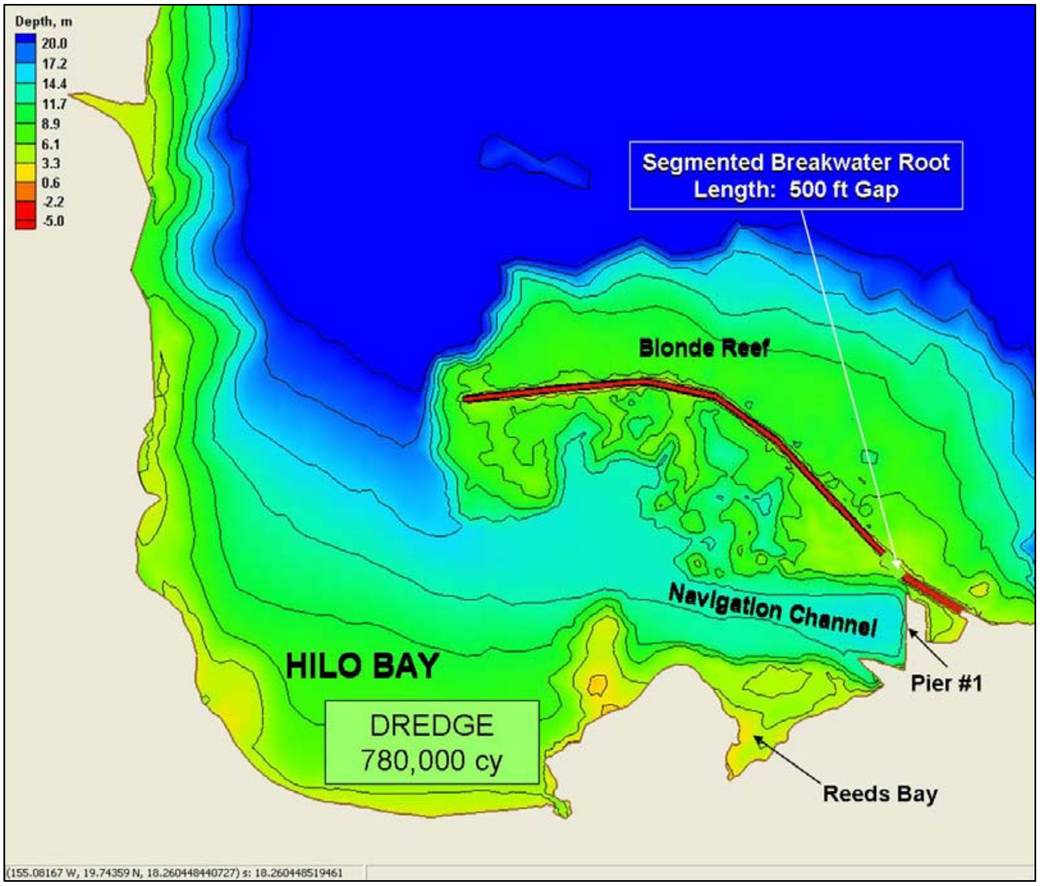

Figure 2-5. Alternative 4

2.6. Alternative 5

Alternative 5 (as shown in Figure 2-6) consists of notching the existing breakwater to provide one gap in the structure's root similar to Alternative 4. A 500-foot offset breakwater would provide increased wave attenuation. The offset breakwater would be constructed oceanward of the existing structure.

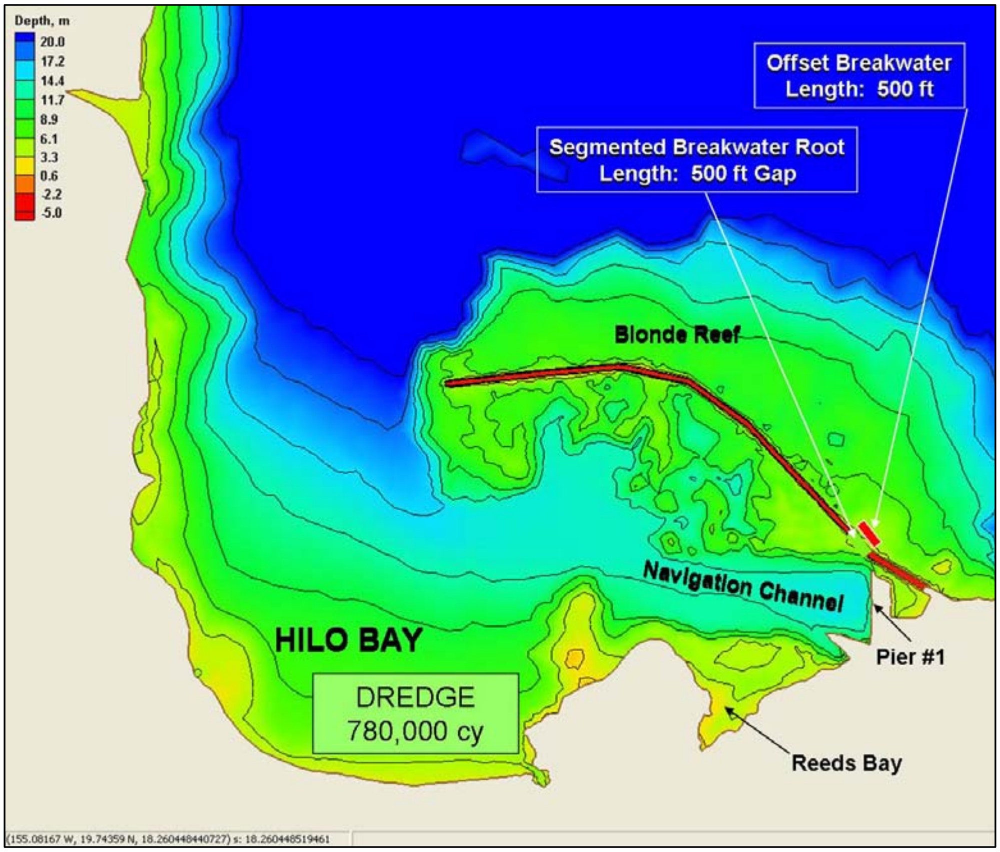

Figure 2-6. Alternative 5

2.7. Assumptions and Limitations of Alternatives

For Alternative 1 it was assumed that removal of 7,500 feet of the existing breakwater would result in significant increase in water circulation within Hilo Bay and in particular the bayfront beach area and Reeds Bay. Complete removal of the structure's cross section (down to pre-construction water depths) was assumed across Blonde Reef to promote wave energy transmission into Hilo Bay. Limitations of this assumption are that increased wave energy transmission could result in increased shoreline erosion and hazardous navigation conditions.

For Alternative 2 and Alternative 3, it was assumed that notching of the existing breakwater would significantly improve water circulation within the bay. A limitation of these alternatives is that notching the breakwater may not provide enough increase in wave energy into the bay to increase water circulation and thereby improve water quality.

Assumptions made for Alternative 4 and Alternative 5 are that tidal induced water circulation would be significantly increased by provision of a means of exchange between the ocean and the bay at the root of the breakwater. It was also assumed that navigation would realize minimal negative impacts due to the implementation of either alternative.

For all alternatives considered, it was assumed that dredging of 780,000 cubic yards of unsuitable material at various locations within the bay to a vertical extent of 3 feet would significantly enhance the chances of improving water circulation and water quality. By dredging unsuitable silty material from the bay, the alternatives may be more successful than otherwise, but large volumes of similar material will still remain in the bay and additional material of marginal quality are likely to enter the bay through subsequent storm water discharges.

3. FIELD DATA COLLECTION

3.1. Waves and Water Circulation Data

Wave and current data collection and processing were completed by the USACE FRF. The data was collected with three Acoustic Doppler Current Profilers (ADCPs). Instrument locations are shown in Figure 3-1 and listed in Table 3-1. The ADCP gages were Teledyne RD Instruments 1200 kHz Workhorse, bottom mounted facing upward with the sensor head approximately 0.45 meters off the bottom.

The gages were deployed on 21 March 2007, and retrieved on 5 June 2007, for a total deployment time of approximately 77 days. ADCP 1 (deployed closest to the entrance channel) was selected for wave and current collection, the other two gages only collected currents. Visual observations of waves at ADCP sites 2 and 3, and analysis of data collected by ADCP 1, indicate that typical wave heights at sites 2 and 3 were too low (nominally below 0.4 meters high) for reliable directional wave estimates to be made with these instruments. ADCP 3 operated only 20 days before the batteries were depleted on 7 April 2007.

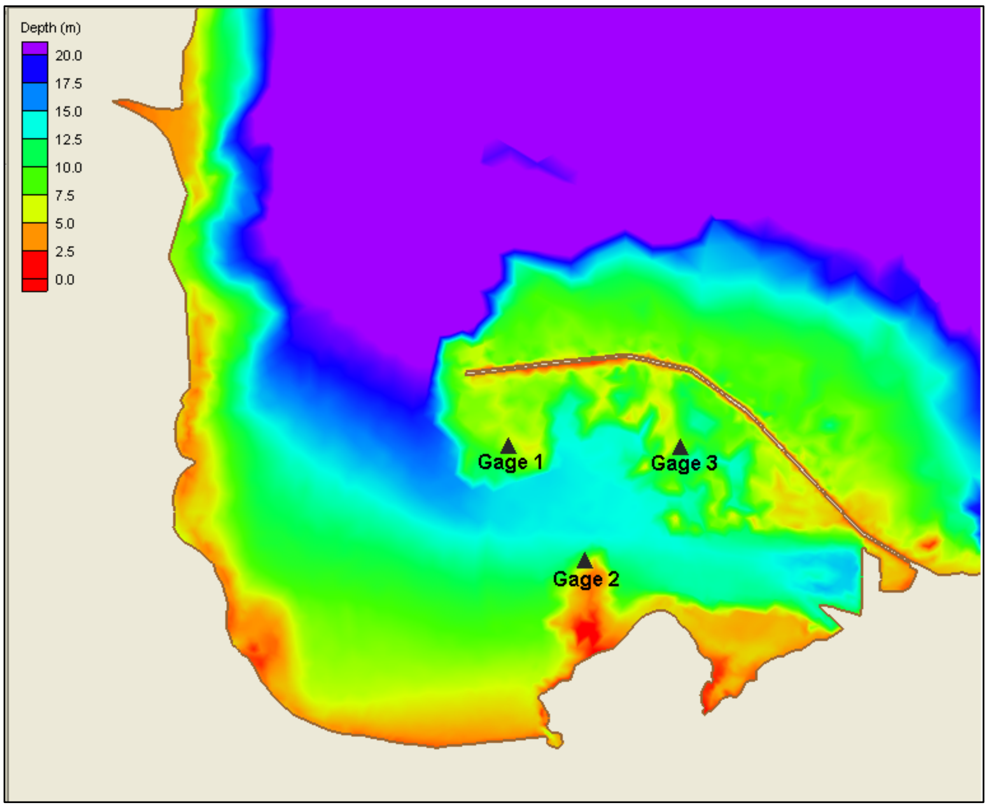

Figure 3-1. ADCP Instrument Locations

Table 3-1. ADCP instrument identifications and locations

Gage	Lat (deg min)	Long (deg min)	Deploy Times (2007)	Depth (m)	Wave/ Current
ADCP 1	19 44.3433	155 4.3783	21 Mar – 5 Jun	6	W/C
ADCP 2	19 44.9000	155 4.1350	21 Mar – 5 Jun	6	C
ADCP 3	19 44.3400	155.3.8317	21 Mar - 5 Jun	6	C

3.1.1. Wave Data Collection

ADCP 1 sampled at 2 Hz for directional wave measurements. Each hourly wave burst was approximately 34 minutes long, starting at the top of each hour, and consisted of 4,096 points. Wave spectra were computed using the RDI "WavesMon v2.1" analysis program. This package computes non-directional spectra from three different parameters; the subsurface orbital velocity, the surface detection signal, and the pressure sensor. The velocity data are used to compute directional spectra. Figure 3-2 displays a typical monthly wave rose for ADCP 1. Measurements for each month are fairly consistent, with waves from the northwest with height never exceeding 1 meter.

3.1.2. Current Profile Data Collection

Current profiles were collected at ADCPs 1, 2, and 3 every 10 minutes from a 200 point average. The gages have four acoustic transducers for measuring currents and a pressure sensor, from which horizontal and vertical current profiles were computed at 0.2 m vertical spacing. The RDI "WavesMon v2.1" program also extracts the current profile data and computes various parameters like vertically integrated currents and quality control (QC) information. Current analysis for the ADCP 1 indicates the surface flow is predominately westward, out of the harbor, as shown in Figure 3-3. Figure 3-4 shows a typical current profile at Hilo Bay, and illustrates the variation in current direction within the vertical water column.

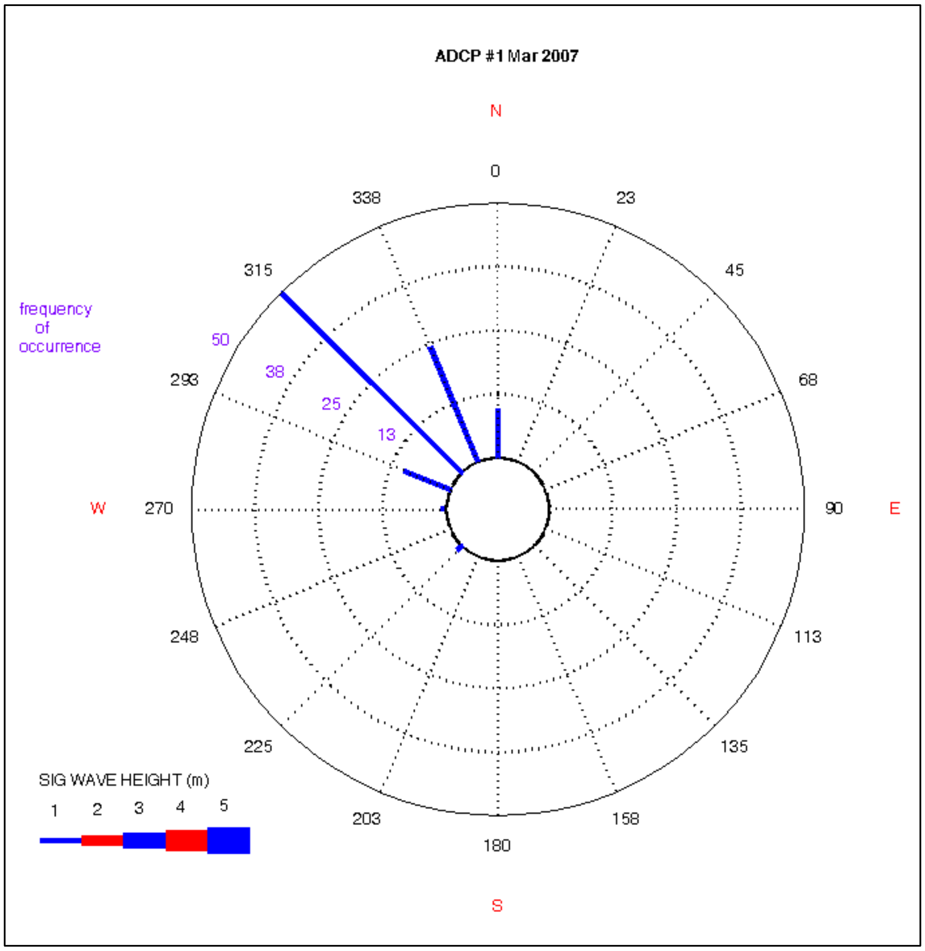

Figure 3-2. Typical Monthly Wave Rose at ADCP 1 (March 2007)

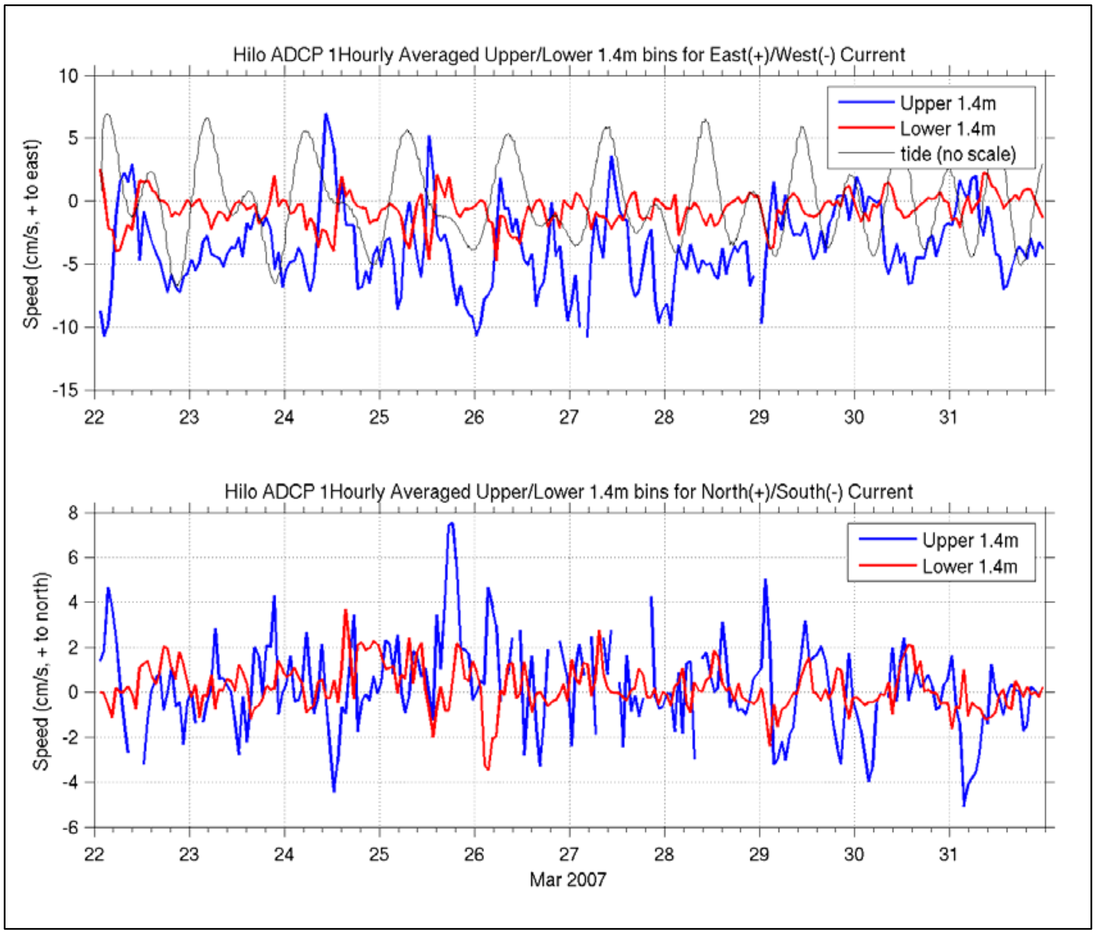

Figure 3-3. Typical Current Measurement Time-Series at ADCP1

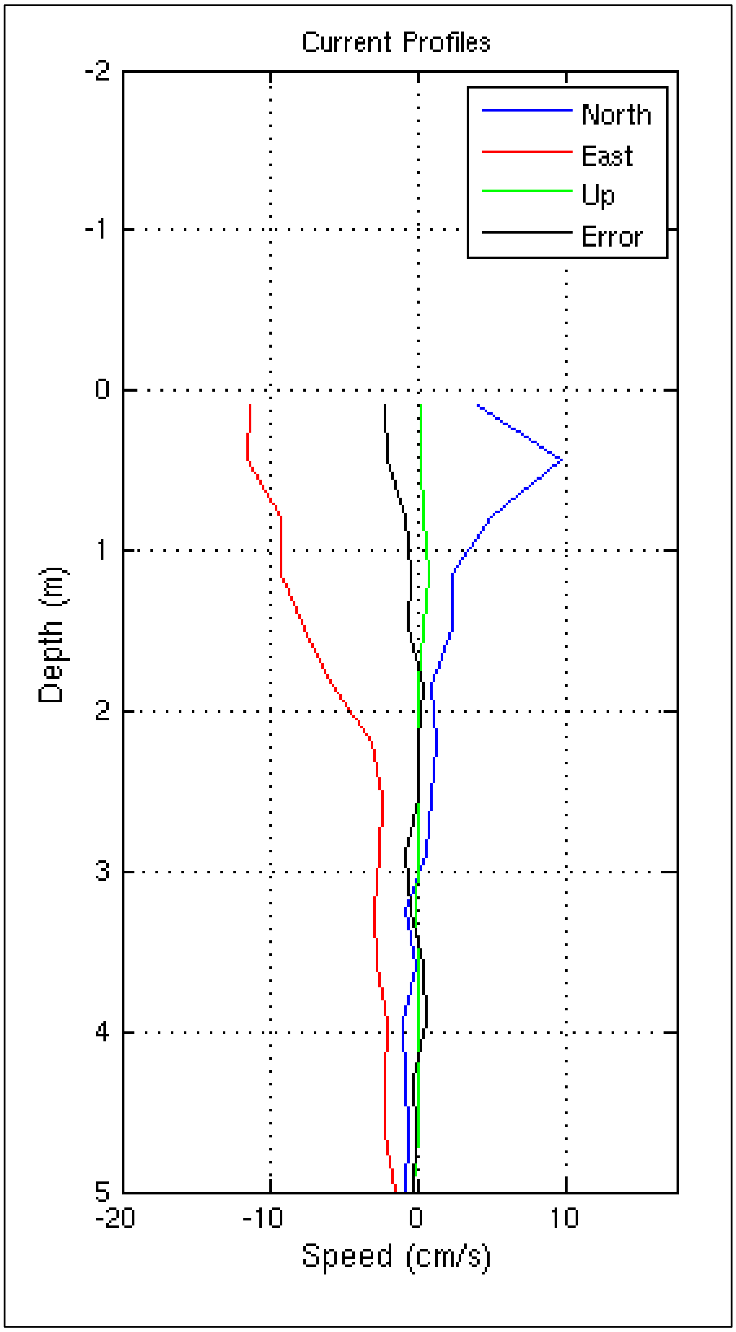

Figure 3-4. Typical Current Profile Snapshot at ADCP1

3.1.3. Current Drogue Data Collection

Current drogues (drifters) were deployed in Hilo Bay to investigate surface and sub-surface water circulation. Four current drogues were designed and built at the CHL Field Research Facility (FRF) that used Global Positioning System (GPS) tracking and radio telemetry for positioning. They were constructed with off-the-shelf plumbing supplies (PVC pipe, vertical risers, rubber unions, hose clamps), a Garmin Geko GPS receivers, and MaxStream (model XStream-PKG-R) radio modems (Figure 3-5). The sails were approximately one meter in cross-section. Surface drogues extended from the air/water interface to a depth of approximately 1 meter. Sub-surface drogues consisted of a floating section containing all of the requisite hardware and a tethered sail section extending through the second meter of the water column (see Figure 3-6). Each Garmin GCP unit internally recorded positions every 5 seconds.

Drogue tracks recorded from 21 to 22 March 2007 are shown in Figure 3-7a. The drogues were deployed in the vicinity of ADCP 1 and ADCP 3 for correlation with the gage data and at or near the mouth of Wailoa Stream. The drogue tracks were generally east to west at both the surface and at depth. Direction of travel for the surface and sub-surface drogues were similar. Surface drogue speeds ranged from 5 centimeters per second (cm/s) to 13 cm/s while the sub-surface drogue speeds ranged from 3 cm/s to 7 cm/s. Overall, the surface drogue speeds were approximately twice that of the sub-surface drogues. Drogue tracks collected during the three other deployments (22-23 March, 5-6 June, and 6-7 June) are shown in Figures 3-7b, 3-7c and 3-7d. Tide stage during drogue deployment is also shown in the figures for reference.

3.2. Water Quality Data

The University of Hawaii at Hilo (UHH) collected the baseline data on sediment and nutrient inputs to the bay, and assessed the response of the bay to these inputs under base and storm flow conditions. This baseline data was used to calibrate and verify the water quality model.

The water quality monitoring specifically examined how storms affect water quality (sediments, nutrients, “Chl a”) in Hilo Bay by comparing conditions in the bay before and following a storm event over a two-year period. A similar design has been successfully used by Ringuet & Mackenzie (2005) to evaluate the effects of storms on water quality and algae in southern Kaneohe Bay, Oahu.

Figure 3-5. Photo of Floating Surface Drogue with GPS Antenna

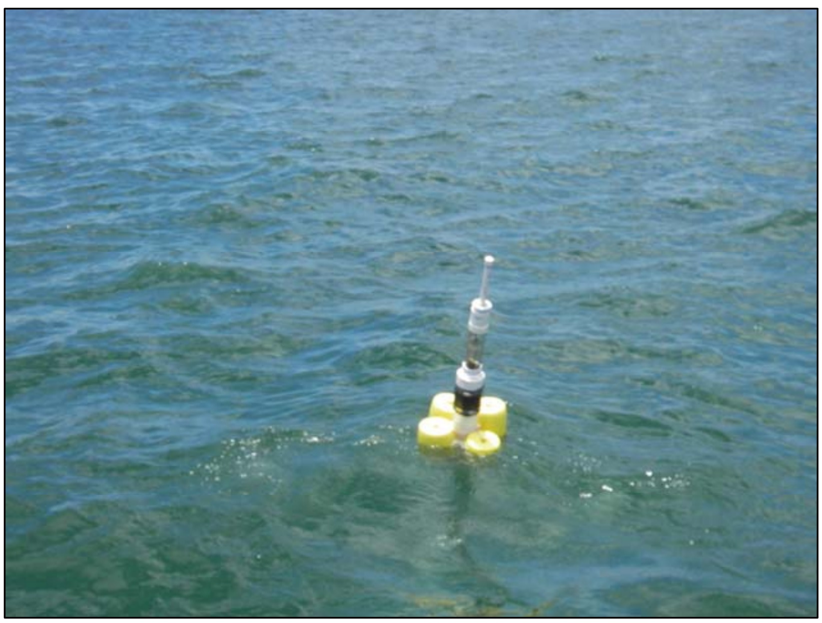

Figure 3-6. Photo of Floating Sub-surface Drogue with GPS Antenna

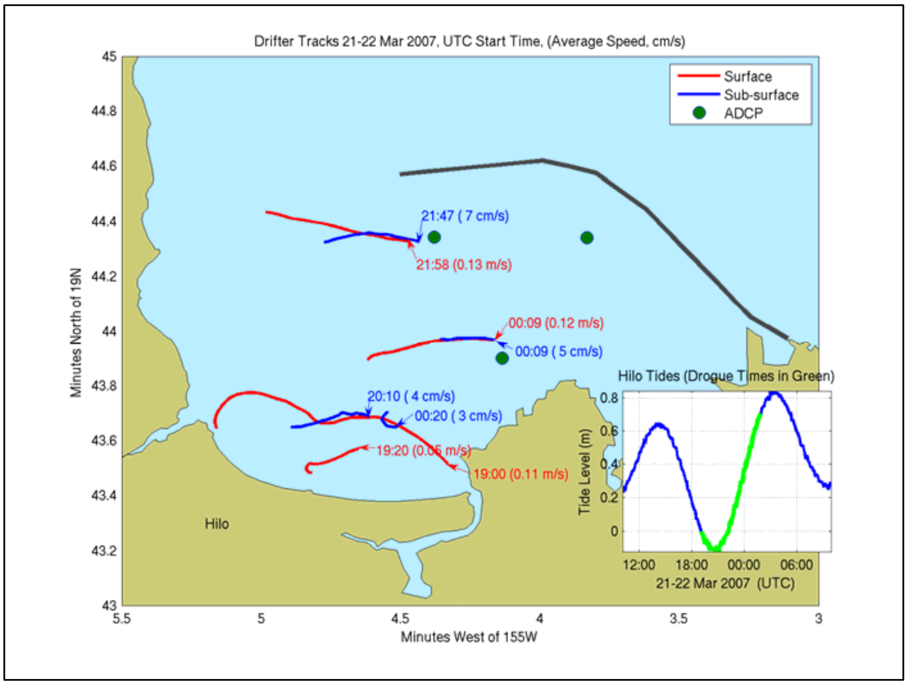

Figure 3-7a. Drogue Tracks between 21 -22 March 2007

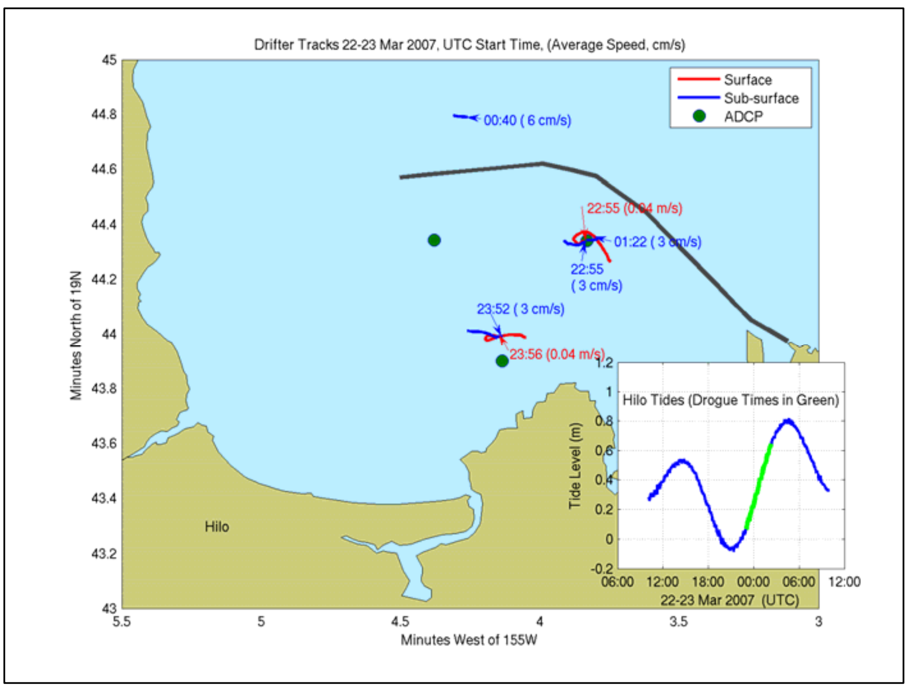

Figure 3-7b. Drogue Tracks between 22 - 23 March 2007

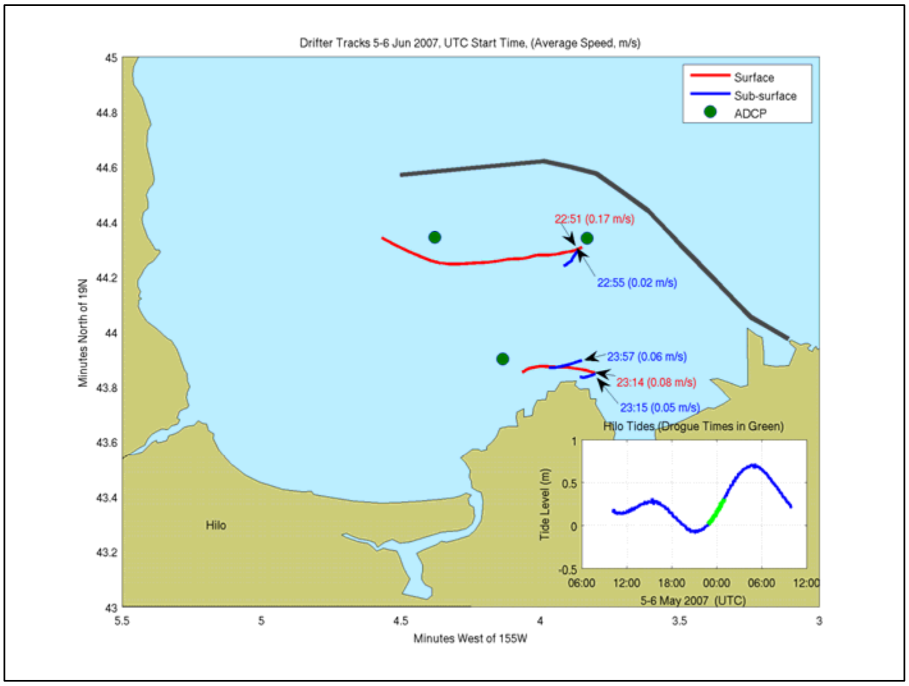

Figure 3-7c. Drogue Tracks between 5 – 6 June 2007

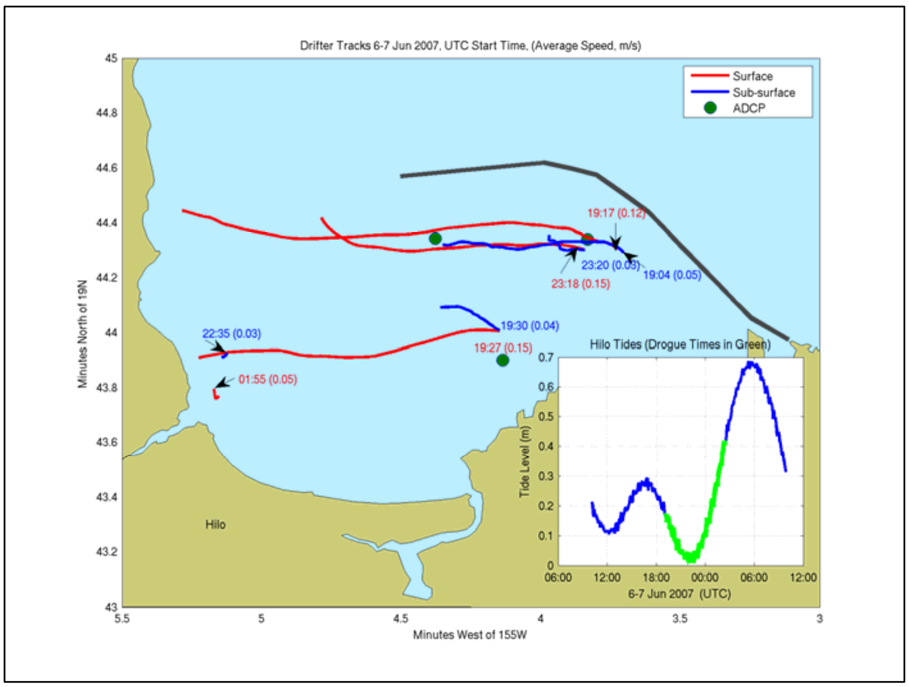

Figure 3-7d. Drogue Tracks between 6 – 7 June 2007

For this monitoring study, eight stations were sampled for suspended sediments, nutrients, and chlorophyll *a* (“Chl *a*”) (Figure 3-8). One station each was located in the freshwater portion of the Wailuku and Wailoa Rivers (S1 and S4). These stations were used to determine the amount of suspended sediments and nutrients entering the bay from surface waters. Four stations were located inside of Hilo Bay. Two Hilo Bay stations were located along a transect following the Wailoa River plume (S5 and S6). The other two Hilo Bay stations were located along a transect following the Wailuku River plume (S2 and S3). This transect was on a slight angle to the northwest of the river’s mouth because previous studies have shown that the Wailuku River plume is deflected northwest in Hilo Bay (Dudley & Hallacher 1991). Two control sites were located outside of the Hilo Bay breakwater (C1 and C2), outside the direct influence of the two rivers.

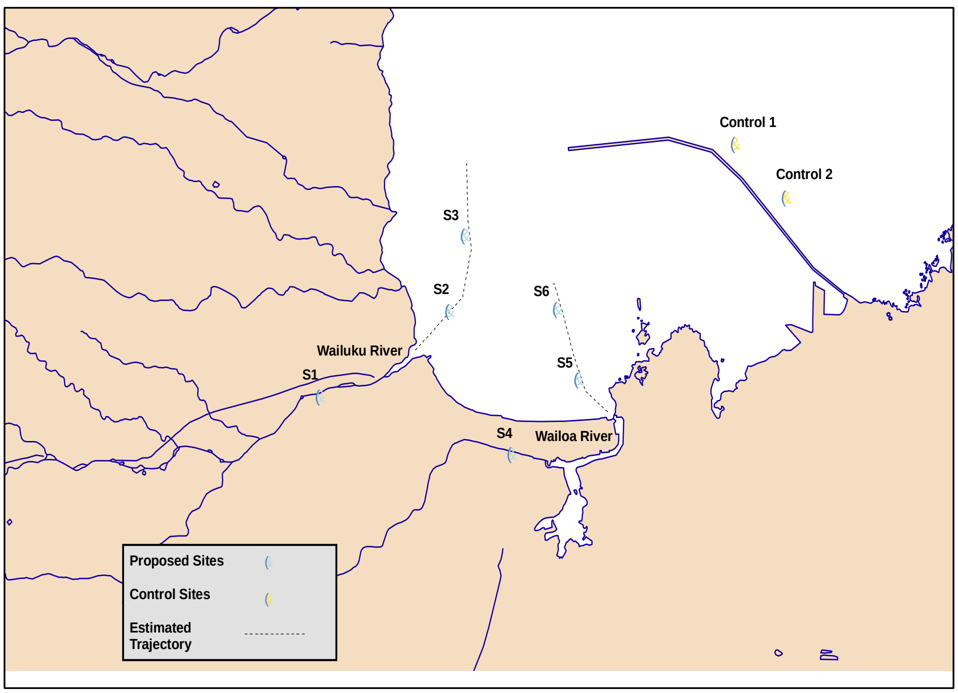

Figure 3-8. UHH Water Quality Monitoring Stations (Wiegner, T. and Mead, L., 2007)

From January 2007 through February of 2008, eight baseflow and four storm events were sampled (Table 3-2). Each station was sampled for suspended sediments, nutrients, and “Chl *a*”. Because the focus of this study was to evaluate water quality in Hilo Bay before and after a storm, water samples were collected from surface waters where river sediments and algae are most likely concentrated due to the bay’s stratification. To characterize the conditions at each station when sampling, physiochemical parameters (salinity, specific conductivity, temperature, dissolved oxygen concentration, dissolved oxygen percent saturation, light penetration) were measured using a YSI multi-parameter meter and a Li-Cor light meter, respectively. Depth profiles for these physiochemical parameters were measured at the six Hilo Bay stations. Meteorological data (rainfall, winds, waves, and tides) were also obtained for the sampling dates. For further detail on the methods and results of the water quality monitoring, refer to Wiegner, T. and Mead, L., (2009).

Table 3-2. University of Hawaii at Hilo Sampling Events through September 2007 (Wiegner, T. and Mead, L., 2009)

Event	Date(s)
Storm 1	1/10/2007 – 1/15/2007
Storm 2	3/1/2007 – 3/6/2007
Storm 3	12/12/2007 – 12/17/2007
Storm 4	1/27/2008 – 2/1/2008
Base 1	3/14/2007
Base 2	5/3/2007 – 5/4/2007
Base 3	6/18/2007 – 6/19/2007
Base 4	7/8/2007 – 7/9/2007
Base 5	7/30/2007 – 7/31/2007
Base 6	9/5/2007 – 9/6/2007
Base 7	10/10/2007 – 10/11/2007
Base 8	11/7/2007 – 11/8/2007

4. HYDRODYNAMIC MODELING

4.1. Circulation Modeling

4.1.1. Model Descriptions

The ADCIRC numerical model was chosen for simulating the long-wave hydrodynamic processes in the study area. Utilizing tidal constituent, wind and atmospheric pressure data, the ADCIRC model can accurately replicate tide induced and storm-surge water levels and currents. The ADCIRC model was developed in the USACE Dredging Research Program (DRP) as a family of two- and three-dimensional finite element-based models (Luettich, Westerink, and Scheffner 1992). ADCIRC can simulate tidal circulation and storm-surge propagation over very large computational domains while simultaneously providing high resolution in areas of complex shoreline configuration and bathymetry. In two dimensions, the model is formulated using the depth-averaged shallow water equations for conservation of mass and momentum. ADCIRC utilizes a standard quadratic parameterization for bottom and wind stress. Furthermore, radiation stress gradient forcing fields, supplied by STWAVE in this application, are applied as a surrogate to wind stress. As such, the radiation stress gradients represent a stress per unit mass of water having units of m^2/s^2 (meters squared per second squared).

The three dimensional numerical hydrodynamic model CH3D-WES (Curvilinear Hydrodynamics in Three Dimensions–Waterways Experiment Station) can be applied in two vertical resolution modes, Z-grid and Sigma–grid. The Z-grid version is documented in Johnson, et al. (1991). The Sigma-grid version, used in this study, is documented in Chapman et al. (1996). The basic Sigma-grid model (CH3D) was developed by Sheng (1986) for WES but has been extensively modified, including the development of the Z-grid version. These modifications have consisted of implementing different basic numerical formulations of the governing equations as well as substantial recoding of the model to provide additional computational efficiency. CH3D-WES performs hydrodynamic computations on a non-orthogonal curvilinear or boundary-fitted planform grid. Physical processes impacting circulation and vertical mixing that are modeled include tides, wind, density effects (salinity and temperature), freshwater inflows, turbulence, and the effect of the earth's rotation.

The boundary-fitted coordinate feature of the model provides grid resolution enhancement necessary to adequately represent deep navigation channels and irregular shoreline configurations of the flow system. The curvilinear grid also permits adoption of accurate and economical grid schematization software. The solution algorithm employs an external mode, consisting of vertically averaged equations, which provides a solution for the free surface displacement for input to the internal mode, which contains the full 3D equations. The 2D vertically, or depth averaged option is used in the present study.

4.1.2. Model Setup and Forcing Data

The development of the ADCIRC grid for determining regional circulation was initiated by using a previously developed finite element mesh that encompasses the entire Hawaiian Island chain in an oval grid boundary (Figure 4-1). This existing mesh used National Geophysical Data Center (NGDC) ETOPO2 bathymetric data to generate deep water bathymetry at a resolution of approximately 2 degrees. The grid was previously used for model studies focusing on Southeast Oahu, and therefore, modifications to the grid were needed to reduce nearshore resolution in that area (from ~ 50m to ~150m) as well as to increase resolution in the present areas of interest, Hilo Bay (Figure 4-2) and Hilo Harbor (Figure 4-3) from ~350m to ~50m.

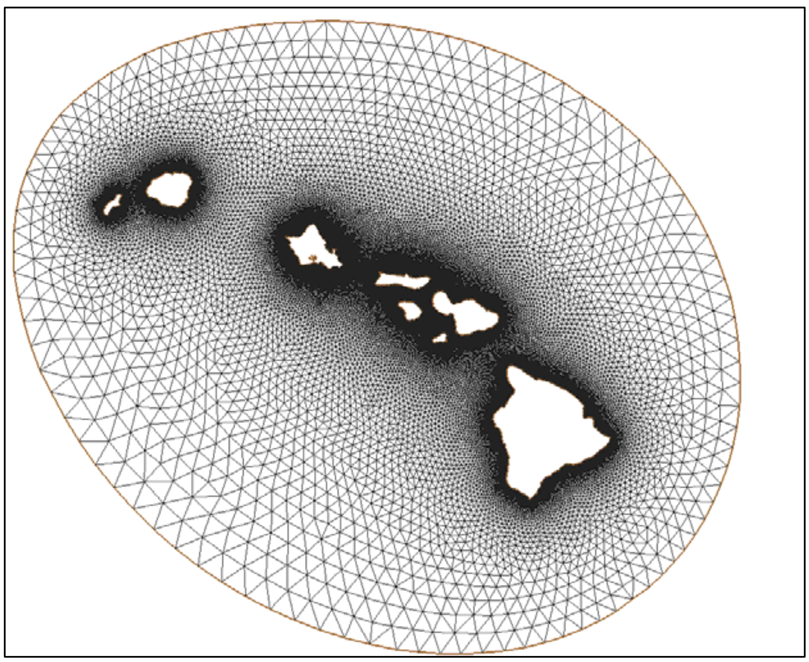

Figure 4-1. ADCIRC Grid for the Hawaiian Islands

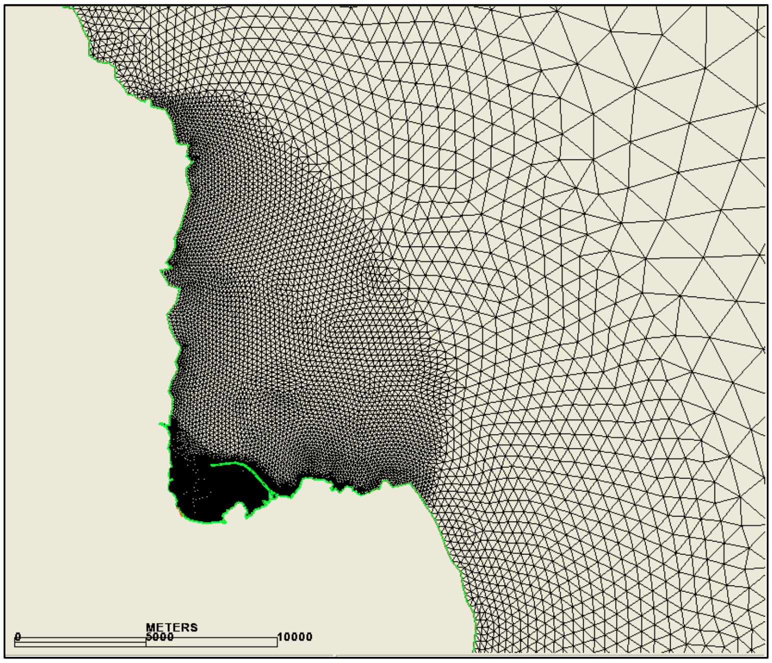

Figure 4-2. ADCIRC Grid for Hilo Bay

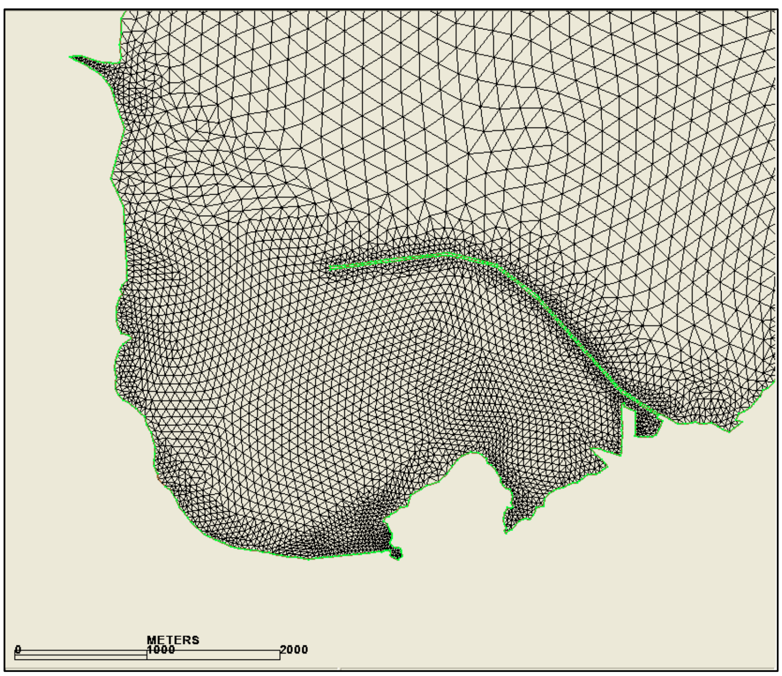

Figure 4-3. ADCIRC Grid for Hilo Harbor

The precision of the Hilo Bay coastline in the grid was improved using several tools including the National Oceanographic and Atmospheric Administration's (NOAA) Coastline Extractor, a georectified 2003 aerial photo of the bay, and a NOAA digital nautical chart. The ADCIRC grid was also improved with several sets of bathymetric data in the Hilo Bay and Hilo Harbor areas. NOAA's National Geophysical Data Center (NGDC) Geophysical Data Management System (GEODAS) database of digital historical surveys was used to update the higher-resolution areas of the grid in intermediate waters both inside and outside the bay. A USACE channel survey dated August 28, 2005 was incorporated into the grid area inside Hilo Harbor, and a 2005 multibeam survey of the subaerial surface of the Hilo Breakwater was used to represent the details of the breakwater foundation and adjacent portions of Blonde Reef. USACE Scanning Hydrographic Operational Airborne LiDAR Survey (SHOALS) bathymetry data was not available for the Hilo Bay area at the time of model setup. All newly incorporated bathymetry sets were converted to the existing mesh coordinate system (Geographic, NAD 83, meters) and vertical datum (Mean Tide Level, meters) for incorporation into the grid. In addition to the existing condition (Figure 4-4), five additional model grids, each based on an alternative breakwater configuration (Figure 4-5), were generated with identical bathymetry and modifications made only to alter the breakwater for alternatives as described in Section 2.

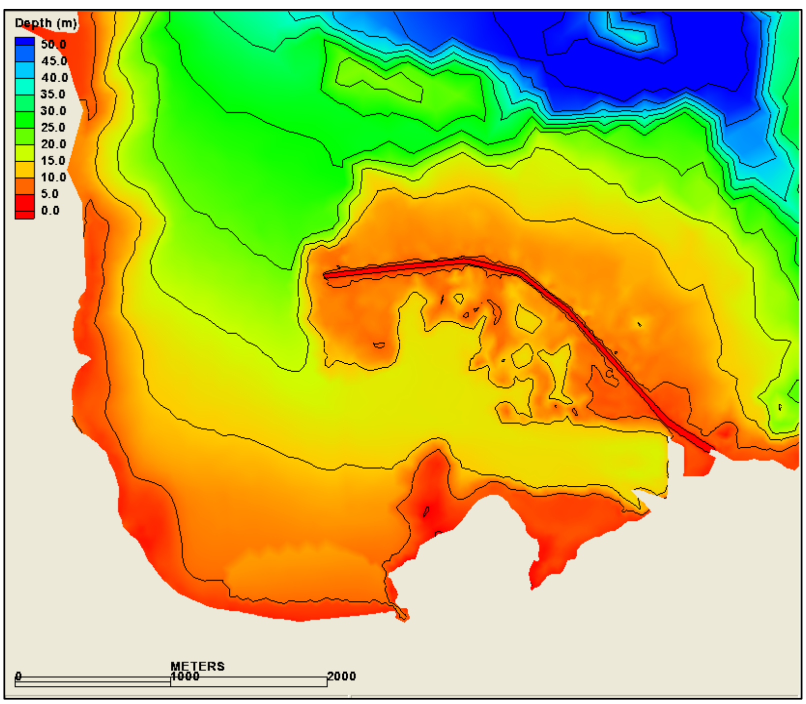

Figure 4-4. ADCIRC Bathymetry for Existing Breakwater Condition

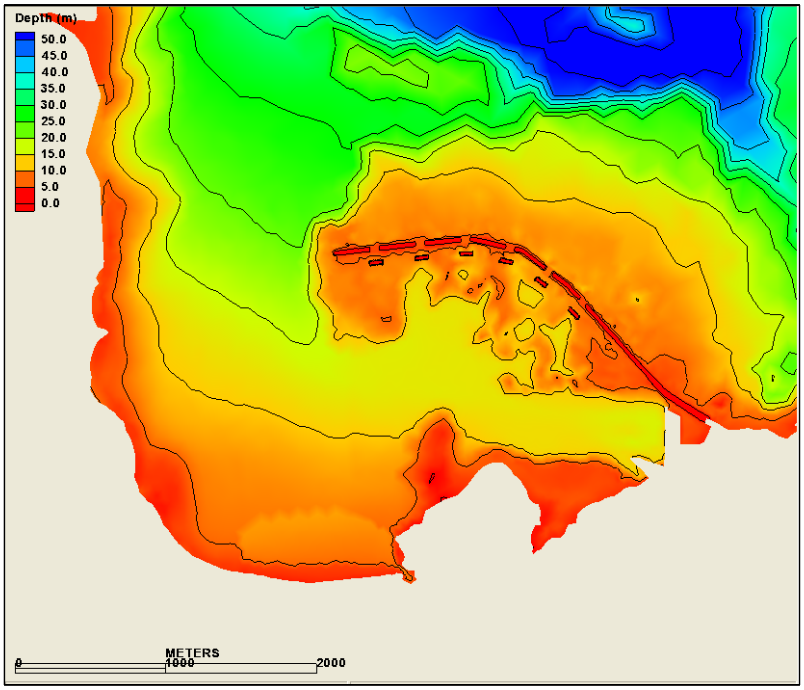

Figure 4-5. ADCIRC Bathymetry for Typical Alternative (Alternative 3)

The ADCIRC grid mesh is forced with the free surface position along the open-water boundary that surrounds the Hawaiian Islands. Tidal forcing conditions were developed for the ocean boundary condition with the LeProvost tidal constituent database (LeProvost et al., 1994). The LeProvost database was applied because it provided a stable solution for the linked model validation time period. Offshore wind fields developed by the National Center for Atmospheric Research (NCAR) and the National Centers for Environmental Predication (NCEP) Reanalysis Project are implemented as the wind forcing condition. The NCEP/NCAR Reanalysis Project is a joint project whose goal is to produce new atmospheric analyses using historical data (1948 onwards) and to produce analyses of the current atmospheric state (Climate Data Assimilation System, CDAS). The quality and utility of the re-analyses are superior to NCEP's original analyses because a state-of-the-art data assimilation is used, more observations are used, and quality control has been improved. Atmospheric pressure fields were not included as forcing data.

Radiation stress gradients were applied from results of the STWAVE model, in order to account for currents generated by wave breaking in the vicinity of the harbor. The STWAVE wave model is discussed later in this section. In addition, approximated stream flows into Hilo Bay from the

Wailuku River were included as input to the ADCIRC runs. These values were determined using daily data from US Geological Survey (USGS) stream gages 1671300 (Wailuku River at Hilo Bay) and 16704000 (Wailuku River at Pi'ihonua), and determining a correlation factor between the two to fill in data gaps. Wailoa River flow was not included as input to the ADCIRC model runs, due to the minimal relative effect that this inflow would have on the large area covered by the grid domain.

A nested CH3D-WES base grid and five breakwater alternative grids were developed using shoreline and bathymetric data from the ADCIRC grid. The entire base Hilo Bay grid with the existing breakwater structure and bathymetry in meters is shown in Figure 4-6. A typical alternative configuration CH3D grid (Alternative 3) is shown in Figure 4-7. Forcing conditions for the CH3D model, including boundary water surface elevations, winds, and Wailuku river flow, were derived from ADCIRC simulations using "output stations" at locations within the ADCIRC grid that correspond to the offshore boundary of the CH3D grid. Radiation stress gradients were applied using values determined from the wave model, in a similar manner to the method used for application to the ADCIRC model.

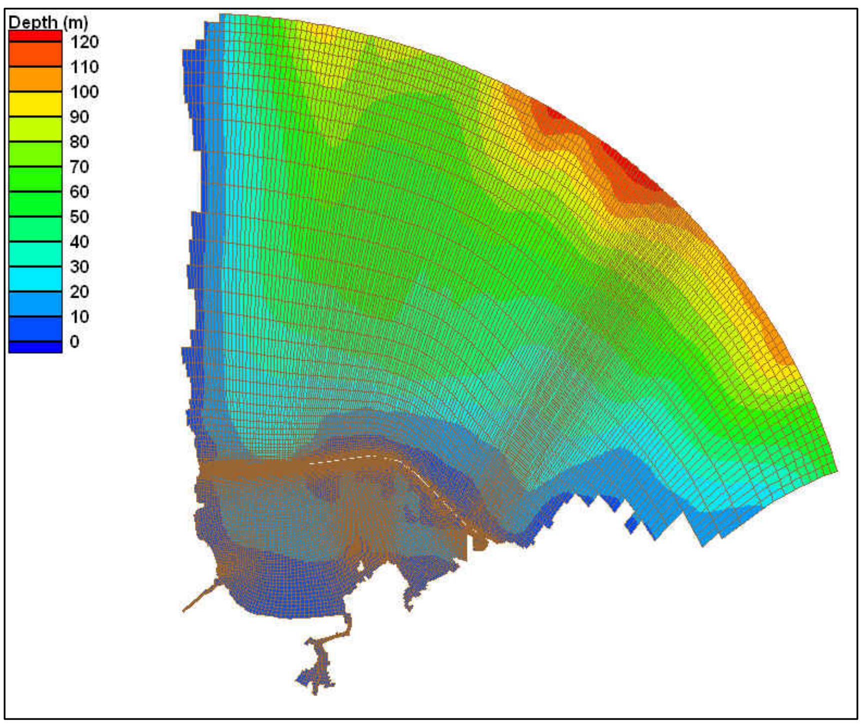

Figure 4-6. CH3D Grid Coverage (Existing Condition)

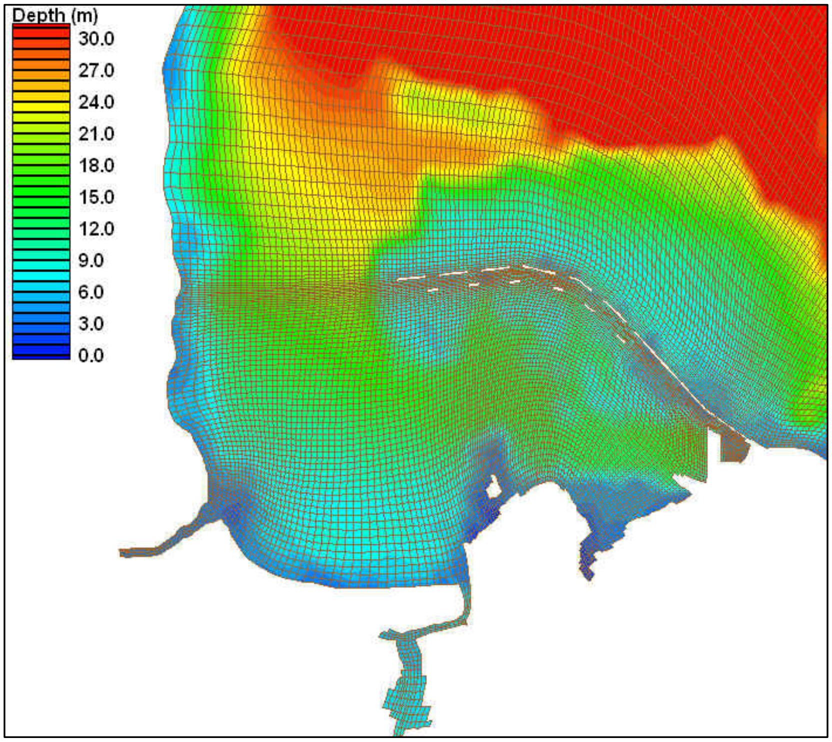

Figure 4-7. CH3D Grid for Typical Alternative (Alternative 3)

4.1.3. Validation and Calibration

A calibration run of ADCIRC results for water level was completed for the period of April 10-24, 2001, and a comparison of model results was made with measured water levels from NOAA tide station 1617760, located near the Hilo Harbor Pier #3 (Figure 4-8). This time period was selected because improved NCEP/NCAR wind fields from Oceanweather, Inc. were available. Oceanweather, Inc utilized Interactive Optimum Kinematic Analysis System (IOKA, Cox et al. 1995) for the generation of these 2001 regional wind fields. In this method, point source measurements and wind estimates derived from satellite scatterometers are used improve the accuracy of the background NCAR/NCEP reanalysis wind fields.

The run included tidal constituents and winds as forcing conditions. The run showed approximate agreement with the tide gage, but some small phase differences were noted, as well as a difference in water levels on the order of approximately 0.2 meters.

A harmonic analysis of tidal constituents was conducted, and based on this; adjustments were made to the tidal boundary conditions. A new calibration run with adjusted tidal constituents resulted in an improved comparison to the predicted tide gage (Figure 4-9). Additional forcing conditions were added, including stream inputs from the Wailuku River and radiation stresses determined from wave transformation model STWAVE, but the resulting changes to water level were negligible.

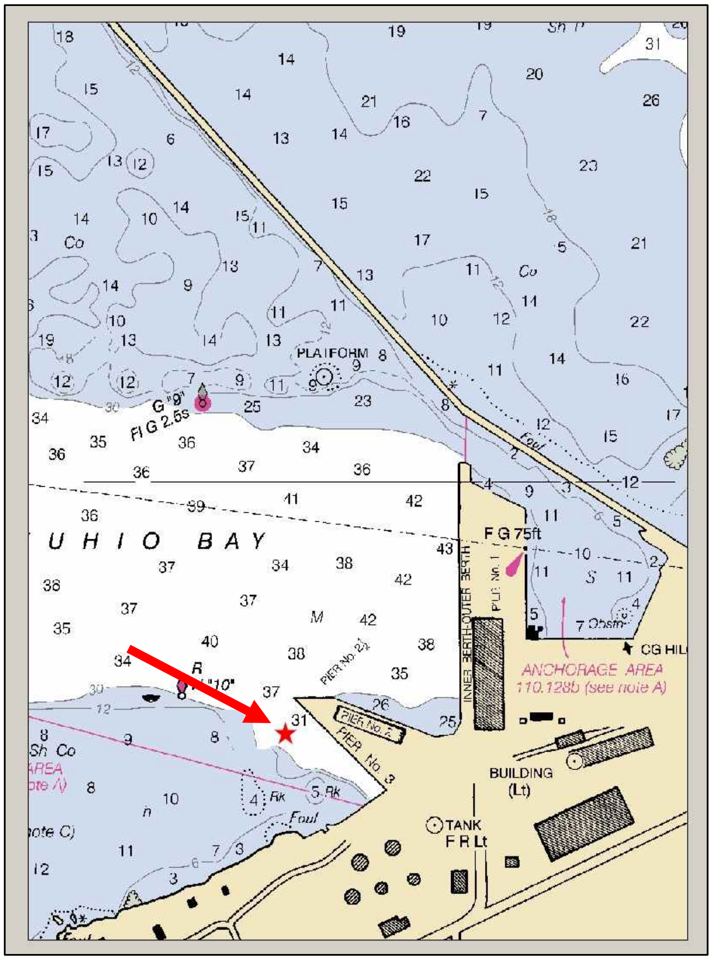

Figure 4-8. NOAA Tide Station 1617760 at Hilo Harbor

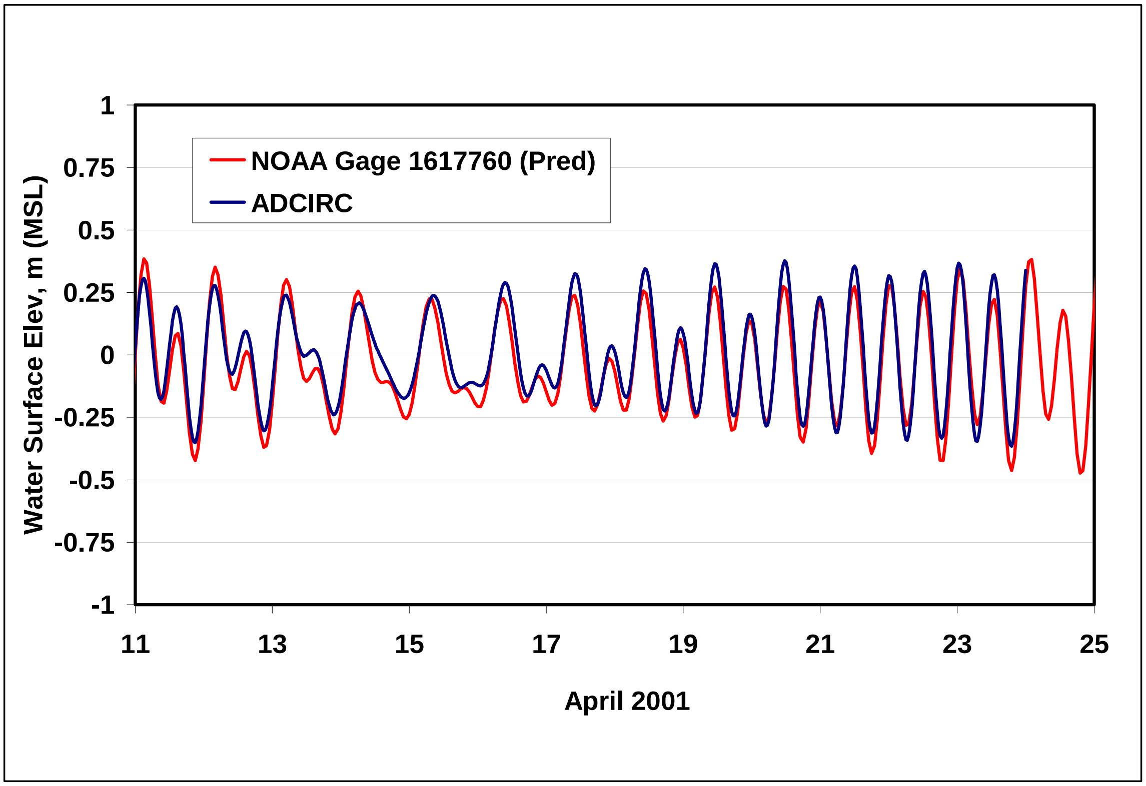

Figure 4-9. ADCIRC Modeled Water Level Compared to Tide Prediction

Depth-averaged tidal calibration of the CH3D-WES model was performed utilizing boundary water surface elevations, wind forcing, and Wailuku river flow derived from the April 2001 ADCIRC simulation. The tide and wind forcing data were updated every 0.5 hours during the simulation. The groundwater inflow from the Wailoa River and Icy Bay was specified as the approximate average low flow of the Wailuku River, which was updated every 24 hours during the simulation. The results of the calibration simulations are presented in Figure 4-10, which show the predicted and measured tides at the Hilo Harbor gage with ADCIRC and CH3D-WES model simulation results. The accurate representation of volume change within the bay is vital to the accurate evaluation of flushing for various alternatives. It is seen in this figure that after sufficient spin-up time, both the ADCIRC and CH3D-WES model simulation results accurately represent the time varying tidal prism within Hilo Harbor. The departure of the gage prediction and model simulations from the gage measurements is a result of atmospheric pressure variation during the model simulation period.

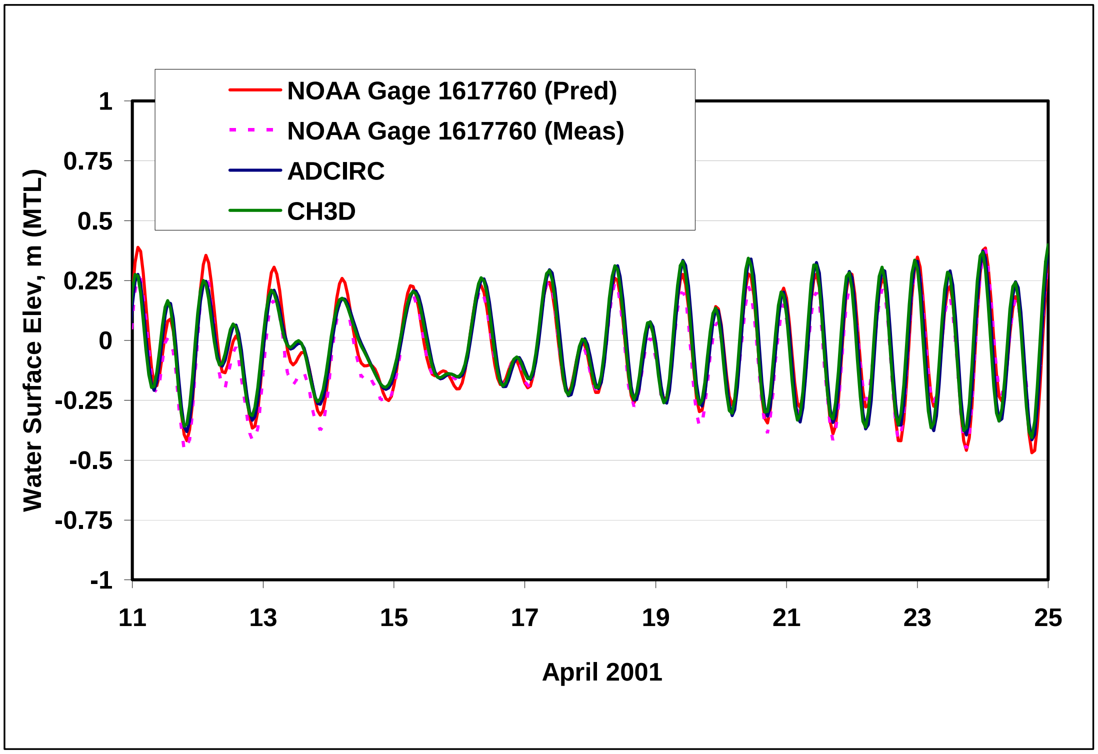

Figure 4-10. ADCIRC & CH3D Comparison to Tide Measurement and Prediction

Subsequent to satisfactory hydrodynamic model calibration, April 2001 simulations using CH3D-WES were performed for the existing condition and five alternative grids to generate hydrodynamic transport files for CE-QUAL-ICM water quality calibration. The hydrodynamic transport data output interval for the water quality model was provided hourly.

4.2. Wave Modeling

4.2.1. Model Description

STWAVE is a spectral wave transformation model, which is capable of representing depth-induced wave refraction and shoaling, current-induced refraction and shoaling, depth- and steepness-induced wave breaking, diffraction, wind-wave growth, wave-wave interaction and whitecapping (Resio 1988, Smith et al. 2001). The purpose of applying nearshore wave transformation models such as STWAVE is to describe quantitatively the change in wave parameters between the offshore and the nearshore because offshore time-series wave data is usually more commonly available. STWAVE has previously been applied to numerous sites with a gently sloping seafloor or small areas of hardbottom. Due to the wide and relatively shallow reef fronting the Hilo Harbor breakwater, this application of STWAVE required the added feature of simulating wave transformation over reefs. Development of a bottom friction capability in STWAVE was completed to address this unique bathymetry specific to the island environment.

4.2.2. Model Setup and Forcing Data

A nested STWAVE grid was developed with a deep water "coarse" grid located so that the offshore grid boundary coincided with the nearest Pacific Wave Information Study (WIS) Hindcast Station (Station 105), See Figure 4-11a. The coarse grid has a resolution of 250 meters. A nearshore "fine" grid was created to continue the transformation into Hilo Bay and Hilo Harbor at a resolution of 25 meters, see Figure 4-11b. Output wave spectra are generated from the coarse grid along a row that overlaps with the fine grid. This spectra is then linearly interpolated along the offshore boundary of the fine grid and used as a forcing condition.

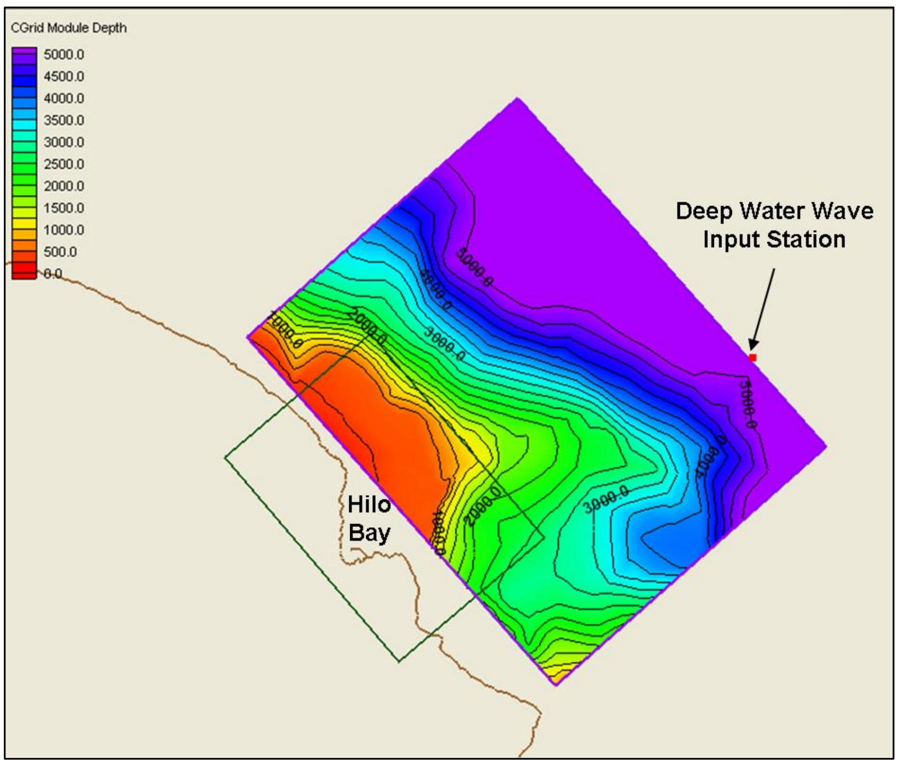

Figure 4-11a. STWAVE Coarse Grid

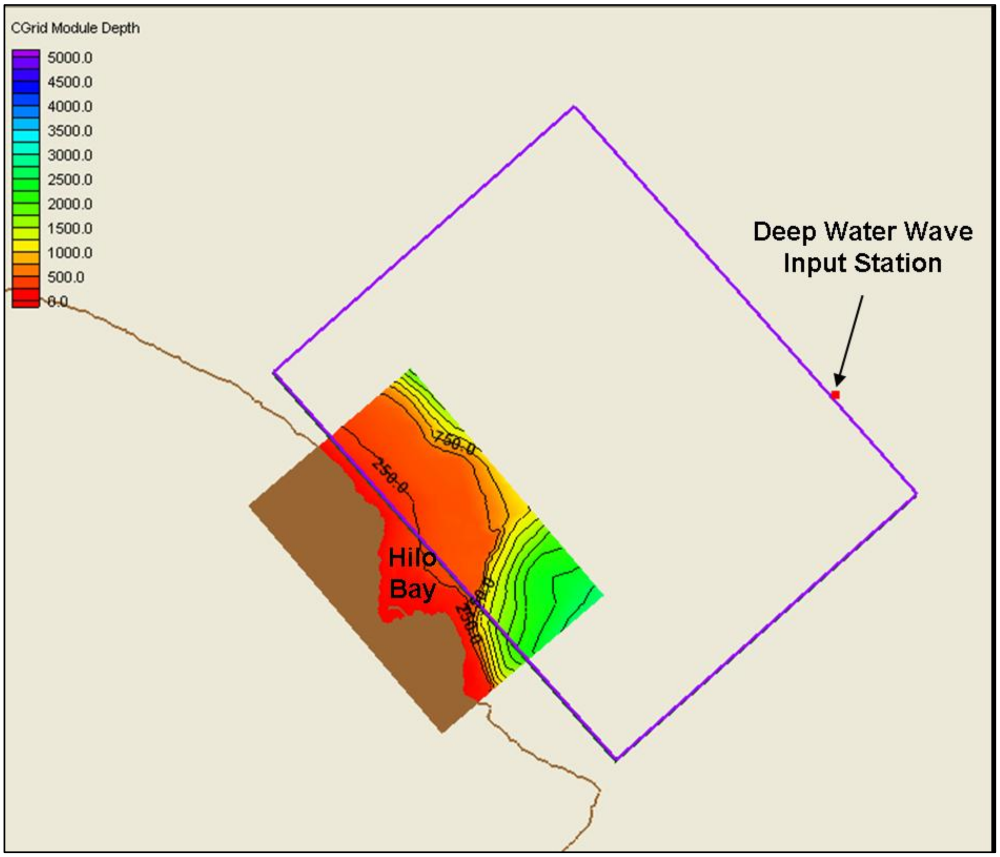

Figure 4-11b. STWAVE Fine Grid

Bathymetry from each of the ADCIRC grids was interpolated onto the STWAVE Cartesian grid for the existing condition (Figure 4-12) as well as each alternative breakwater configuration (Figure 4-13), respectively, with smoothing adjustments to the STWAVE grid cells for land boundaries and the breakwater structure made as needed.

Incident wave spectra were generated at the coarse grid offshore boundary using a parametric spectral shape together with a directional spreading function and based on wave parameters (wave height, period, and direction), as determined from various wave data sources including WIS and National Data Buoy Center (NDBC) buoys, corresponding to the different run periods. A variable Manning friction coefficient (n= 0.020 for non-reef, n = 0.20 for reefs) was used on the fine grid to incorporate the friction effects over Blonde Reef. These friction values were based on previous applications of STWAVE in a reef environment along the coast of Southeast Oahu (Cialone, et al., 2008).

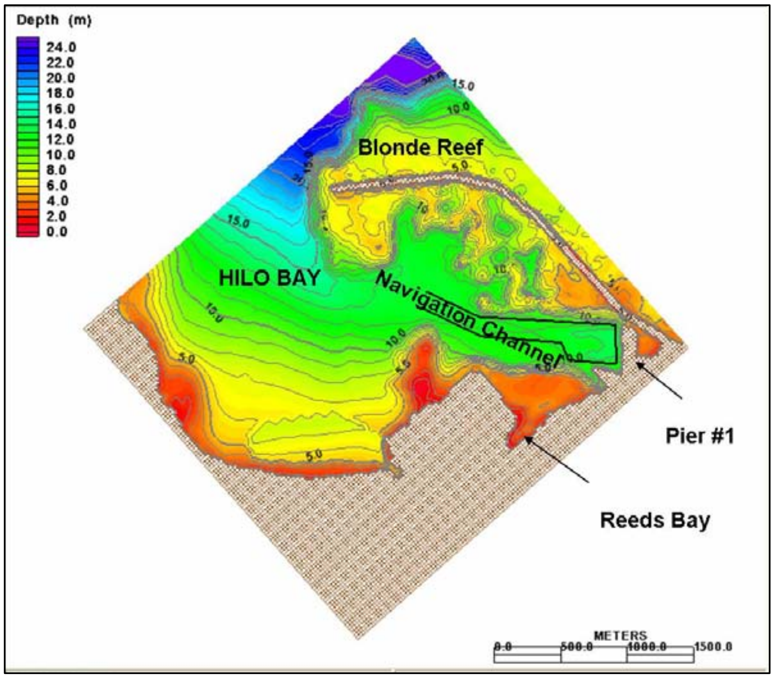

Figure 4-12. Detailed Bathymetry of STWAVE Grid for Existing Condition

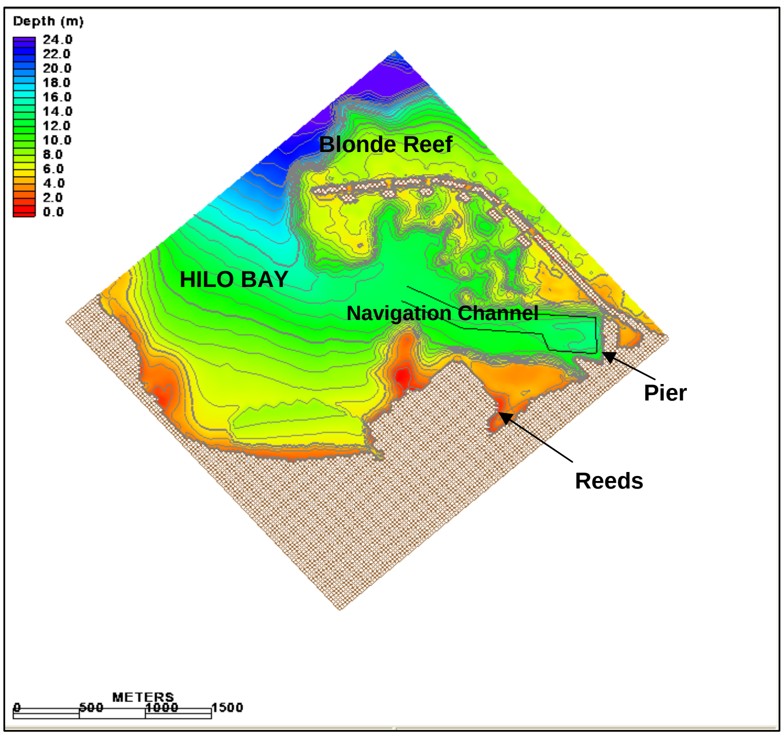

Figure 4-13. Detailed Bathymetry of STWAVE Grid for Typical Alternative (Alt. 3)

4.2.3. Validation and Calibration

STWAVE was run for the April 10 – 24, 2001 time period using WIS hindcast data from Station 105 as offshore input, in order to contribute radiation stress gradients to the ADCIRC and CH3D calibration runs for that time period. STWAVE was also run for the period of March – June 2007 and results were compared to wave data collected during the March – June 2007 instrument deployment period, for the validation and calibration of the wave model only. For the calibration period during March – June 2007, the WIS station data at Station 105 was not available to use as the incident offshore wave condition. The nearest directional wave data available for this time was at NDBC Station 51001, northwest of the island of Kauai. A transformation from the NDBC Station to the STWAVE boundary was completed using WAVTRAN (Gravens, Kraus, and Hanson, 1991).

As discussed in Thompson and Scheffner (2004), the WAVTRAN model calculates spectral transformation of waves during propagation from one depth to another shallower depth, taking into account shoreline orientation and wave sheltering. The model assumes that sea and swell waves have an energy spectrum that follows the Texel, MARSEN, ARSLOE (TMA) spectral form (Bouws et al.1985). Directional spread is calculated by 4th and 8th power cosine functions. Wave transformation calculation is dependent on the shoreline orientation because bottom contours are assumed parallel to the shoreline. If wave sheltering is included, wave energy coming from directions specified by a sheltered angle band is deleted from the spectrum. Typically, sheltering is applied as needed to remove wave energy from any direction which is blocked from a straight-line approach to the site by protruding land forms. Wave transformation calculation is dependent on the shoreline orientation, in order to capture the sheltering effects of the island chain.

In this case, an angle of 10 degrees was implemented in WAVTRAN to incorporate the sheltering effect of the Hawaiian Island chain from northwest waves at the offshore boundary of the STWAVE grid. Figure 4-14 shows the general bathymetry of the island chain, the location of NDBC Station 51001, the STWAVE coverage area, and a 10 degree sheltering angle, in comparison with a 20 and 30 degree sheltering angle. Based on this bathymetry, a 10 degree sheltering angle was considered appropriate. This process effectively deleted any wave energy in the NDBC 51001 buoy spectra from west of 318 degrees True North. This “reduced” set of refracted wave parameters in hourly increments was then further reduced and processed into 6-hour incremental wave spectra at the STWAVE coarse grid boundary as a deep water input condition to the model. A constant water level equivalent to Mean High Water (0.254 meters above Mean Tide Level) was used within the entire STWAVE domain. A compiled model run of the coarse and fine grids was completed for 22 March 2007 through 9 June 2007 at 6-hour increments to develop a nearshore time series at the instrument where waves were measured (ADCP 1).

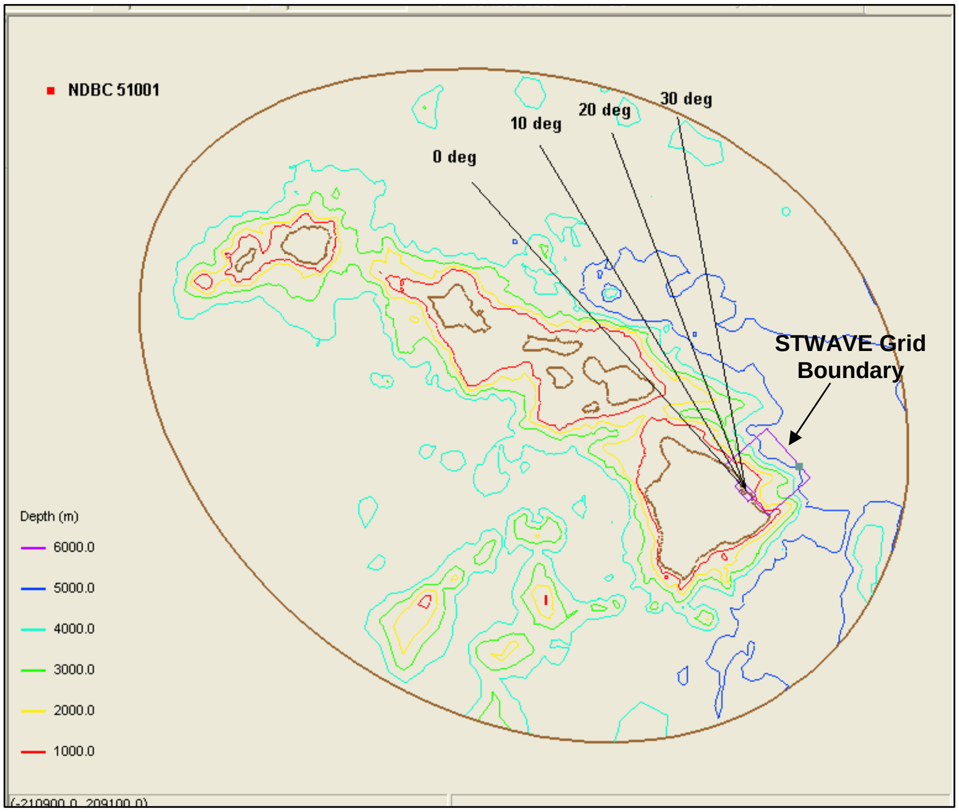

Figure 4-14. Sheltering Angle used for Wave Transformation with WAVTRAN

The nearshore time series extracted from the model run at ADCP 1 was advanced 36 hours in time based on calculations of average wave celerity (determined by average wave period) and distance from NDBC buoy 51001 to the offshore boundary of the STWAVE grid. This adjustment was made to accommodate for the lag time between the real-time data at the NDBC buoy and the time that these waves would reach the boundary offshore of Hilo Bay.

The comparison of the model time series wave height to the measured gage data at ADCP 1 was relatively good, capturing the trends in wave height fluctuation, but with a slight bias toward lower wave heights in the model results (Figure 4-15). Wave height at NDBC buoy 51001 and wave height used at the STWAVE offshore boundary after transformation using WAVTRAN is also shown in this time series. Some adjustments were made to the Manning friction factor in an attempt to better calibrate the model to the gage data; however, due to the relatively small and concentrated location of the reef area and the distance from the reef to the instrument location, these adjustments did not improve the agreement significantly.

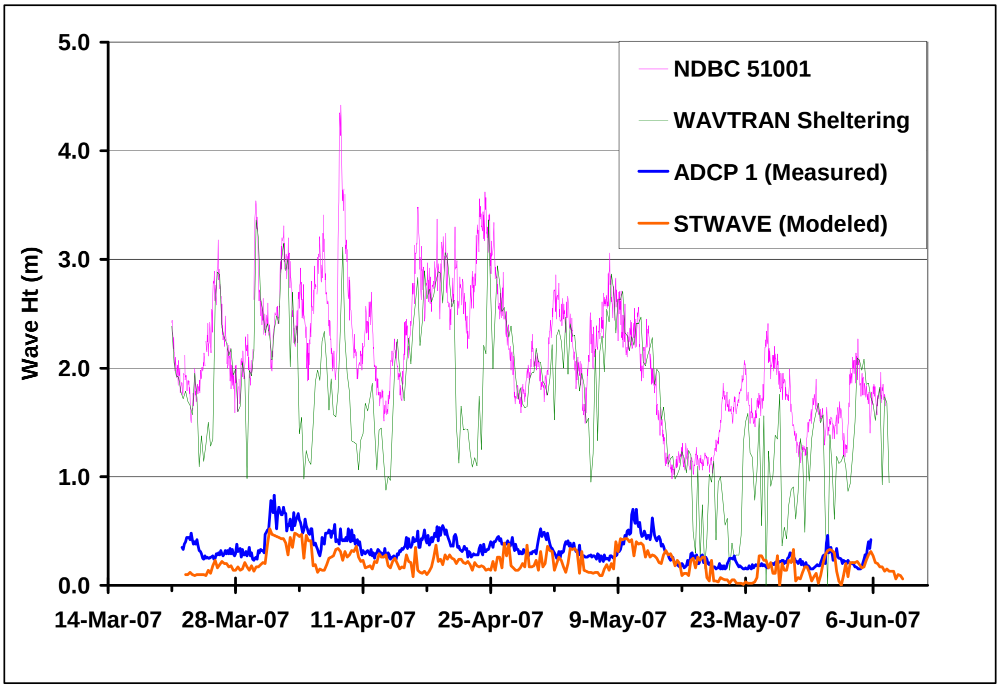

Figure 4-15. Wave Height Comparison (STWAVE vs. ADCP1)

The agreement of the model with measured wave periods was also generally good; however, the model appears to overpredict wave period at several times, while missing intermittent higher wave periods recorded by the instrument (Figure 4-16). Wave direction was also compared for model results vs. gage data. Due to the strong diffractive effects on waves moving past the breakwater to the instrument location, it is not entirely surprising that agreement between the model wave direction and measured wave direction is not in substantial agreement.

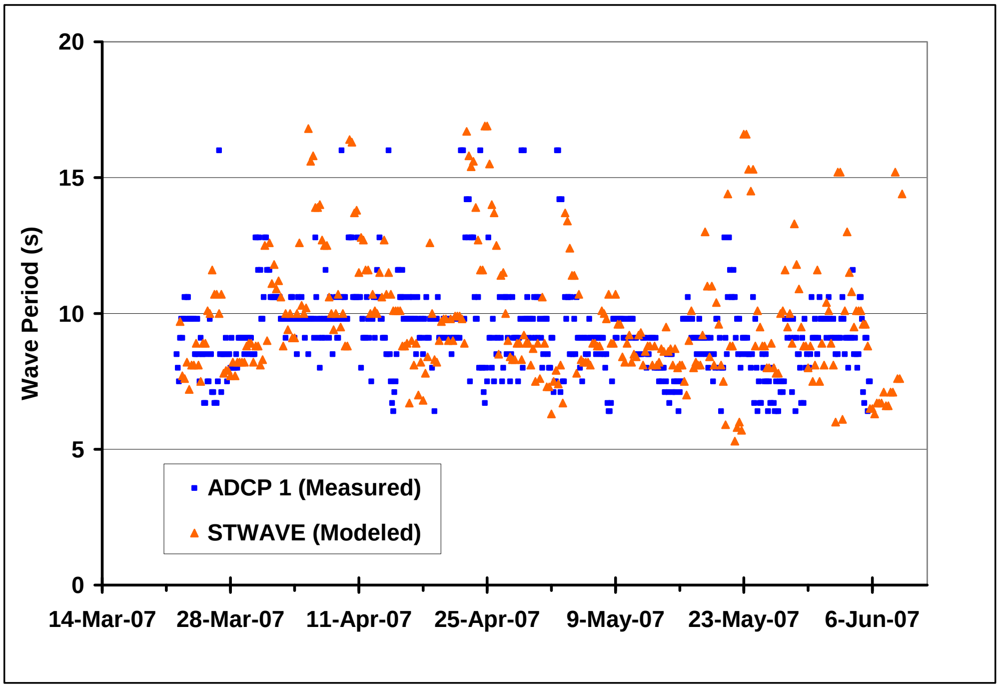

Figure 4-16. Wave Period Comparison (STWAVE vs. ADCP1)

The model-predicted wave direction spans a very small window, while the measured wave direction varies widely, though both are primarily from the northwest (coming from the direction of the harbor entrance), as shown in Figure 4-17. It is also possible that the wave gage captured the direction of some reflected or wind-generated wave energy that is not accounted for in STWAVE. Overall, it was felt that since the wave energy was well-represented by STWAVE in terms of wave height and period, that the model was validated sufficiently to determine relative changes in wave energy due to the alternative breakwater modifications.

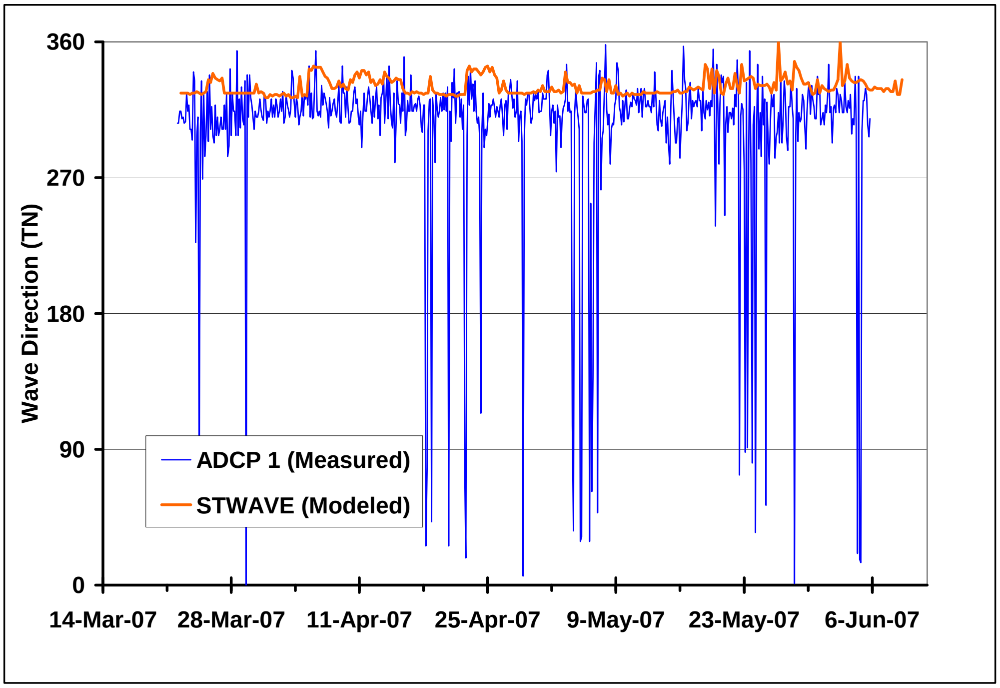

Figure 4-17. Wave Direction Comparison (STWAVE vs. ADCP1)

4.3. Combined Wave and Circulation Modeling

4.3.1. Radiation Stress Gradients in STWAVE

Radiation stress is the flux of momentum which is carried by ocean waves. When these waves break, that momentum is transferred to the water column, forcing nearshore currents. As such, the radiation stress gradients represent a stress per unit mass of water having units of m^2/s^2. This effect on currents (and in turn circulation) is important in this model application due to the wave breaking that occurs on Blonde Reef, in the vicinity of the breakwater and Hilo Harbor entrance. Radiation stress is calculated in STWAVE based on linear wave theory. Gradients in radiation stress are calculated in STWAVE to provide wave forcing to external circulation models to drive nearshore currents and water level changes (i.e., wave setup and setdown) (Smith et al. 2001). Fields of radiation stress gradients, both x and y components, are provided for each wave condition run in STWAVE, over the entire model domain.

4.3.2. Application of Radiation Stress Gradients in ADCIRC

Outputs of the radiation stress field over the fine STWAVE grid were reformatted for use in the ADCIRC and CH3D models in order to account for wave generated currents. A separate computer program was used to spatially interpolate the radiation stress gradient solution from STWAVE to the ADCIRC grid at 6 hour intervals (the same interval that offshore wave conditions were updated in STWAVE). The application of radiation stress gradients in ADCIRC resulted in increased current velocities where wave breaking occurs, along the shoreline and on the outside of the breakwater across Blonde Reef. Current velocities were increased due to the effect of waves breaking on Blonde Reef by an order of magnitude of approximately 0.5 meters/second (m/s).

4.3.3. Radiation Stress Gradients and Water Levels in CH3D

The CH3D-WES wind subroutine was modified to accept radiation stress gradient forcing from the spatially interpolated solution file used for the ADCIRC application. Non-trivial values (values exceeding 0.0001 m^2/s^2) were extracted from the radiation stress gradient file and applied along the seaward side of the breakwater and exposed shoreline. As in ADCIRC, the radiation stress gradient forcing is applied as a supplement to wind stress. The update interval of the radiation stress gradient forcing during the CH3D-WES simulations was also 6 hours.

4.4. Modeling Simulation of February – March 2007

The primary modeling simulation during this project was completed for the dates of 19 February 2007 through 19 March 2007. This time range was selected because it encompassed the following wave, wind, and flow events: tradewind/wave conditions, northwest swell waves, Kona wind/wave conditions, light and variable wind conditions, a rain event (above average river flow), and a dry period (below average river flow). A time series of various meteorological conditions is shown in Figure 4-18, with the various events labeled. In addition, UHH water quality data had been collected at two instances during this period, one baseflow event (‘Base 1’ on 14 March 2007) and one storm event (‘Storm 2’ during 1 - 6 March 2007). Use of this time period for the primary modeling simulation would therefore enable examination of the effects of various breakwater alternatives under several weather conditions, in addition to verifying the CEQUAL-ICM model to the UHH water quality data.

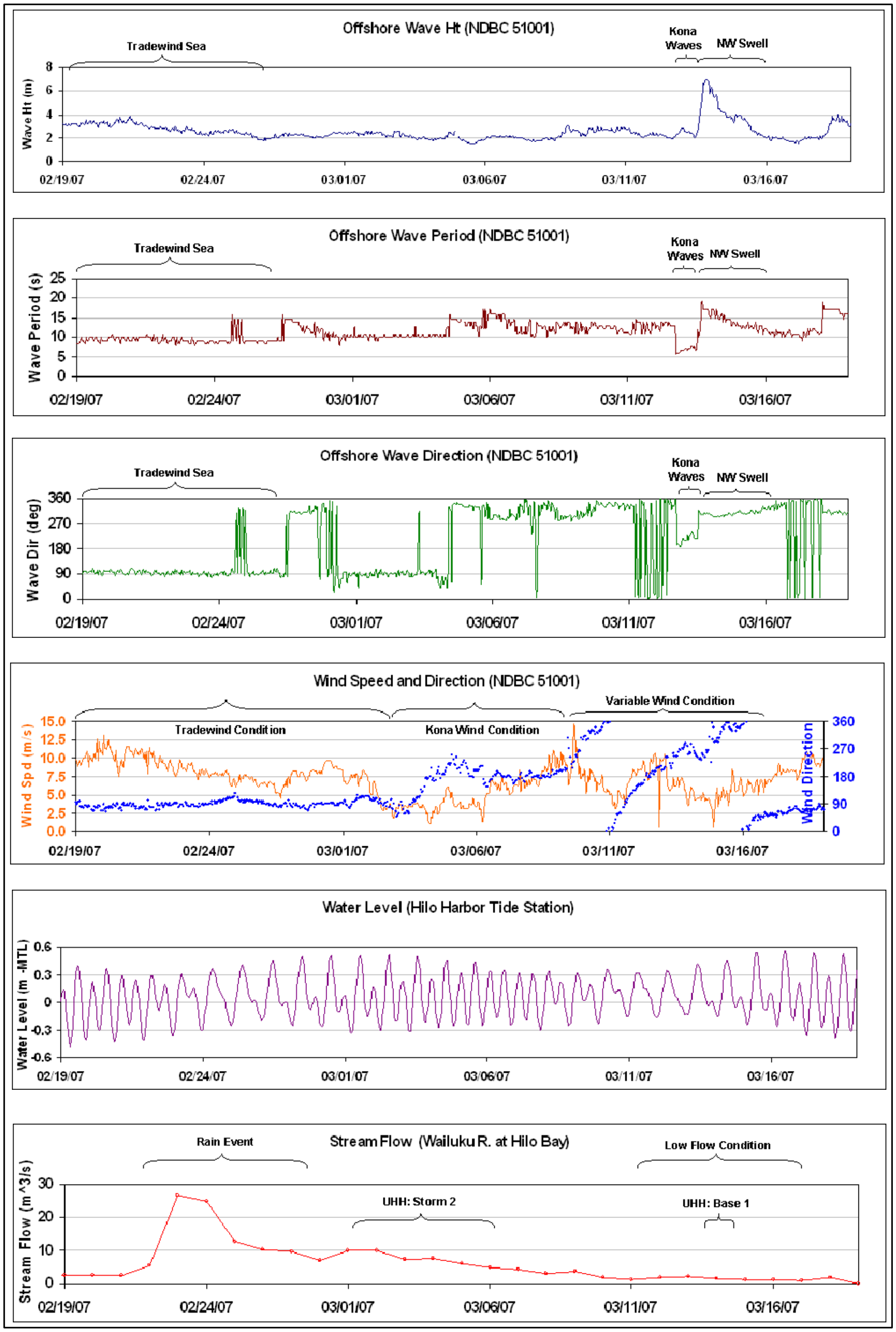

Figure 4-18. Meteorological Conditions during 19 February – 19 March 2007

4.4.1. Forcing Data

The forcing data used during this modeling simulation is similar to the data used as input for the validation and calibration runs of STWAVE, ADCIRC, and CH3D-WES. Offshore wave data was not available from Pacific WIS Hindcast Data for the February – March 2007 time period, so directional wave data from NDBC buoy 51001 (parameters of wave height, period and direction shown in Figure 4-18) was again transformed to the STWAVE boundary using WAVETRAN, and used to generate wave spectra using a parametric spectral shape at 6 hour intervals. Water level in STWAVE was again held constant at Mean High Water for wave runs through both the coarse and fine wave grids. Spatially varying Manning's friction coefficients of n= 0.020 for non-reef and n = 0.20 for reefs were also applied in the manner as the calibration run. Radiation stress gradients from STWAVE output were interpolated for application in ADCIRC and CH3D grids.

The harmonic-adjusted LeProvost tidal constituents used in the calibration run of the ADCIRC model were applied again, with modifications made in phase start time to correspond to the March 2007 run start time. NCEP/NCAR Reanalysis wind fields were obtained for February and March 2007 and applied in the ADCIRC model. As mentioned, radiation stress gradient fields from the STWAVE model runs were interpolated to the ADCIRC mesh and applied to the circulation model run for this time period in areas where wave breaking occurs. Stream flow input at the Wailuku River was incorporated using the daily USGS stream gage data and applying the correlation factor previously determined to simulate flow levels at the entrance to Hilo Bay.

Forcing conditions for the CH3D model (boundary water surface elevations, winds, and Wailuku river flow) were again derived from ADCIRC simulations using "output stations" at locations within the ADCIRC grid that correspond to the offshore boundary of the CH3D grid. Radiation stress gradients were applied using values determined from the wave model at 6 hour intervals, in the same method used during calibration runs. Wailoa River and Icy Bay groundwater flow was again specified as the approximate average low flow of the Wailuku River, and updated every 24 hours during the simulation.

4.4.2. Harbor Alternative Runs

STWAVE runs for each alternative were completed for the 19 February – 19 March 2007 time period at an interval of six hours. As discussed, radiation stress gradients were passed forward to the ADCIRC and CH3D models throughout the 30 day simulation. ADCIRC simulations were completed for the same time period using the existing and five alternative meshes, all had identical input forcing. Water surface elevation, wind, and

Wailuku river flow were extracted for the entire time series for each alternative and used to force CH3D-WES. CH3D-WES simulations using tide, wind and radiation stress gradient forcing were performed to generate ICM hydrodynamic transport files for the base grid and five alternative grid configurations.

The results of the February – March 2007 STWAVE runs were evaluated in order to determine the changes to wave energy that would occur with implementation of the various breakwater alternatives. Wave height everywhere within the harbor was used as the primary indicator of an increase in wave energy; therefore, a relative difference between the wave heights for the existing breakwater configuration and each alternative was used to evaluate the various proposed configurations. These wave height differences were calculated for each alternative over the entire run period. It is not feasible to show the wave difference plots throughout the entire time series, so snapshots during a predominant tradewind condition only are shown for each alternative (Figures 4-19a through 4-19e). A wave height difference of 1.0 meter or greater within the navigation channel was chosen as the evaluation criterion for bringing forward an alternative breakwater configuration for water quality modeling. As shown in the following figures, this criterion removed Alternative 1 (removal of the outer 7,500 feet of the existing breakwater and construction of a new 2,000-foot long interior breakwater) from further consideration and water quality modeling, after flushing simulation was completed.

Alternative 1 resulted in a marked increase in wave energy within the harbor as would be expected due to the drastic reduction in breakwater length (Figure 4-19a). An increase in wave height of 1.0 meter or greater is shown within a large portion of Hilo Harbor, including the outer portion of the navigation channel. The maximum increase within the harbor is 1.65 meters at several locations inside the previous breakwater alignment. This alternative breakwater configuration continues to provide sheltering at the interior of the harbor and navigation channel, with wave height differences in the range of 0.0 to 0.2 meters. A significant increase in wave energy approaching the Hilo Bay shoreline is evident by the green shading in the figure, indicating a wave height increase of between 0.4 and 0.6 meters along the shoreline. As mentioned, this significant increase in wave energy in the harbor and channel removed this alternative from further consideration following flushing simulations.

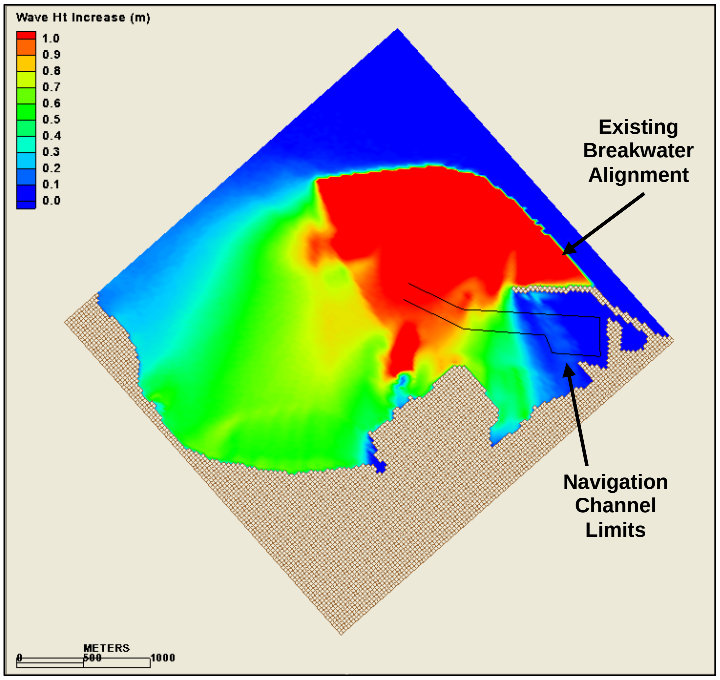

Figure 4-19a. Typical Wave Height Increase for Alternative 1

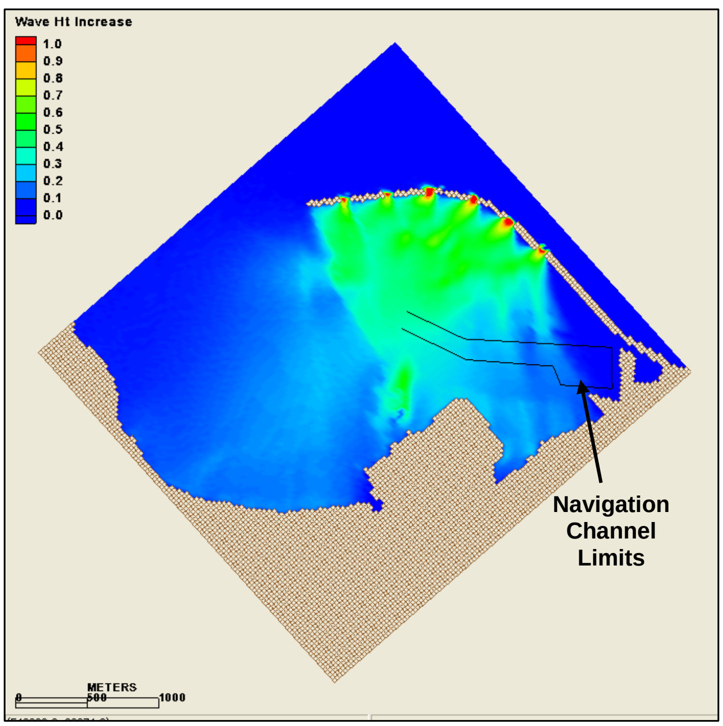

Figure 4-19b. Typical Wave Height Increase for Alternative 2

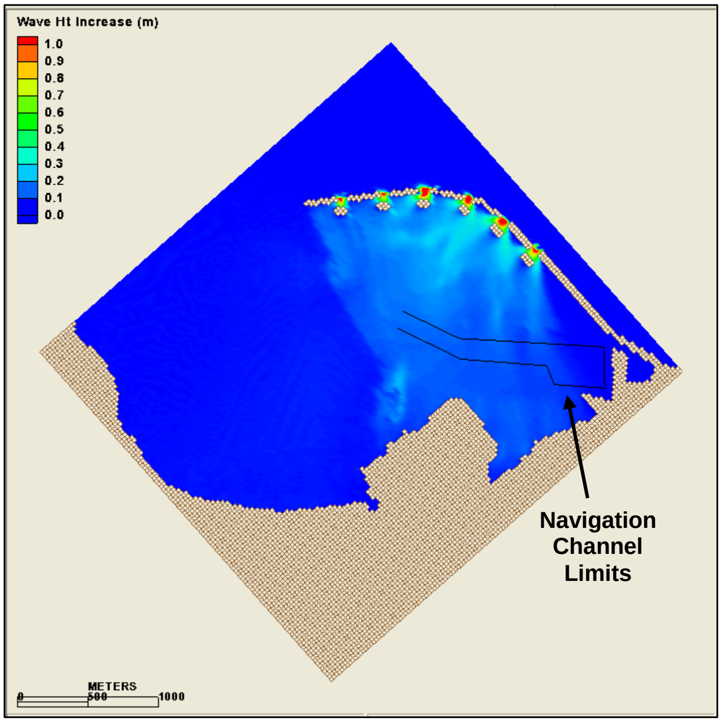

Figure 4-19c. Typical Wave Height Increase for Alternative 3

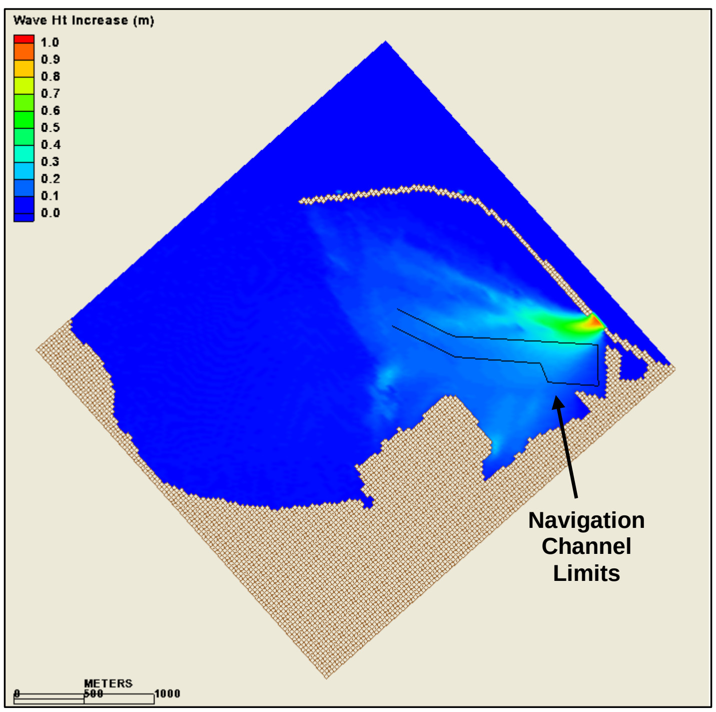

Figure 4-19d. Typical Wave Height Increase for Alternative 4

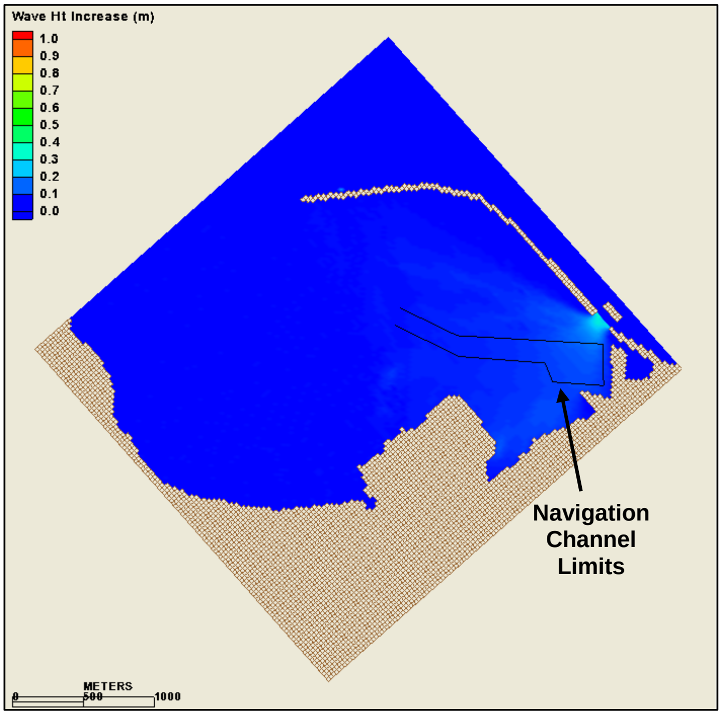

Figure 4-19e. Typical Wave Height Increase for Alternative 5

Alternative 2 (placing six gaps in the outer reach of the breakwater) also shows an increase in wave height within the harbor (Figure 4-19b). Wave height increase exceeds 1.0 meter within the gaps, which is not unexpected since there is no wave occurring here under existing conditions. The maximum increase in wave height in the harbor (not including area within the gaps) is 0.85 meters just inside the gaps, and the maximum increase in wave height within the navigation channel is 0.34 meters. Waves at the Hilo Bay shoreline are increased between 0 and 0.15 meters for this alternative. This alternative breakwater configuration also continues to provide sheltering at the interior of the harbor and navigation channel, with wave height differences in the range of 0.0 to 0.2 meters. This alternative was brought forward for further consideration of flushing characteristics and water quality improvement.

Alternative 3 shows a smaller increase in wave energy than Alternative 2 due to the additional interior detached breakwaters present (Figure 4-19c). Again, the largest overall increase in wave height is in the breakwater gaps, where no waves are transmitted under existing conditions. The greatest wave height increase in the harbor aside from this occurs between the gaps and the detached breakwaters at 0.6 to 0.85 meters. The maximum wave height increase within the navigation channel is 0.1

meters. Wave energy at the shoreline is not increased measurably for this alternative due to the added protection provided by the detached breakwaters. Wave energy at the interior of the channel and at the vessel piers is also virtually unchanged for this alternative. This alternative was brought forward for further consideration of flushing characteristics and water quality improvement.

Alternative 4 (single gap at breakwater root) shows a somewhat focused area with an increase in wave height in comparison with the existing breakwater configuration (Figure 4-19d). Wave height increases are limited to the interior of the breakwater, near the entrance to the small boat harbor. Again, the maximum wave height increase occurs in the gap; however, the area just interior of the gap shows the largest increase otherwise at 0.84 meters. The largest increase in wave height within the channel for this alternative is 0.3 meters at the location closest to the breakwater gap. Wave energy at the shoreline is not increased measurably for this alternative and increases in wave height at the vessel piers are less than 0.1 meter for this case. This alternative was brought forward for further consideration of flushing characteristics and water quality improvement.

Alternative 5 shows only a minimal amount of increase in wave energy within the harbor, due to the addition of an exterior detached breakwater (Figure 4-19e). The maximum increase in wave height within the harbor is directly interior of the gap and is approximately 0.26 meters. The largest increase in wave height within the channel is 0.11 meters at the location closest to the gap. Similar to Alternative 4, wave energy at the shoreline is not increased measurably for this alternative and increases in wave height at the vessel piers are less than 0.1 meter for this case. This alternative was brought forward for further consideration of flushing characteristics and water quality improvement.

Evaluation of the ADCIRC and CH3D-WES simulations for February – March 2007 was limited to a verification that water levels for both models compared well with tide gage data from NOAA tide station 1617760 at Hilo Harbor, as shown in Figure 4-20. Since these models were previously shown (during the validation stage) to provide a satisfactory representation of circulation within the harbor, the hydrodynamic data from CH3D-WES between February – March 2007 was passed to the water quality model as forcing data. The flushing studies conducted with CE-QUAL-ICM are a better indicator of the changes in circulation and flushing patterns due to each alternative breakwater configuration, and are detailed in Section 5.2.2 of this report.

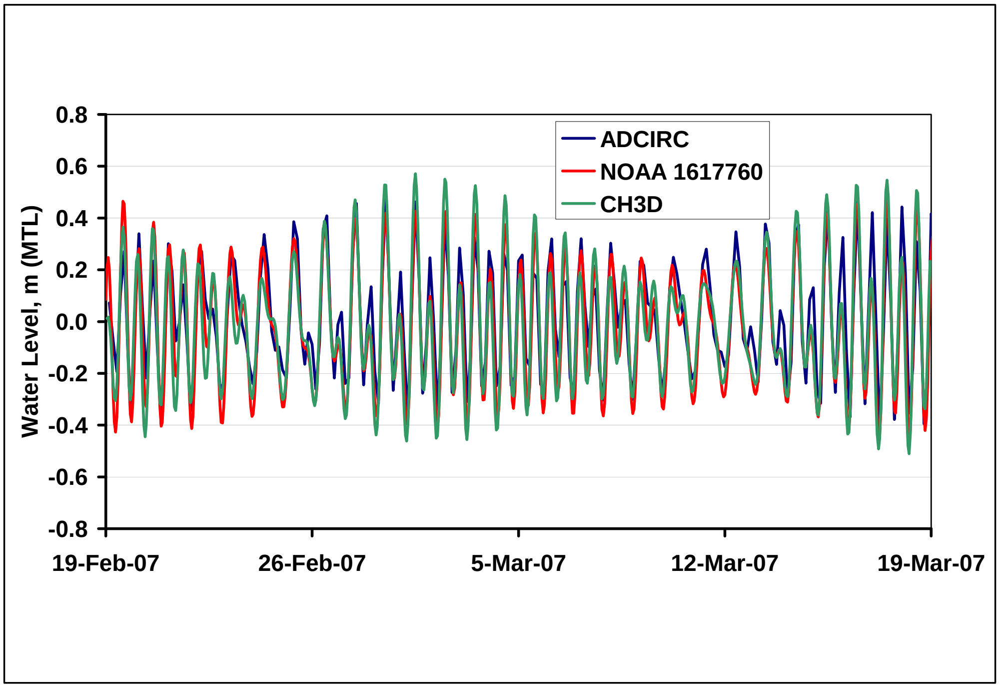

Figure 4-20. Water Level Validation for 19 February – 19 March 2007 Run Period

5. WATER QUALITY MODELING

5.1. Water Quality Model

5.1.1. Model Description

CE-QUAL-ICM (ICM) was designed to be a flexible, widely applicable, state-of-the-art eutrophication model. Initial application was to Chesapeake Bay (Cerco and Cole, 1994). Since the initial Chesapeake Bay study, the ICM model code has been generalized with minor corrections and model improvements. Subsequent additional applications of ICM included the Delaware Inland Bays (Cerco et al. 1994), Newark Bay (Cerco and Bunch, 1997), the San Juan Estuary (Bunch et al. 2000), Florida Bay (Cerco et al. 2000), St. Johns River (in preparation) and Port of Los Angeles (in preparation). Each model application employed a different combination of model features and required addition of system-specific capabilities.

General features of the model include:

a. Operational in one-, two-, or three-dimensional configurations
b. Twenty-two +state variables including physical properties.
c. Sediment-water oxygen and nutrient fluxes may be computed in a predictive sub-model or specified with observed sediment-oxygen demand rates (SOD)
d. State variables may be individually activated or deactivated.
e. Internal averaging of model output over arbitrary intervals.
f. Computation and reporting of concentrations, mass transport, kinetics transformations, and mass balances.
g. Debugging aids include ability to activate and deactivate model features, diagnostic output, volumetric and mass balances.
h. Operates on a variety of computer platforms. Coded in ANSI Standard FORTRAN F77.

ICM is limited by not computing the hydrodynamics of the modeled system. Hydrodynamic variables (i.e., flows, diffusion coefficients, and volumes) must be specified externally and read into the model. Hydrodynamics may be specified in binary or ASCII format and are usually obtained from a hydrodynamic model such as the CH3D_WES model (Johnson et al. 1991).

The foundation of CE-QUAL-ICM is the solution to the three-dimensional mass-conservation equation for a control volume. Control volumes correspond to cells on the model grid. CE-QUAL-ICM solves, for each volume and for each state variable, the equation:

Equation 5-1:

$$\frac{\delta V_j C_j}{\delta t} = \sum_{k=1}^{n} Q_k C_k + \sum_{k=1}^{n} A_k D_k \frac{\delta C}{\delta x_l} + \Sigma S_j$$

in which:

V_j = volume of j^{th} control volume (m^3)
C_j = concentration in j^{th} control volume ($g\ m^{-3}$)
t, x = temporal and spatial coordinates
n = number of flow faces attached to j^{th} control volume
Q_k = volumetric flow across flow face k of j^{th} control volume ($m^3\ s^{-1}$)
C_k = concentration in flow across face k ($g\ m^{-3}$)
A_k = area of flow face k (m^2)
D_k = diffusion coefficient at flow face k ($m^2\ s^{-1}$)
S_j = external loads and kinetic sources/sinks in j^{th} control volume ($g\ s^{-1}$)

Solution of Equation 5-1 on a digital computer requires discretization of the continuous derivatives and specification of parameter values. The equation is solved explicitly using upwind differencing or the QUICKEST algorithm (Leonard 1979) to represent C_k. The time step, determined by stability requirements, is usually five to fifteen minutes. For notational simplicity, the transport terms are dropped in the reporting of kinetics formulations.

Deleted: Equation 5-1

Deleted: Equation 5-1

Formatted: Font: 12 pt

Formatted: Font: 12 pt, Do not check spelling or grammar

Formatted: Font: 12 pt

Formatted: Font: 12 pt

Formatted: Font: 12 pt, Do not check spelling or grammar

Formatted: Font: 12 pt

CE-QUAL-ICM incorporates 22 state variables in the water column including physical variables, multiple algal groups, and multiple forms of carbon, nitrogen, phosphorus and silica (Table 5-1). Two zooplankton groups, microzooplankton and mesozooplankton, are available and can be activated when desired.

Table 5-1.Water Quality Model State Variables

Temperature	Salinity
Fixed Solids	Cyanobacteria
Diatoms	Other Phytoplankton
Dissolved Organic Carbon	Refractory Particulate Organic Carbon
Labile Particulate Organic Carbon	Nitrate + Nitrite Nitrogen
Ammonium	Dissolved Organic Nitrogen
Refractory Particulate Organic Nitrogen	Labile Particulate Organic Nitrogen
Total Phosphate	Dissolved Organic Phosphorus
Refractory Particulate Organic Phosphorus	Labile Particulate Organic Phosphorus
Chemical Oxygen Demand	Dissolved Oxygen
Dissolved Silica	Particulate Biogenic Silica

5.1.2. Model Setup

Modifications to the circulation pattern in Hilo Harbor have the potential to impact water quality conditions in the harbor. The various proposed breakwater alternatives will each result in a unique circulation pattern which may redistribute materials in the harbor. Only by using a water quality model can the impacts from the different configurations be compared with each other on an equal basis.

The first step in applying a water quality model is to define the problem and the level of modeling required to address that problem. A model such as ICM can be applied with varying levels of sophistication. The complexity of the water quality model application depends upon a number of features including the nature of the water quality problem to be investigated, data availability, and funding. Below are some possible types of water quality modeling efforts that can be applied for a study.

1. Eutrophication – Involves the modeling of dissolved oxygen, algae, nutrients, and carbon. Realistic loads (observed or estimated) are required for all major discharges in the system. In addition, information on constituent concentrations is required for development of boundary conditions and for calibration. Sediment processes could either be specified or simulated with a sediment diagenesis model. This is the most involved approach in time and money and would provide the most defensible results provided there is an adequate database for model development.

2. DO/BOD/SOD – This approach is similar to number 1 except that all oxygen demand is specified as a Biochemical Oxygen Demand (BOD). Sediment Oxygen Demand (SOD) is specified as a constant rate and together with BOD are the only sinks for DO. Information is required on DO and BOD levels throughout the system for cursory model calibration. Information (observed or estimated) is required for all significant discharges. While less involved than level 1, this approach still requires some calibration

3. DO/OD/SOD No calibration – This approach is similar to the second approach but with more simplified processes. Rather than BOD, a zero-order, background oxygen demand (OD) in units of mg/L/day is used. No loads are input. Boundary concentrations are held constant. OD and SOD are sinks for DO. No reaeration is allowed. The value for background OD is assumed. No model calibration is required. Dissolved oxygen is essentially modeled as a non-conservative tracer. Relative changes in DO can be determined by comparing results from a base condition simulation (present conditions) to a simulation made with a proposed island. The driving mechanism in this approach is that localized

circulation changes result in differences in residence time which impact dissolved oxygen.

4. Residence Time - This approach does not provide a measure of dissolved oxygen but a measure of the impact that circulation changes have on the time that water stays in a certain area. Assuming that oxygen demands are the same throughout the system, an increase in residence time would indicate a decrease in flushing and a decrease in DO.

There are advantages and disadvantages to the different approaches listed above. The more comprehensive efforts require the most data and time. Less rigorous approaches require less time and a more modest amount of data. They rely more on inferences and assumptions and are better suited for screening studies.

Since the focus of the current study is an investigation of possible changes to circulation for the purpose of improving in-harbor water quality a limited suite of constituents was applied. The constituents modeled are listed in Table 5-2.

Table 5-2. Hilo State variables

Temperature	Particulate Organic Carbon
Salinity	Ammonia
Dissolved Oxygen	Nitrate
Dissolved Organic Carbon	Phosphate

These constituents are adequate to capture changes in the water quality conditions in the Hilo harbor system as a result of any breakwater modification.

The computational grids used for the Hilo Harbor water quality modeling effort are the same as those used in the CH3D-WES modeling effort, Figures 4-6 and 4-7. The ICM and CH3D-WES grids are identical except that one row of cells is deleted in the water quality grid along the outer (ocean) boundary of the hydrodynamic model grid. These cells are removed from the water quality grid due to differences between the way ICM and CH3D-WES handle flows at ocean boundaries. CH3D-WES specifies a water surface elevation or head condition at the ocean boundary while CEQUAL-ICM requires a flow for the face along the boundary. Removing cells along the ocean boundary has no impact upon water quality computations on the interior of the grid. Grid information is contained in Table 5-3 for base and the five alternative cases.

Table 5-3. CEQUAL-ICM Grid Characteristics			
Alternative	**Description**	**# Cells**	**#Flow Faces**
0	Existing (Base)	16110	31870
1	Shortened Breakwater	16042	31786
2	Multiple Gaps on Breakwater	16146	31948
3	Multiple Gaps on Breakwater with Harborside Detached Breakwaters	16112	31851
4	Single Nearshore Gap on Breakwater near shore	16124	31903
5	Single Nearshore Gap on Breakwater with Oceanward Detached Breakwaters	16106	31856

5.2. Modeling Simulation of February – March 2007

5.2.1. Forcing Data

A certain amount of information is required to “drive” CEQUAL-ICM. This information defines the conditions that exist initially throughout the system, the conditions at the boundaries from which inflow/outflow rates and conditions are obtained, and meteorological data which impacts the heat exchange and temperature in the system. This in turn impacts the rates at which chemical and biological processes occur. The following information is required for an application of CEQUAL-ICM:

Meteorological data for Lyman Field Hilo, HI (Meteorological station 912850) was obtained for the period of 01 Jan 2007 through 15 Oct 2007. This data was processed and daily equilibrium temperatures and heat exchange coefficients generated for the desired periods (Eiker 1977).

Bathymetry and flow information are all obtained directly from CH3D. The ICM grid captures its physical properties from the CH3D-WES grid. Cell volumes, surface areas, and depths in ICM are the same as used in CH3D. Flow information is averaged in CH3D-WES and output for every flow face. Procedures and techniques are used so that the flow fields generated by CH3D-WES are the same flow fields used in ICM to transport water quality constituents.

A clear distinction needs to be made between initial and boundary conditions and comparison data. Comparison data have no effect on model performance - they are used only to assess model performance. Initial and boundary conditions are of greater importance because they directly affect model performance.

Constituent boundary condition information was obtained from data collected in support of this study by the University of Hawaii at Hilo, (Wiegner and Mead, 2009). This information consisted of temperatures and concentrations of the constituents modeled. The Hilo water quality model had four boundaries; Wailuku River, Wailoa River, Reed's Bay, and open ocean boundary. Data from Wiegner and Mead (2009) station S1 was used for the boundaries of the Wailuku River and S4 for the Wailoa River. Information from S4 was also used for the boundary conditions in the Reed's Bay inflow. Data from stations C1 and C2, located outside of the breakwater were used for conditions at the ocean boundary.

5.2.2. Flushing Studies

The purpose of this study was to determine to what degree flushing inside Hilo harbor would be impacted by changes in the breakwater configuration. Therefore, a primary focus of the water quality modeling was to simulate conditions that would exist for these configurations and compare them against conditions for the existing configuration. A powerful way to do this is via the use of tracer flushing simulations. In these cases, a conservative, i.e., non-reacting substance is introduced into the system and its concentration is monitored with time. Since the substance is conservative, any change in concentration is the result of the movement and dilution of that substance. There is no decay, uptake, or creation. The only manner via which the tracer can leave the model domain is to be transported out a boundary.

A benefit of using a tracer to investigate flushing versus traditional water quality constituents is that the modeler defines the location and magnitude of the tracer. Tracers can be applied initially over select portions of a system or discharged continuously with a tributary or outfall. When conventional water quality constituents are used, there may or may not be enough gradient in the values to definitively determine the change in flushing.

Several different types of tracer flushing tests were investigated. In different tests, tracers were loaded at the headwaters of the Wailuku and Wailoa Rivers, the ocean boundary, and selected locations in the interior of the system. The tracer test that was most illuminating from a flushing point of view was the one where all cells inside the breakwater had initial tracer concentrations of 10 mg/l. All cells outside the breakwater had initial concentrations of 0 mg/l and as did all boundary flows. This test was repeated for all scenarios under consideration.

Shown in Figure 5-1 are eighteen locations inside and outside of Hilo Harbor where tracer concentrations were monitored. Stations S2, S3, S5, S6, C1, and C2 correspond to stations sampled by Wiegner and Mead. Stations A1 through A12 were selected in order to get insight on conditions at locations in the system that had not been sampled.

Flushing tests were run using hydrodynamics information from February and March 2007. This is the same period used for the water quality calibration. As shown in Figures 5-2 through 5-19, all breakwater configurations tested resulted in improved flushing, i.e., decreased tracer concentrations, at all locations monitored. This behavior was definitively observed in plan view images of concentration contours, Figure 5-20 through 5-24.

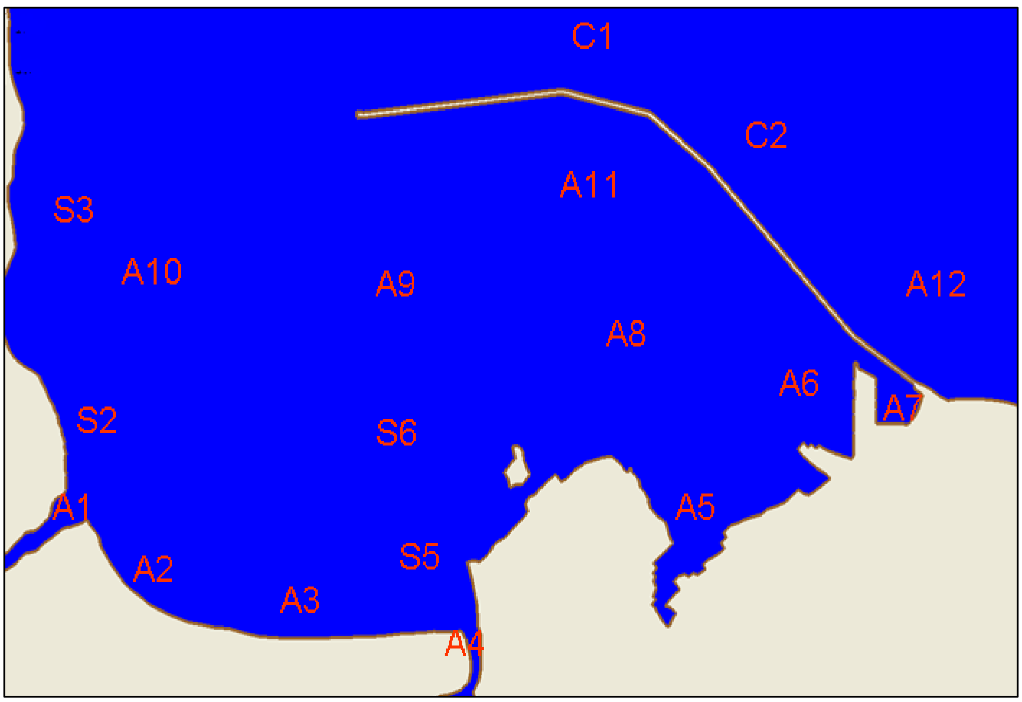

Figure 5-1. Hilo Bay time series comparison

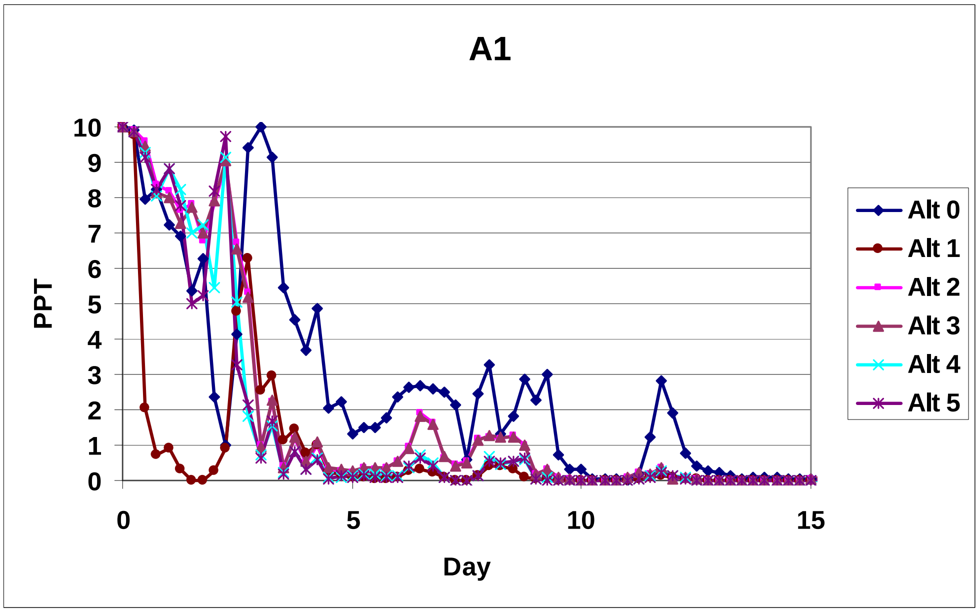

Figure 5-2. Tracer concentrations harbor flushing test at station A1

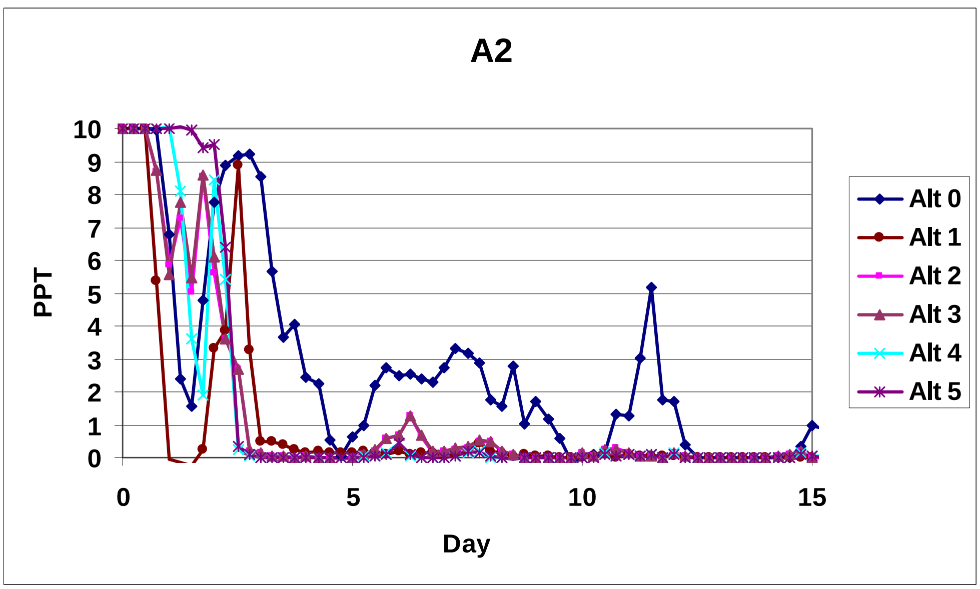

Figure 5-3. Tracer concentrations harbor flushing test at station A2

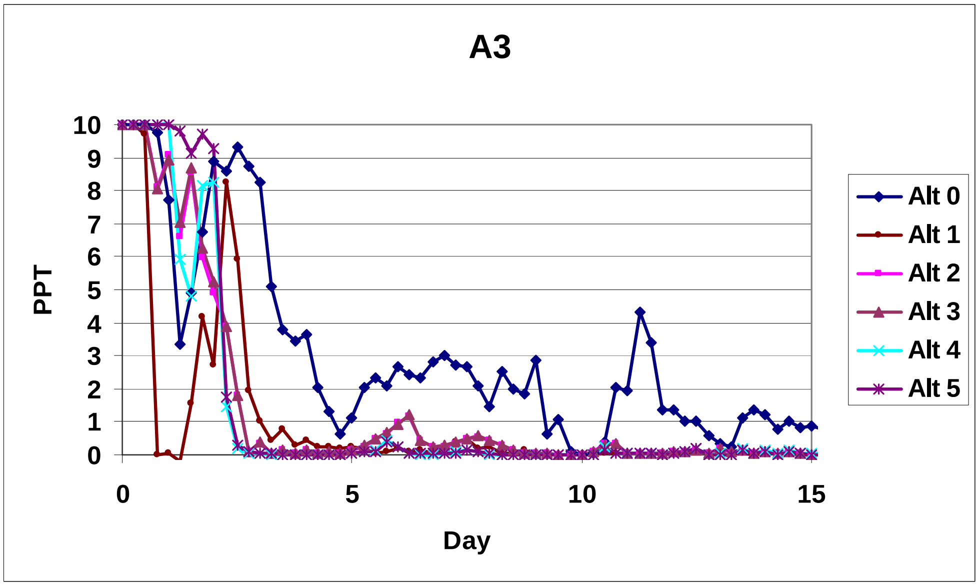

Figure 5-4. Tracer concentrations harbor flushing test at station A3

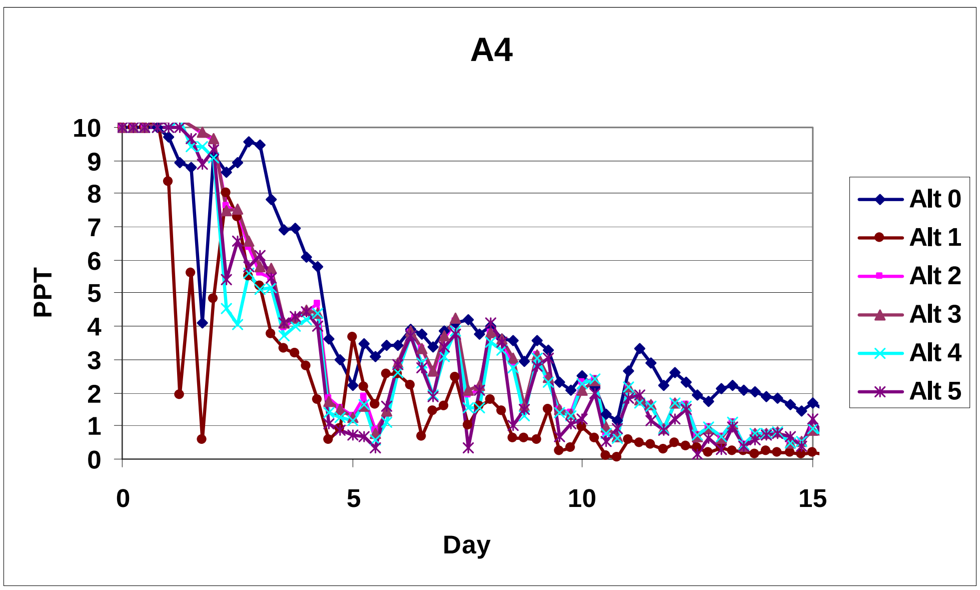

Figure 5-5. Tracer concentrations harbor flushing test at station A4

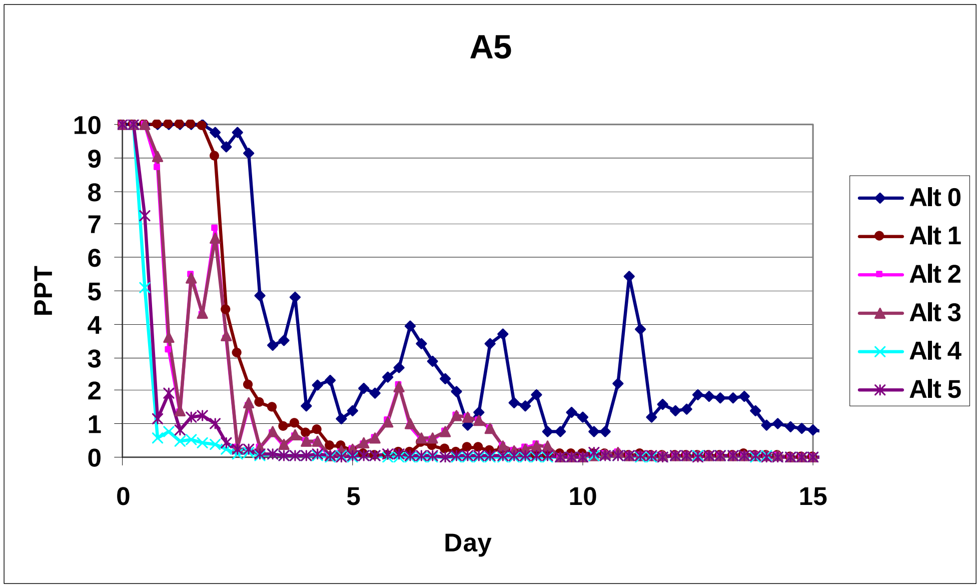

Figure 5-6. Tracer concentrations harbor flushing test at station A5

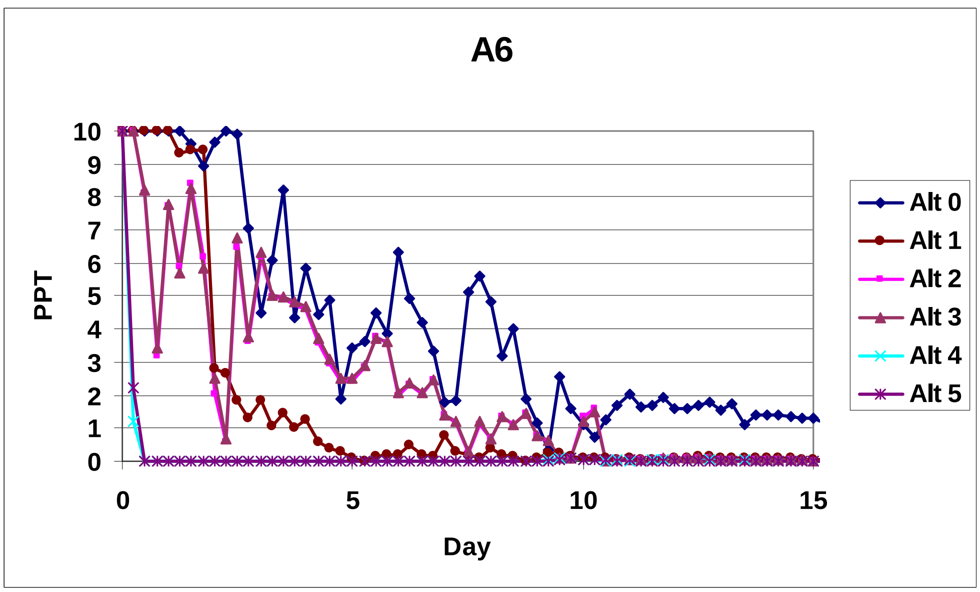

Figure 5-7. Tracer concentrations harbor flushing test at station A6

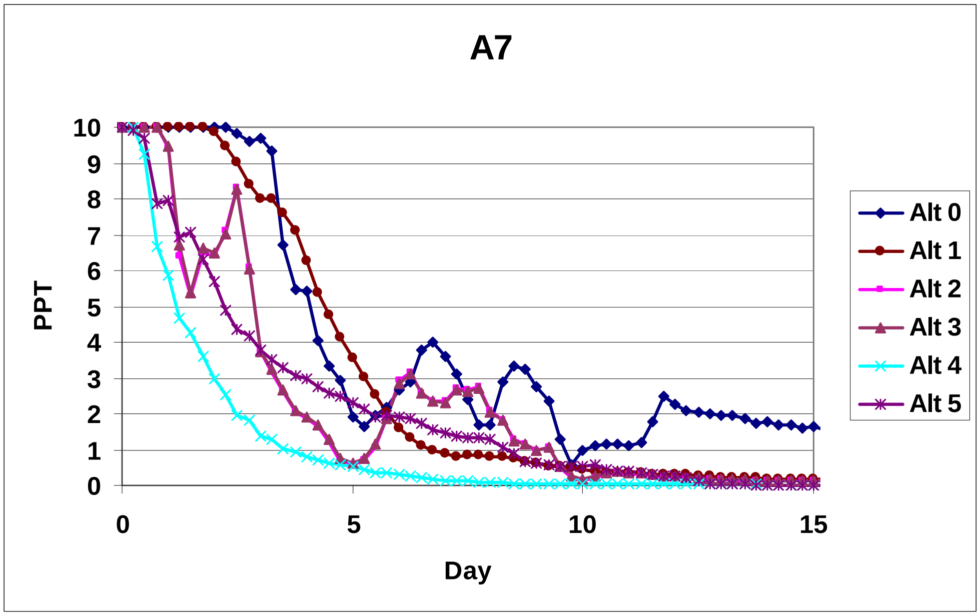

Figure 5-8. Tracer concentrations harbor flushing test at station A7

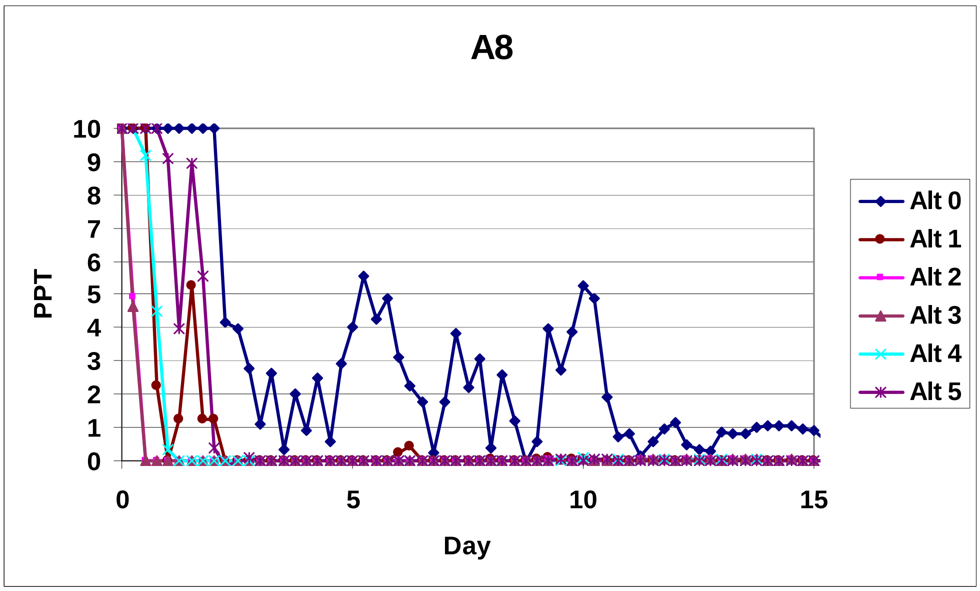

Figure 5-9. Tracer concentrations harbor flushing test at station A8

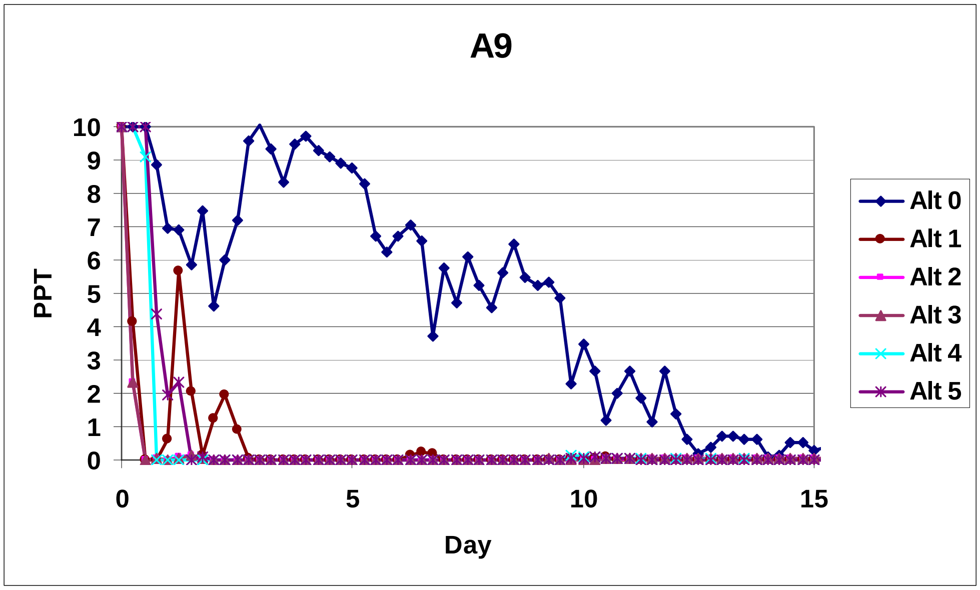

Figure 5-10. Tracer concentrations harbor flushing test at station A9

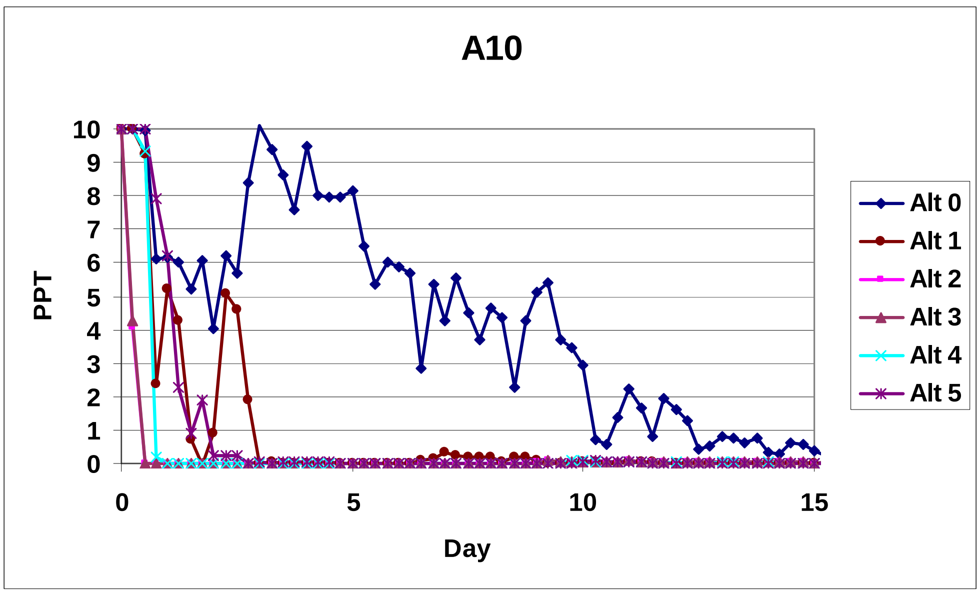

Figure 5-11. Tracer concentrations harbor flushing test at station A10

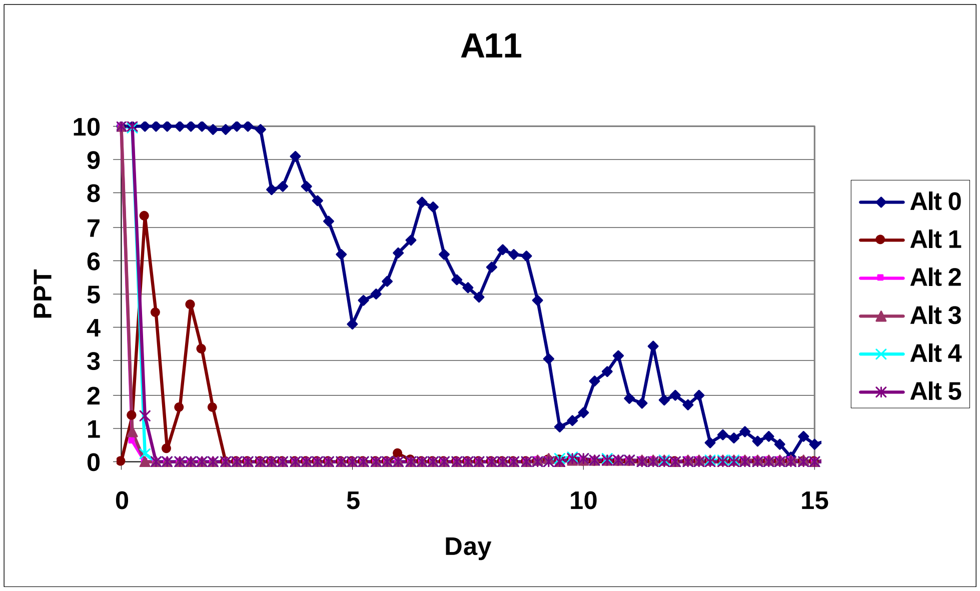

Figure 5-12. Tracer concentrations harbor flushing test at station A11

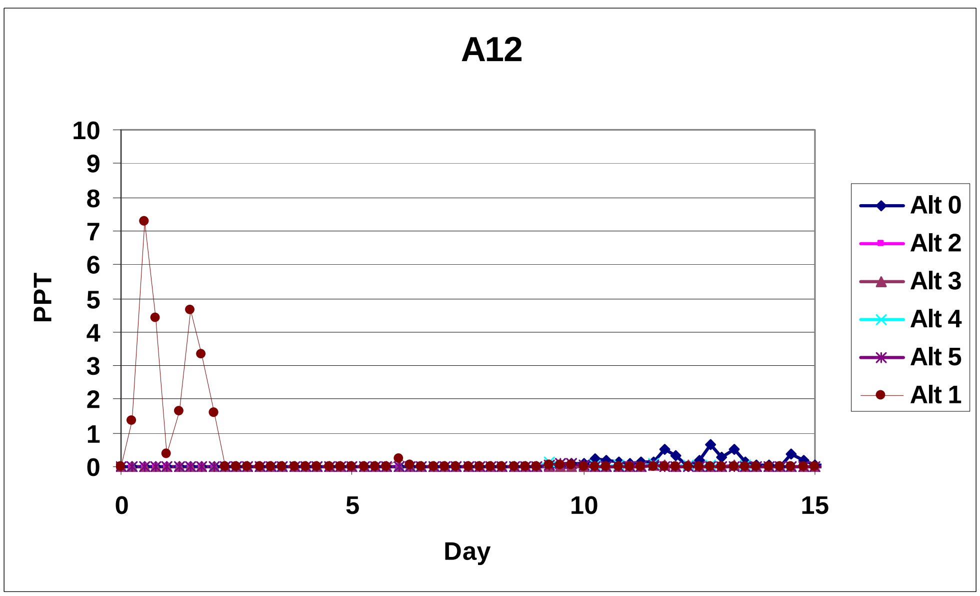

Figure 5-13. Tracer concentrations harbor flushing test at station A12

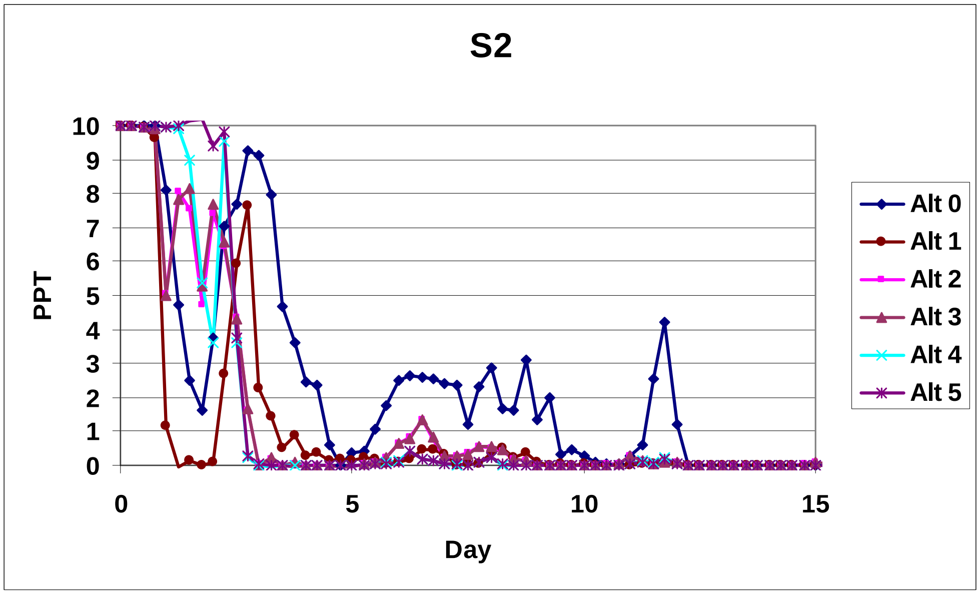

Figure 5-14. Tracer concentrations harbor flushing test at station S2

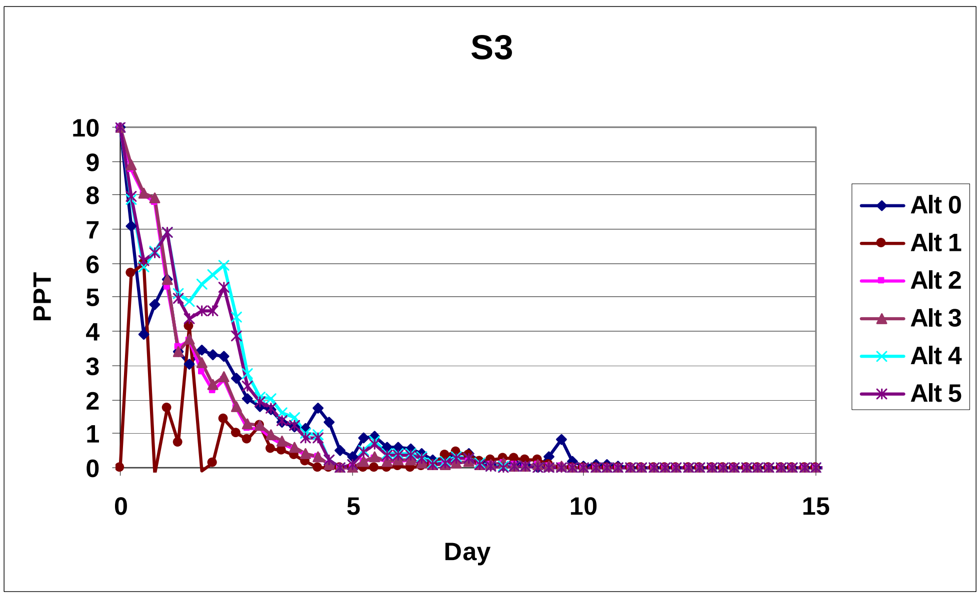

Figure 5-15. Tracer concentrations harbor flushing test at station S3

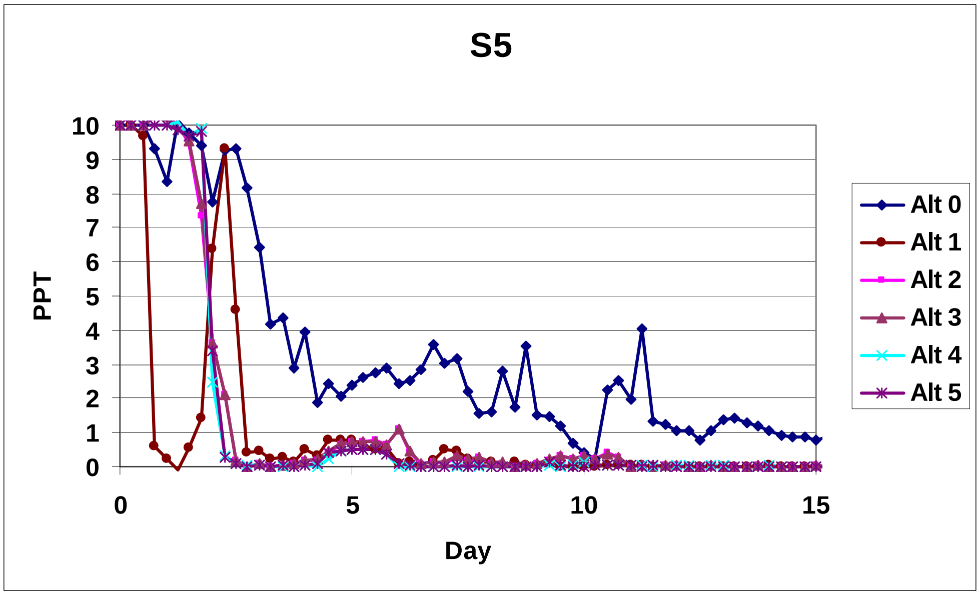

Figure 5-16. Tracer concentrations harbor flushing test at station S5

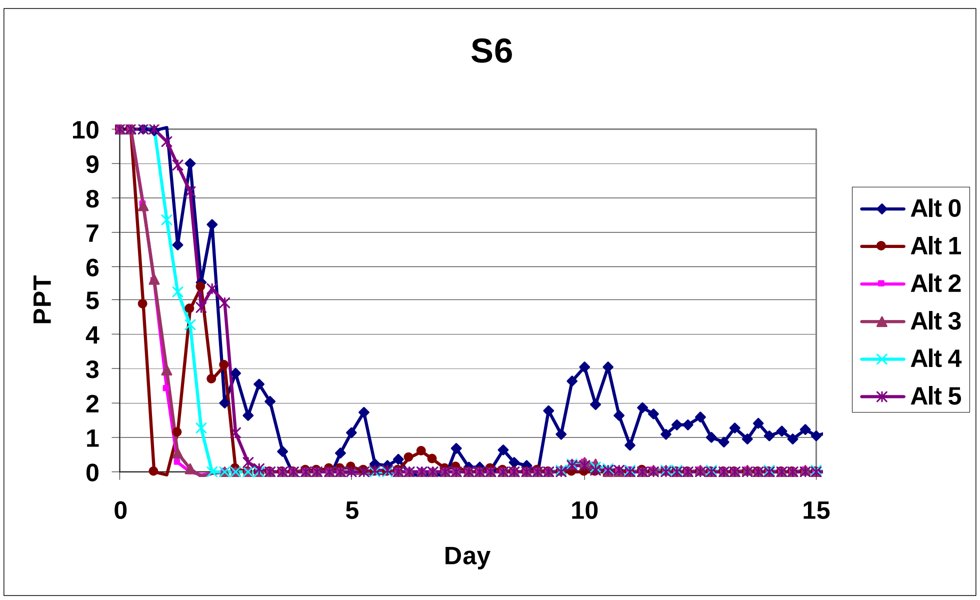

Figure 5-17. Tracer concentrations harbor flushing test at station S6

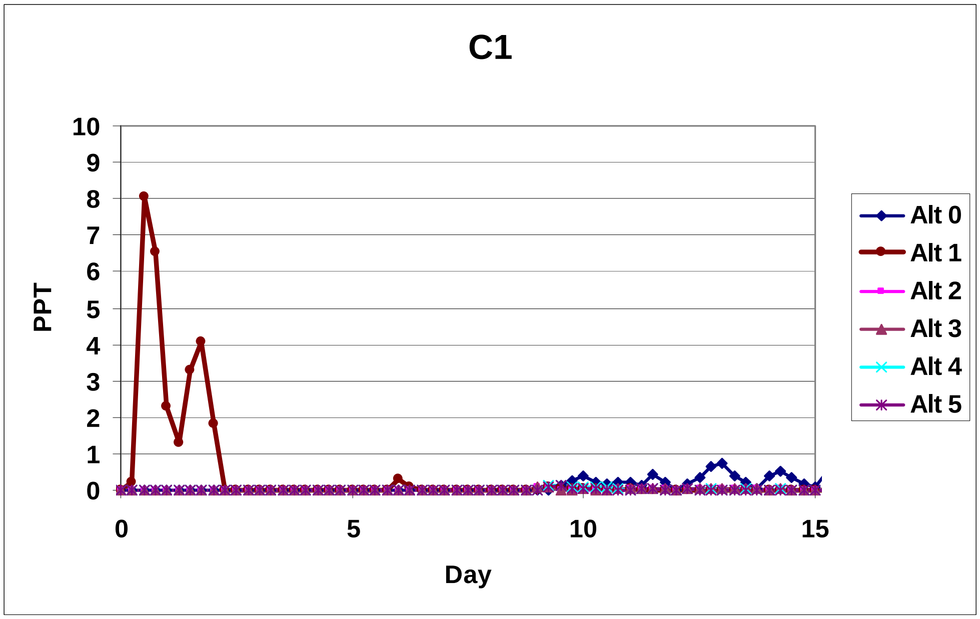

Figure 5-18. Tracer concentrations harbor flushing test at station C1

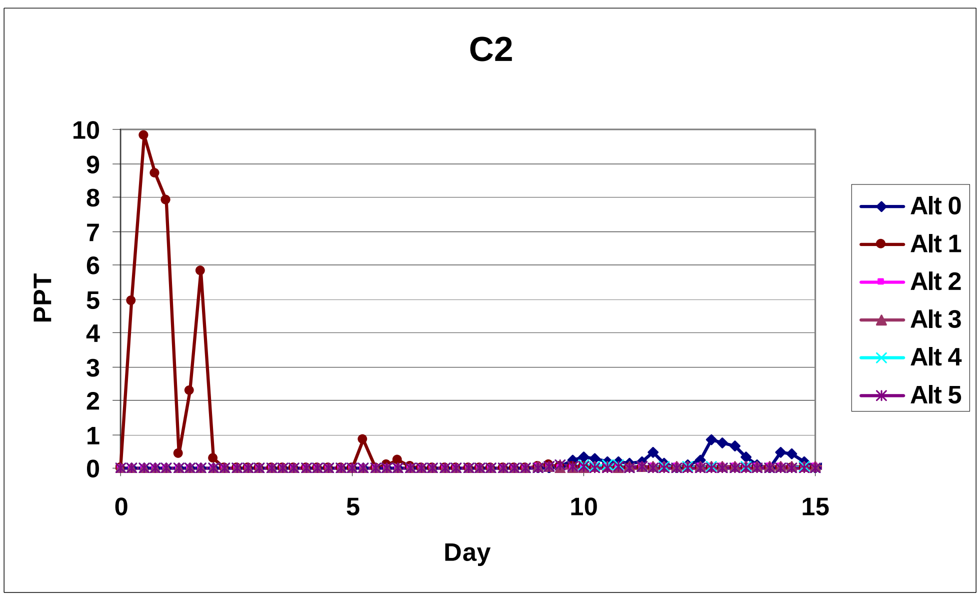

Figure 5-19. Tracer concentrations harbor flushing test at station C2

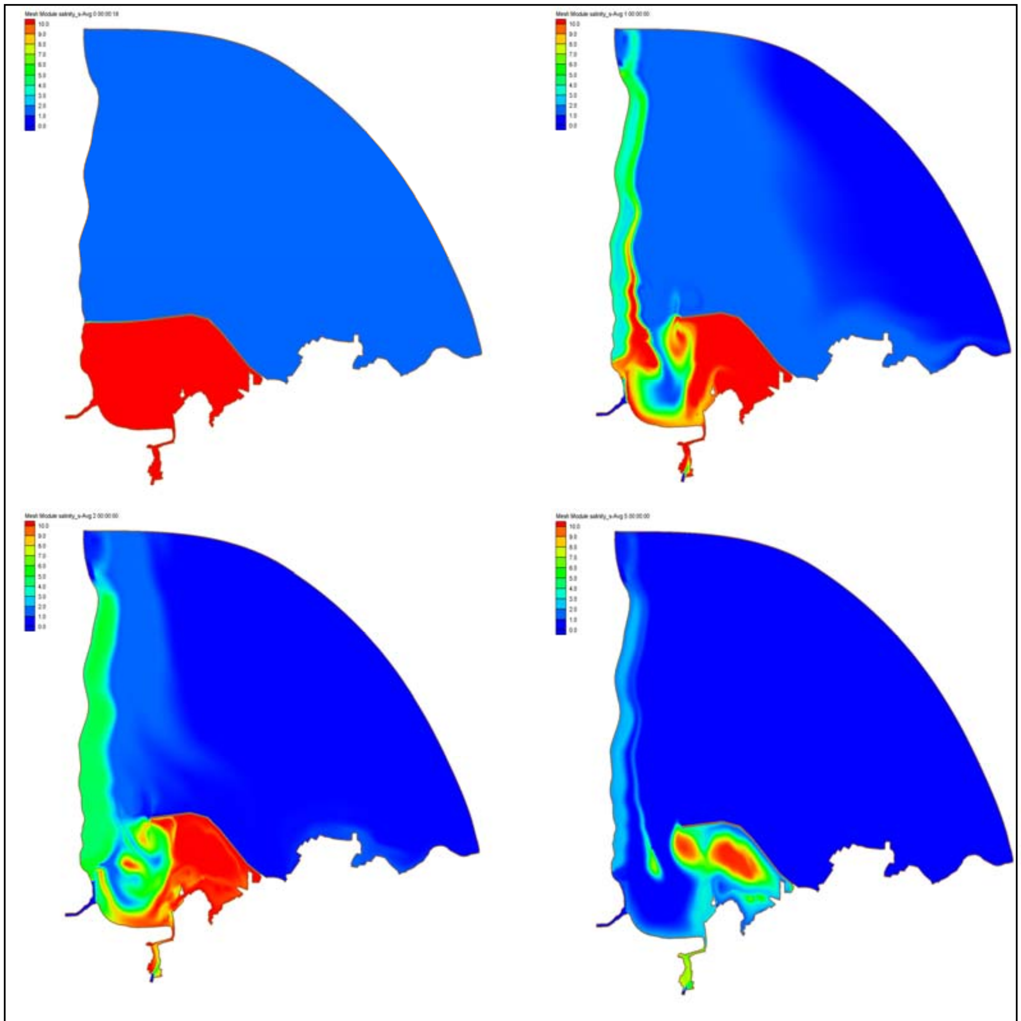

Figure 5-20. Tracer concentrations in flushing test Alt. 0 (base case) for (left to right from upper left) days 0, 1, 2, and 5.

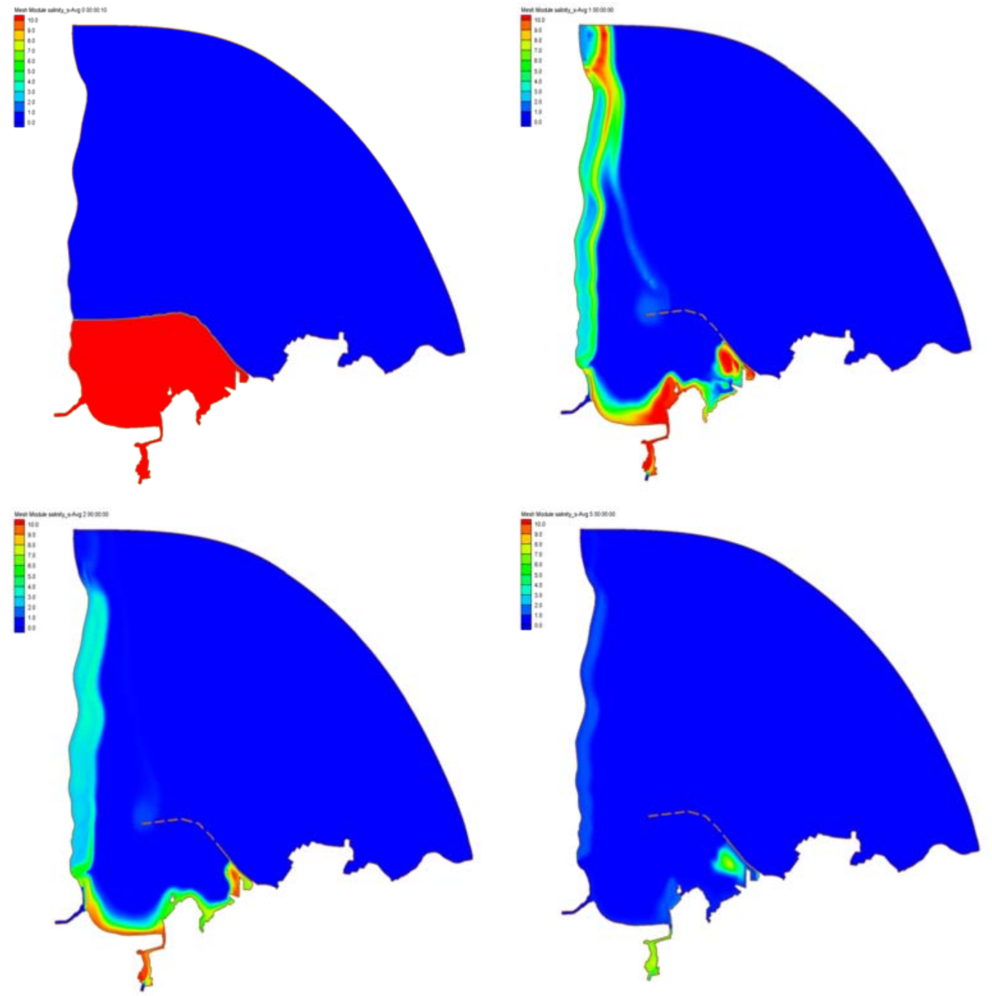

Figure 5-21. Tracer concentrations in flushing test Alt. 2 (multiple gaps in outer breakwater) for (left to right from upper left) days 0, 1, 2, and 5

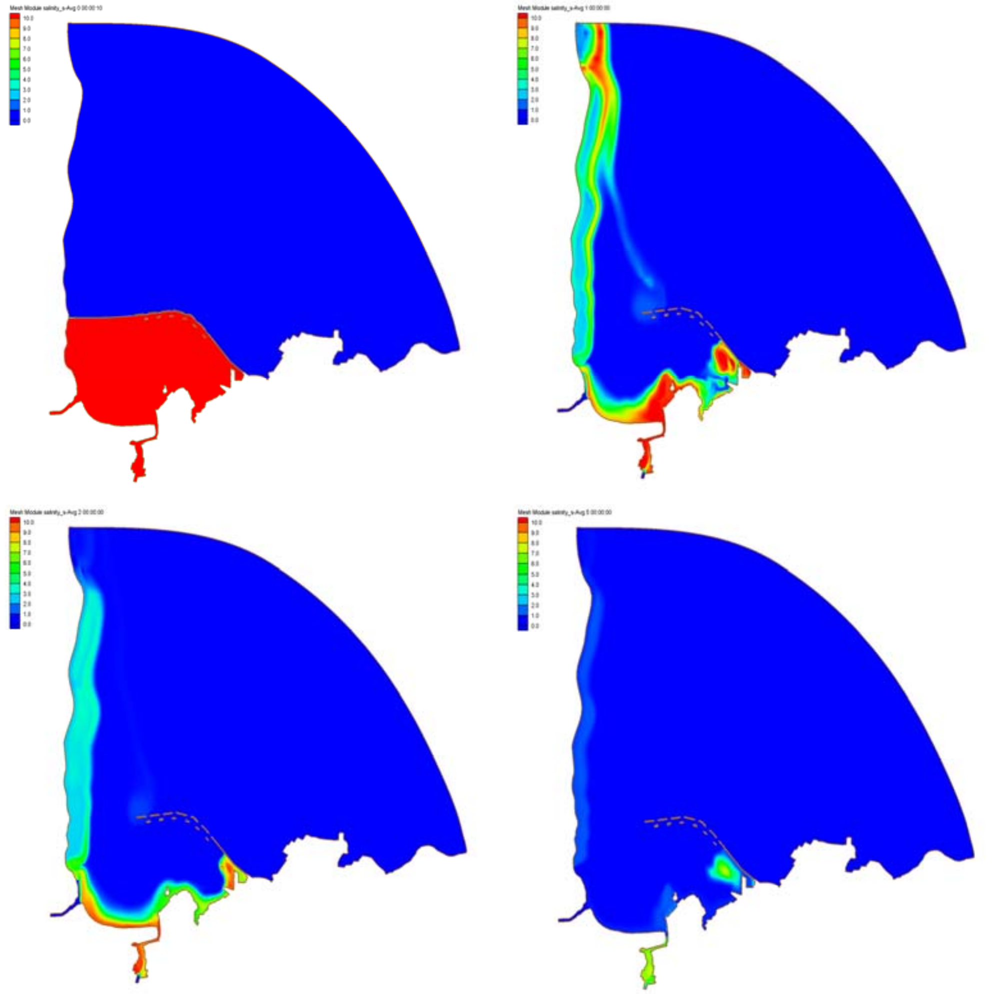

Figure 5-22. Tracer concentrations in flushing test Alt. 3 (multiple gaps in outer breakwater with interior groins) for (left to right from upper left) days 0, 1, 2, and 5

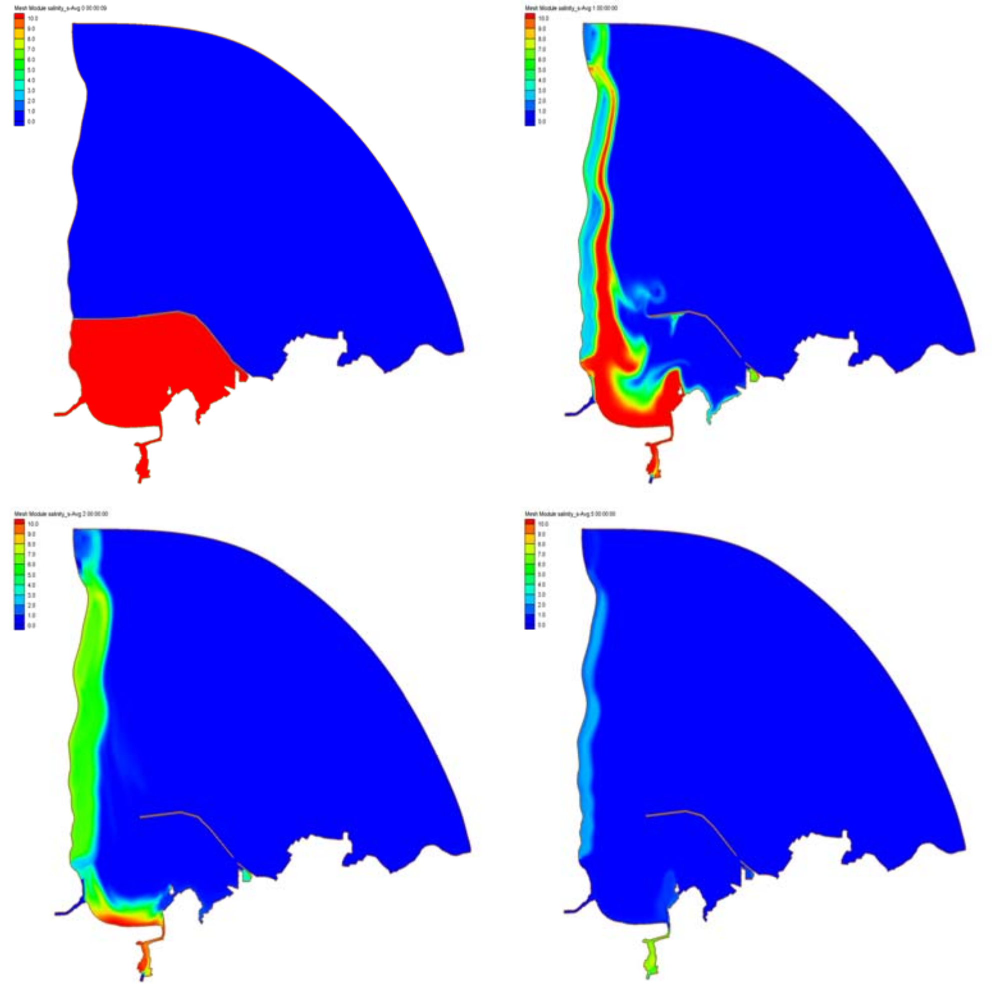

Figure 5-23. Tracer concentrations in flushing test Alt. 4 (single gap in breakwater) for (left to right from upper left) days 0, 1, 2, and 5

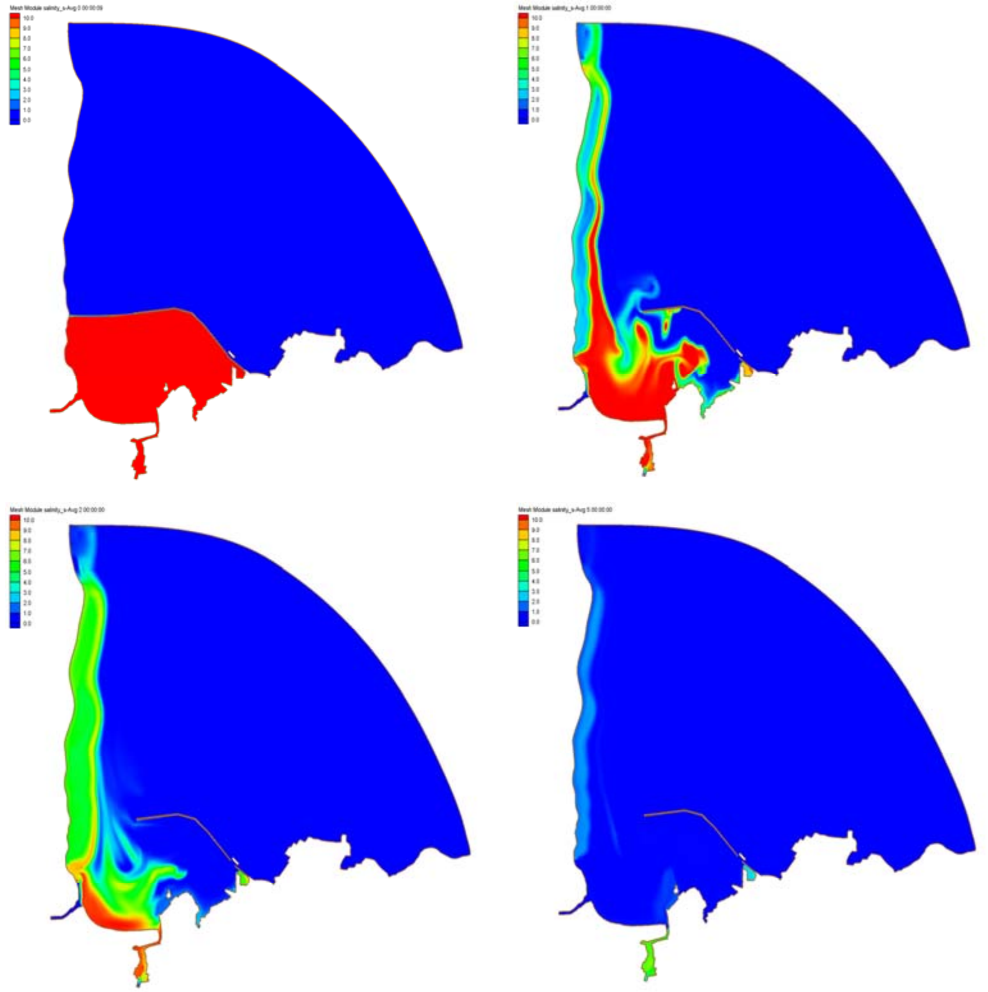

Figure 5-24. Tracer concentrations in flushing test Alt. 5 (single gap in breakwater with external groin) for (left to right from upper left) days 0, 1, 2, and 5

Further indication of the impact that the different alternatives have on circulation is shown in Table 5-4. Figures 5-25 through 5-29 illustrate the flows at the harbor entrance. By definition, positive flows are out of the harbor, negative are into the harbor. As indicated for the exiting case, Alternative 0, there is little net flow out of the harbor mouth.

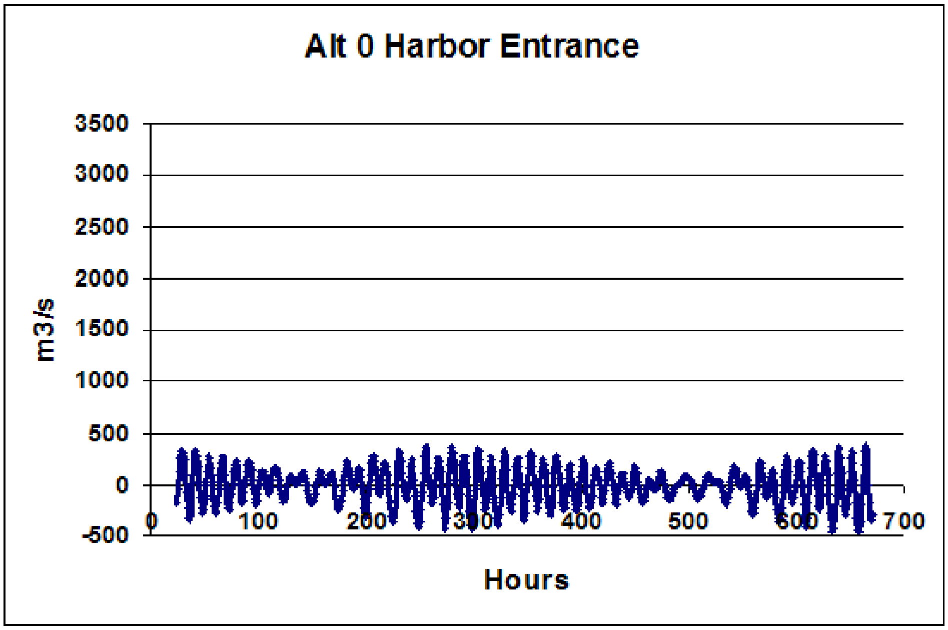

Figure 5-25. Harbor mouth flow rate during water quality modeling period for Alt. 0.

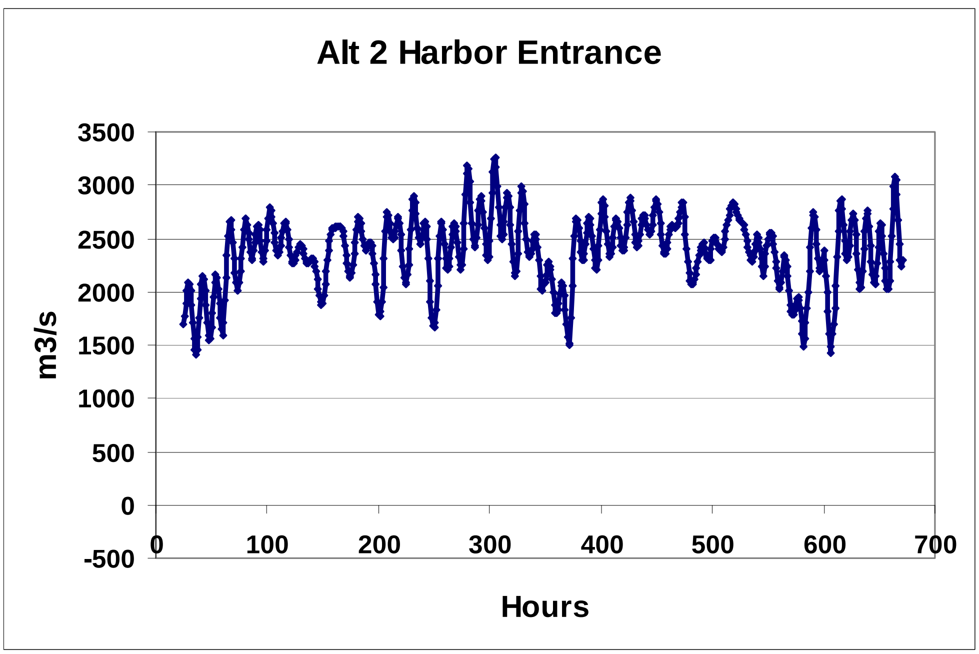

Figure 5-26. Harbor mouth flow rate during water quality modeling period for Alt 2

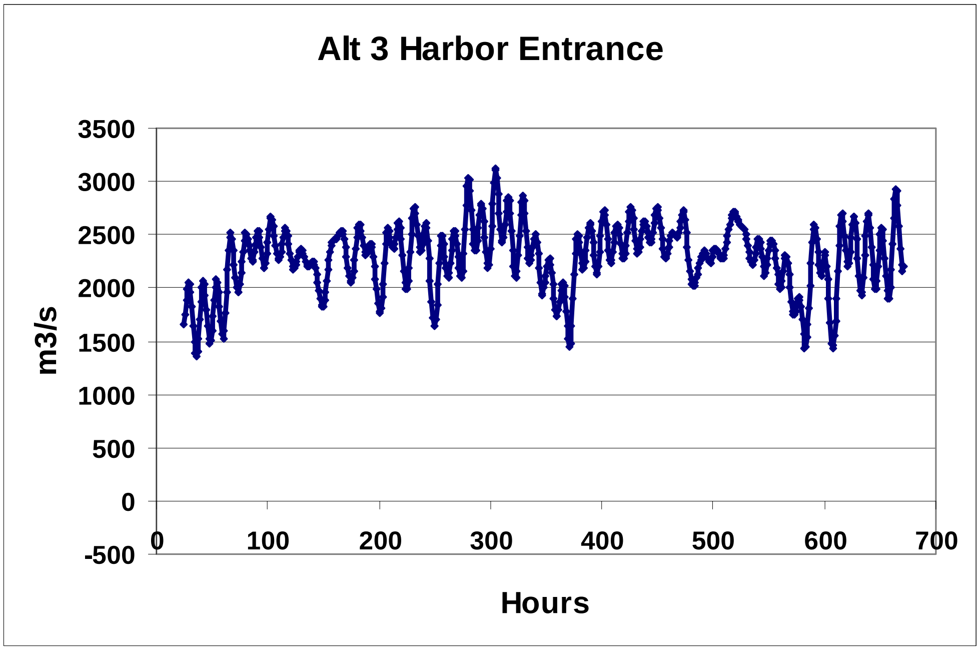

Figure 5-27. Harbor mouth flow rate during water quality modeling period for Alt. 3

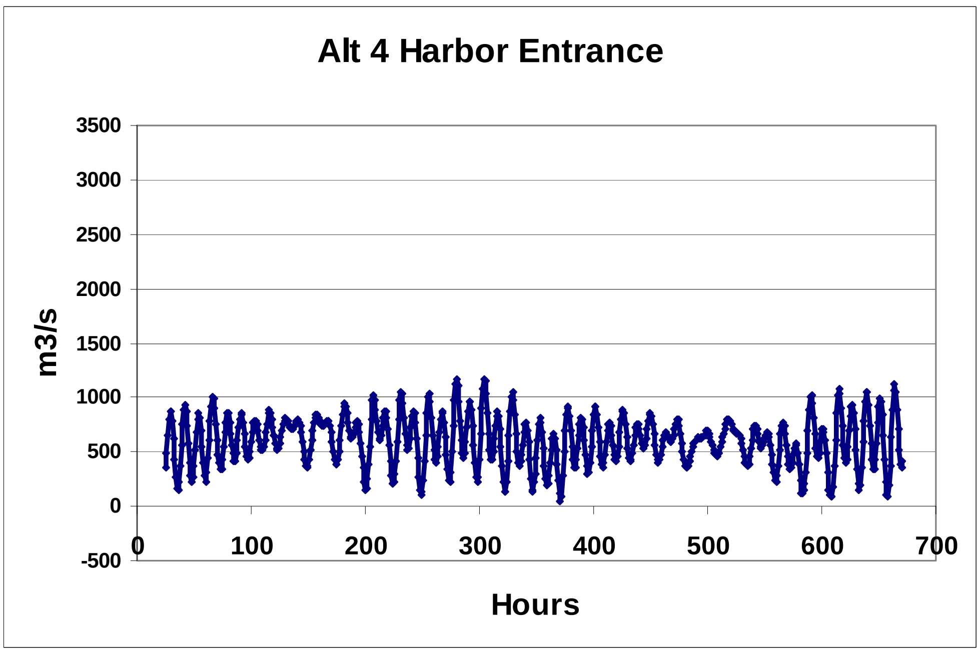

Figure 5-28. Harbor mouth flow rate during water quality modeling period for Alt. 4

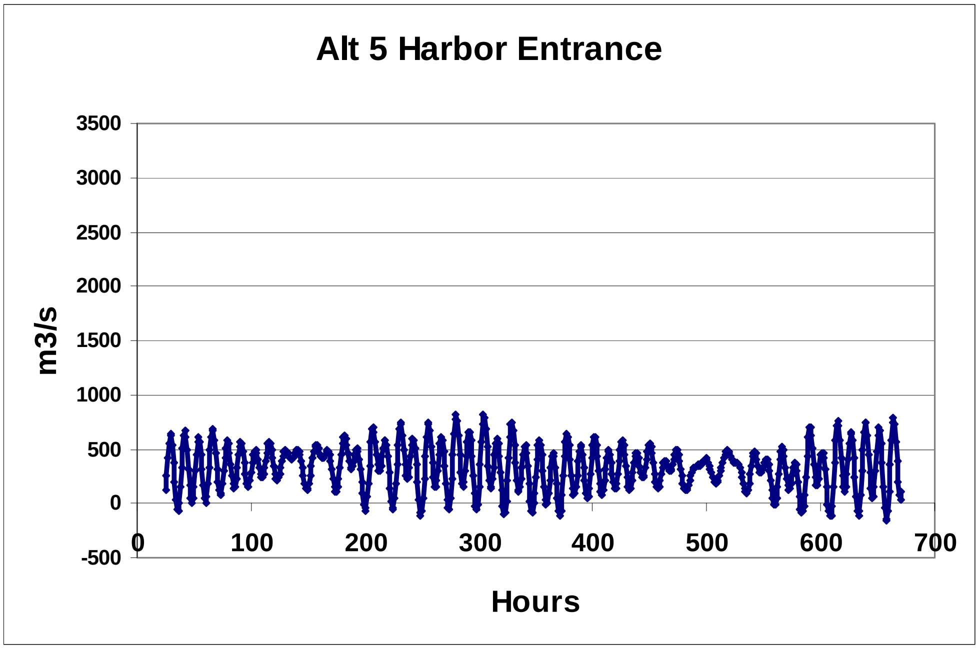

Figure 5-29. Harbor mouth flow rate during water quality modeling period for Alt. 5.

This is understandable as the only difference between the inflow and outflow at the mouth are the freshwater flows from the streams emptying in the harbor. The negative value for Alternative 0 is attributed to the beginning and ending of the simulation not corresponding to the same time in the tidal cycle. When these results are compared against the alternatives with breakwater openings, there is a net outflow at the harbor mouth. This outflow is generated by water entering the harbor through the causeway gaps. As a result there is a rapid net transport of material out of the harbor in comparison to the existing conditions where material is led much longer.

Table 5-4. Net flows at Hilo Harbor Mouth

Alternative	**Description**	**Net Flow M^3/s**
0	Existing (Base)	-6.9
2	Multiple Gaps on Breakwater	2380.3
3	Multiple Gaps on Breakwater with interior groins	2291.8
4	Single Nearshore Gap on Breakwater	606.0
5	Single Nearshore Gap on Breakwater with exterior groin	332.3

5.2.3. Validation to UH Water Quality Data

Prior to application to Hilo Harbor for water quality simulations, CEQUAL-ICM was calibrated using observed data collected by the University of Hawaii at Hilo (Wiegner and Mead 2007). The same period was used for calibration as was used for the subsequent alternative evaluation scenarios. The University of Hawaii at Hilo data was used to generate boundary conditions for the Wailuku and Wailoa Rivers and the ocean Boundary. Boundary condition information is shown in Table 5-5.

Table 5-5.Water Quality Boundary Conditions

Constituent	Ocean	Wailuku	Wailoa
Temperature (C)	23	23	23
Salinity (ppt)	35	0	0
Dissolved Oxygen (mg/l)	6.0	5.0	5.0
Suspended Solids (mg/l)	14.3	20	21
DOC (mg/l)	1.0	1.0	0.3
POC (mg/l)	0.1	0.2	0.2
Ammonia (mg/l)	0.002	0.01	0.003
Nitrate (mg/l)	0.02	0.05	0.3
Dissolved Inorganic Phosphorus (mg/l)	0.001	0.001	0.001

Model output was compared against observed data collected at stations in the harbor and outside of the breakwater, Figures 5-30 to 5-38. In some cases these data were profile samples. In these cases, all data for that day regardless of depth were plotted on the graph.

Overall the model appears to do a good job of representing general trend in dissolved oxygen, temperature, and salinity during the period it was applied, Figures 5-30 through 5-32. Model structural ability, i.e., two-dimension, depth average, limits the model's ability to capture three dimensional effects evident in some of the data. For example, ICM in 2-D mode is unable to capture the variation of dissolved oxygen and salinity with depth in Hilo Harbor. In the case of dissolved oxygen, the observed variation with depth is likely the combined result of the processes of reaeration and sediment oxygen demand and physical stratification. When the system is modeled as depth average, the effects of stratification are not included. With that said, the model does do a good job of capturing the trends of the dissolved oxygen observations in the system.

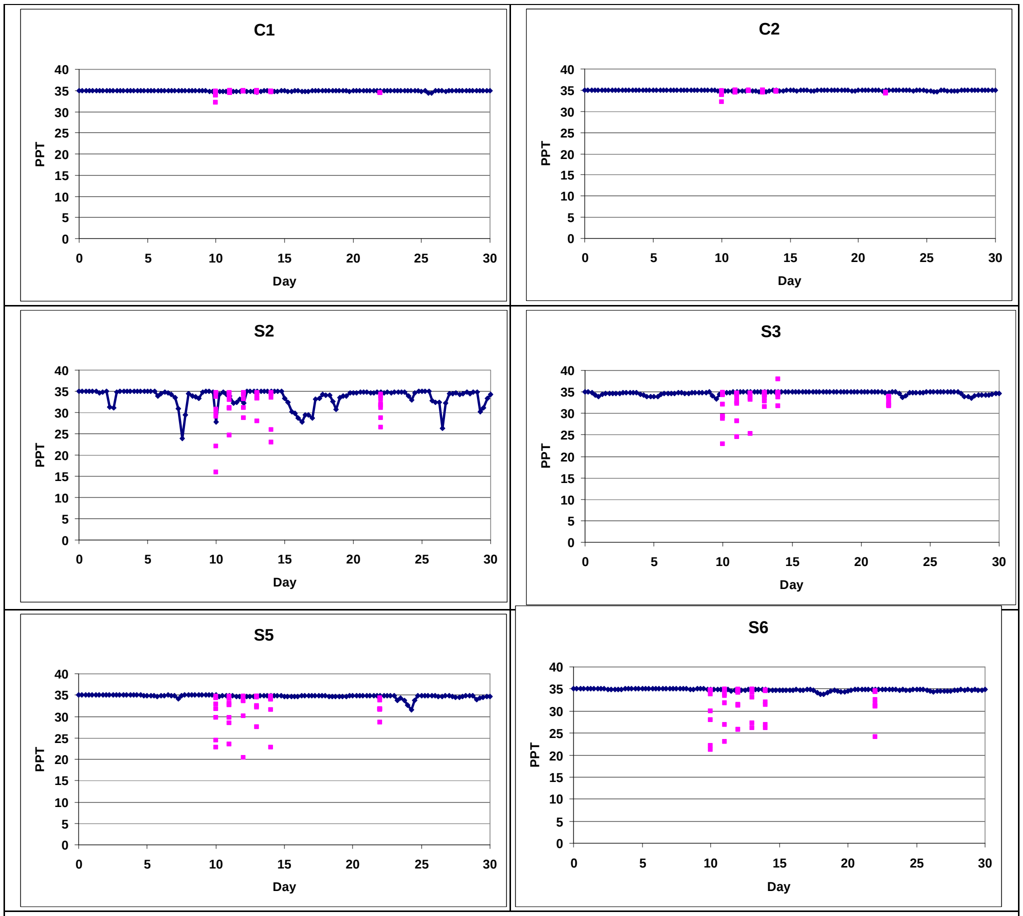

Figure 5-30. Salinity

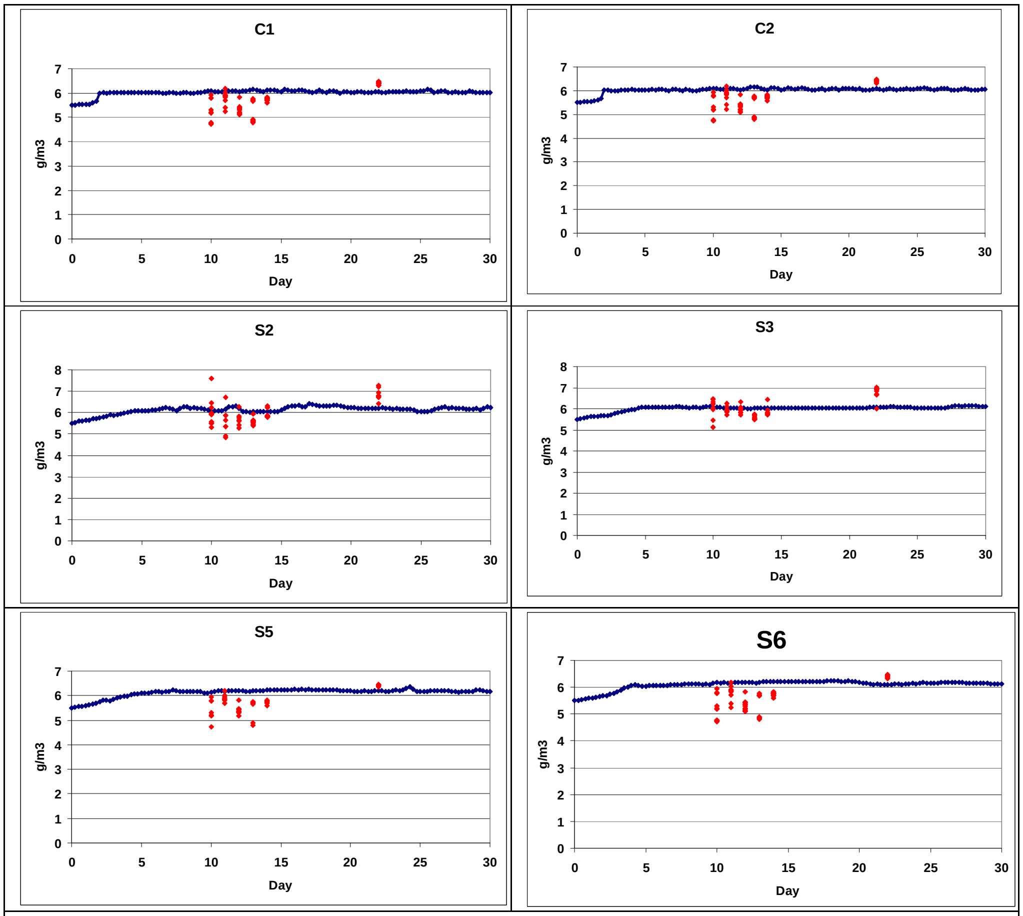

Figure 5-31. Dissolved Oxygen

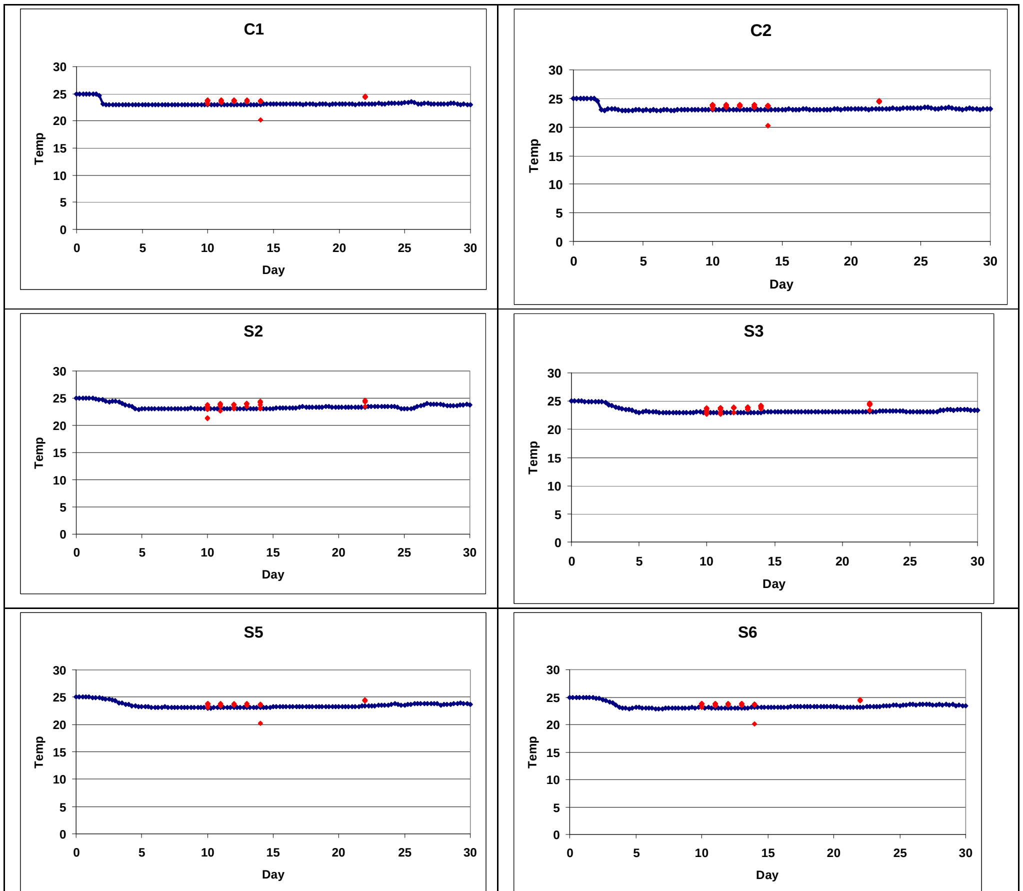

Figure 5-32. Temperature

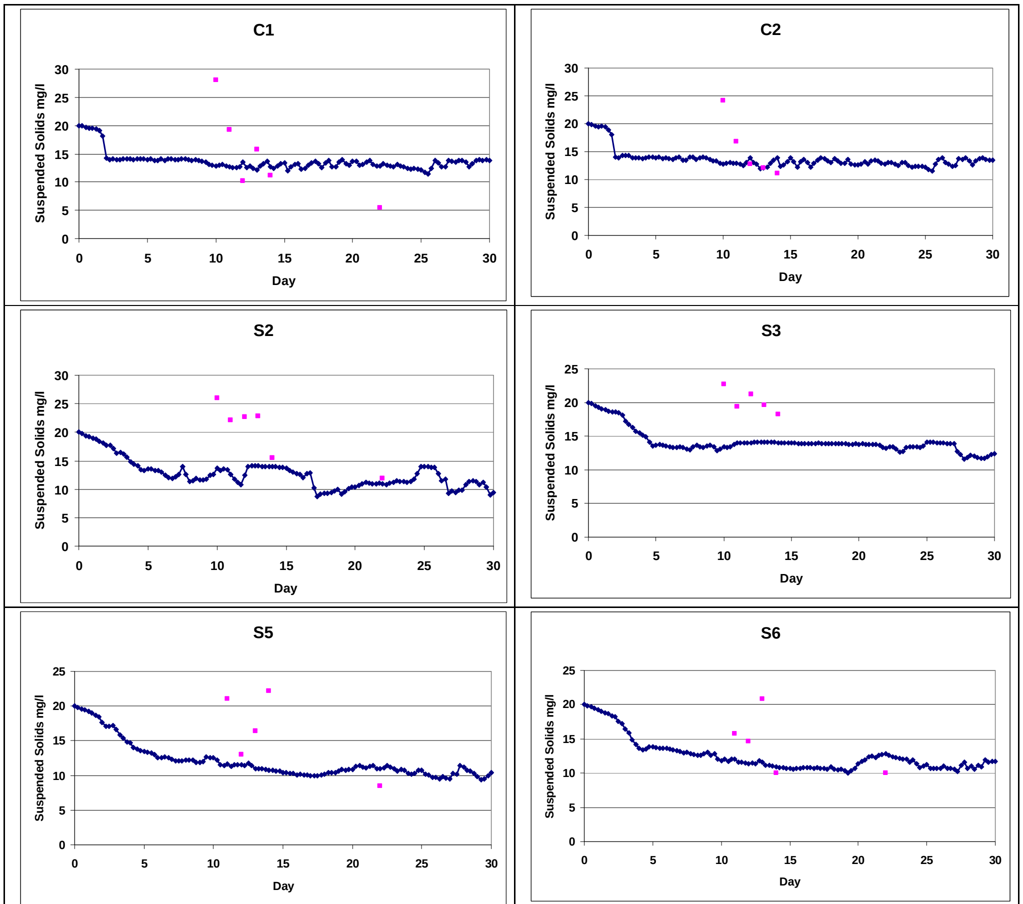

Table 5-33. Suspended Solids

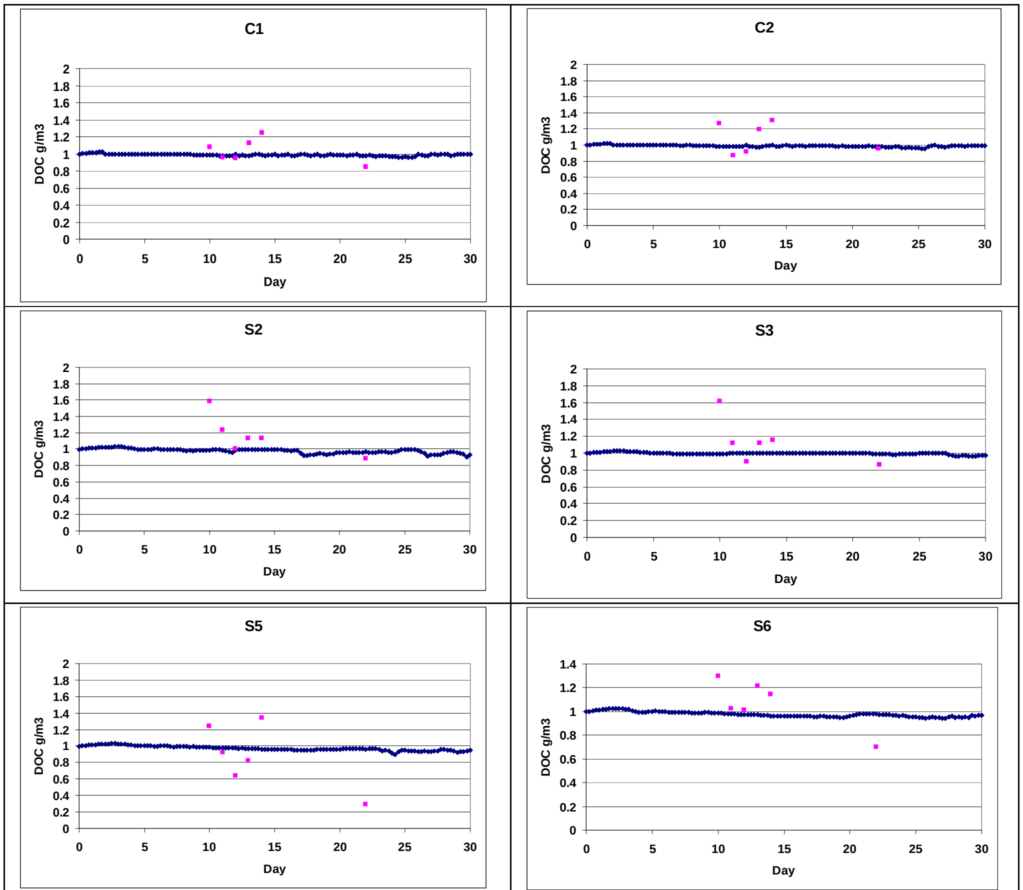

Figure 5-34. Dissolved Organic Carbon

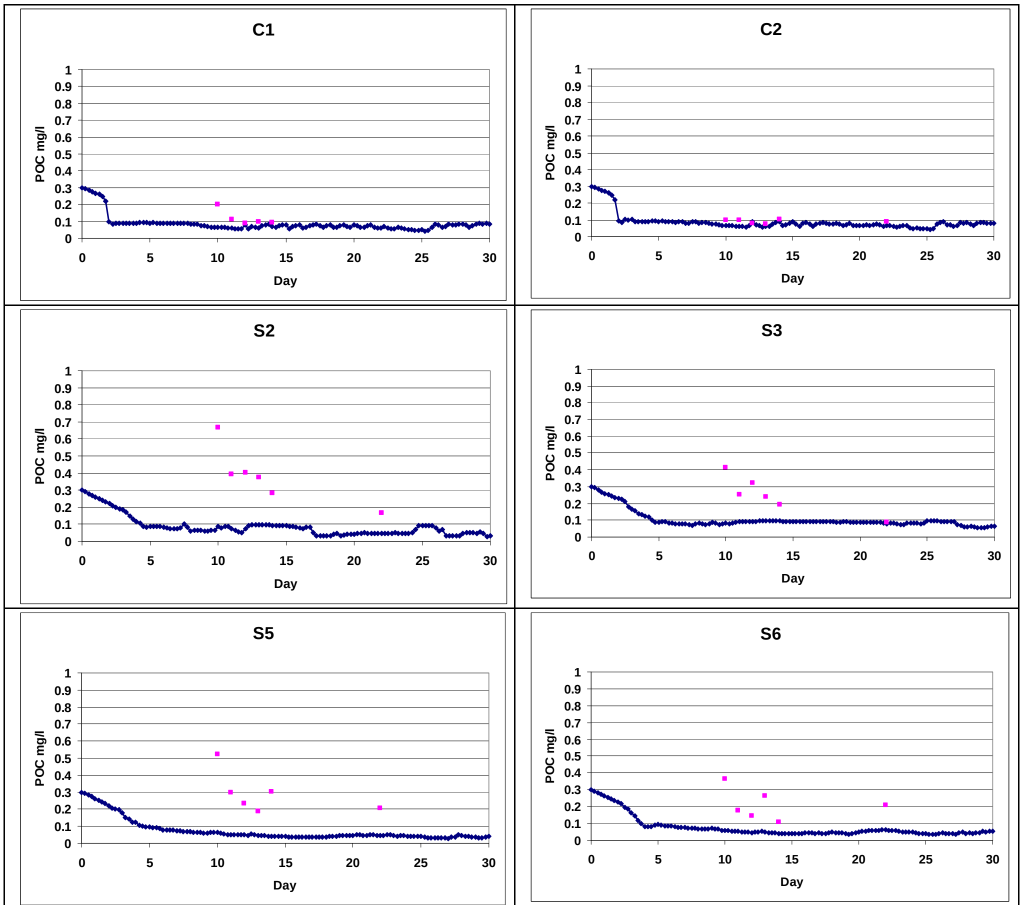

Table 5-35. Particulate Organic Carbon

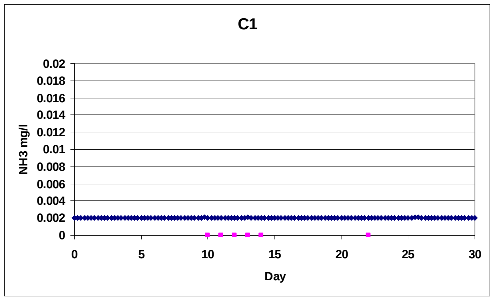

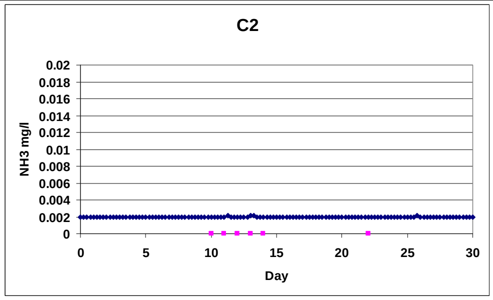

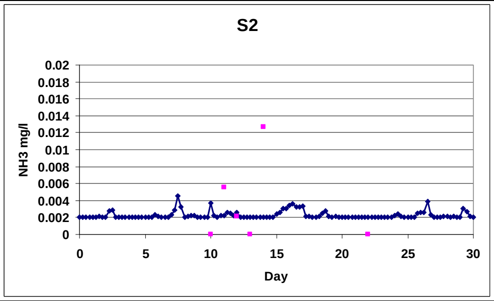

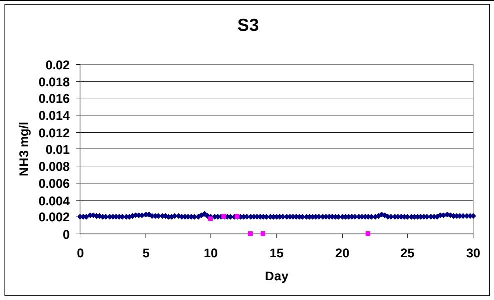

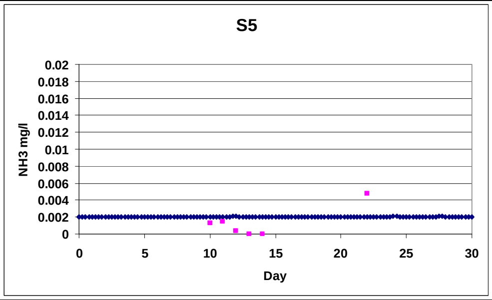

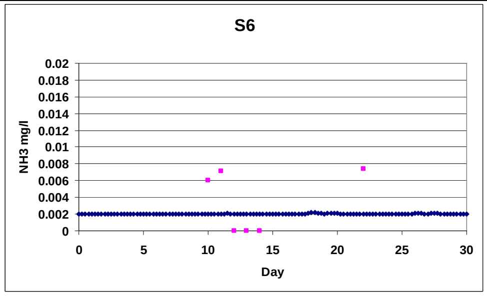

Table 5-36. Ammonia

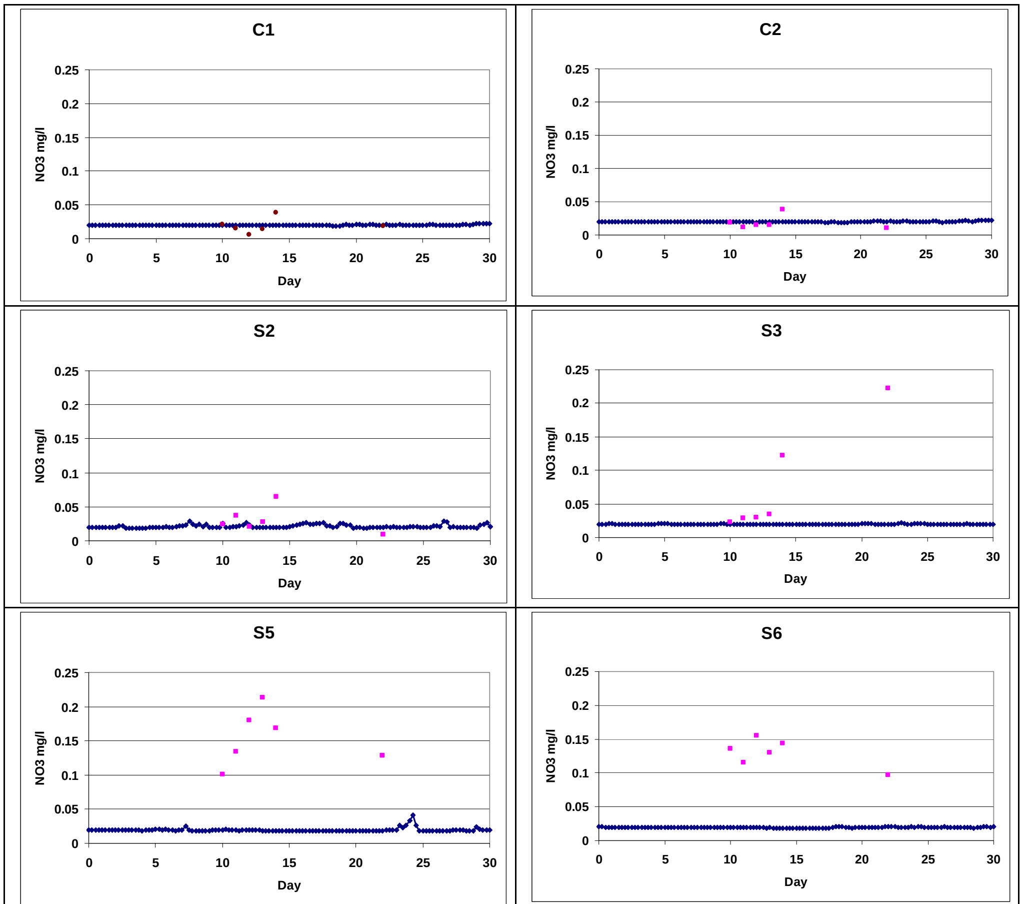

Figure 5-37. Nitrate

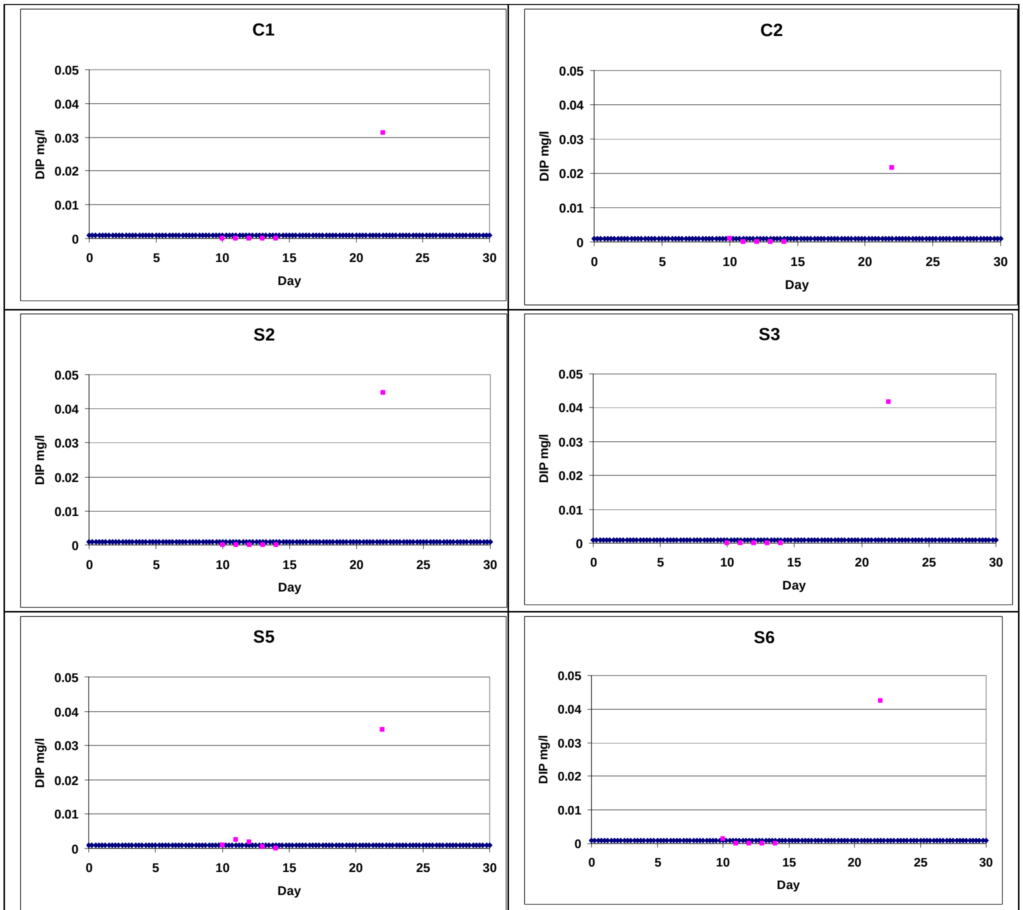

Table 5-38. Dissolved Inorganic Phosphorus

Similar results are evident on the inner portions of the system, stations S2, S3, and S5, where the observed salinity profiles indicated significant freshening near the surface. A two dimensional model is unable to capture this. When freshening in the model does occur, it is represented as a decrease in the overall salinity of the water column as was evident at station S2.

Suspended solids model results, Figure 5-33, indicated fairly constant values after a few days of simulation. Values at open water stations showed spikes between model days 10 and 15 (March 2-7). in the meta-data for the observed data, this period is listed as a being a storm. Of interest is the fact that the tributary suspended solids concentrations during this period were much less that the values observed in open water.

As the model is driven by values based on the tributary observations, the model will not capture this behavior. Possible reasons for the open water observations exceeding the tributary values are that there were other un-measured sources of suspended solids besides the Wailuku and Wailoa rivers. As the observed values during this period at stations C1 and C2 were also elevated, it is thought that some sediment resuspension was ongoing. This would increase solids levels in open waters irregardless of tributary loadings.

Model results for Dissolved Organic Carbon, DOC, are good, Figure 5-34. There is a little fluctuation in observed values associated with a storm event around day 9. The model does a good job of capturing the conditions in the system both inside and outside of the breakwater.

Model results for Particulate Organic Carbon, POC, were low, Figure 5-35. Results for stations C1 and C2 were representative. Predictions inside of the harbor were lower than observed. However, considering the low magnitude of the observed values, the model performed adequately.

Model results for ammonia indicated that the model consistently over-predicted observed levels of 0.000 at many stations, Figure 5-36. In instances where ammonia levels were measured above 0.000, they were associated with run-off events and were still small.

Model results for nitrate indicate that there is little variation throughout the period simulated, Figure 5-37. Observed data demonstrate more volatility associated with runoff events. Some of the observed values such as at Station S3 exceed values which are in the observed data   This is felt to be an indication of there being loadings to the system that are not currently captured in the model. Model prediction for stations C1 and C2 are slightly high but still representative.

Observed data for total dissolved phosphorus indicated that values throughout the system were consistently near 0, Figure 5-38. The model was able to capture this behavior. However on model day 22 (March 14, 2007) observed total dissolved phosphorus values ranging from 0.022 – 0.042 mg/l were observed at all stations. No other values within an order of magnitude of these values were observed throughout the nine month sampling effort. Consequently, the water quality model did not capture this behavior as there was nothing in the model to generate these conditions. It is believed that these data either represent a loading, process not in the model, or were bad data.

5.2.4. Harbor Alternative Runs

Water quality simulations were made for alternatives 2, 3, 4, and 5 using the same model set up and time period as was used for calibration. Alternative 1 was dropped from further modeling after flushing tests and wave model results. Total simulation time was for 30 days. Model results for the different harbor configurations were extracted for the same 18 stations as were used for model calibration. The first 15 days of the simulation were plotted against Alternative 0 (Base) results. These are shown in Figures 5-39 to 5-47.

Results indicate that the conditions at the stations plotted for all alternatives were similar. The base condition results for the constituents simulated were also similar to those observed for the four harbor configurations evaluated. The overall similarity of the harbor alternative configurations is attributed to two things. First, all alternative configurations evaluated exhibited greatly increased circulation in comparison to the base case. As such, the waters inside of the harbor breakwater were mixed with and rapidly replaced by water from outside of the breakwater. This is supported by the flushing results presented earlier. Secondly, the depth average approach used in the model prevented the creation of vertical structure in the water column which could have resulted in more differences as it was displaced by the added mixing of the harbor alternative simulations. For example, in a three dimensional representation, low dissolved oxygen levels at certain portions of the system might be impacted differently by the various flow fields resulting from the different harbor alternatives considered.

There were some differences in the base results and the four harbor alternative results. These differences appear to be the result of delays in flushing in the base case as opposed to the alternatives. The fact that differences were not numerically great at all times should not be ignored. Conditions inside the harbor and outside were very similar in the model. Therefore mixing of waters from outside of the harbor with the waters inside did not necessarily result in large changes in concentrations or temperature. This is somewhat an artifact of the two dimensional nature of the model.

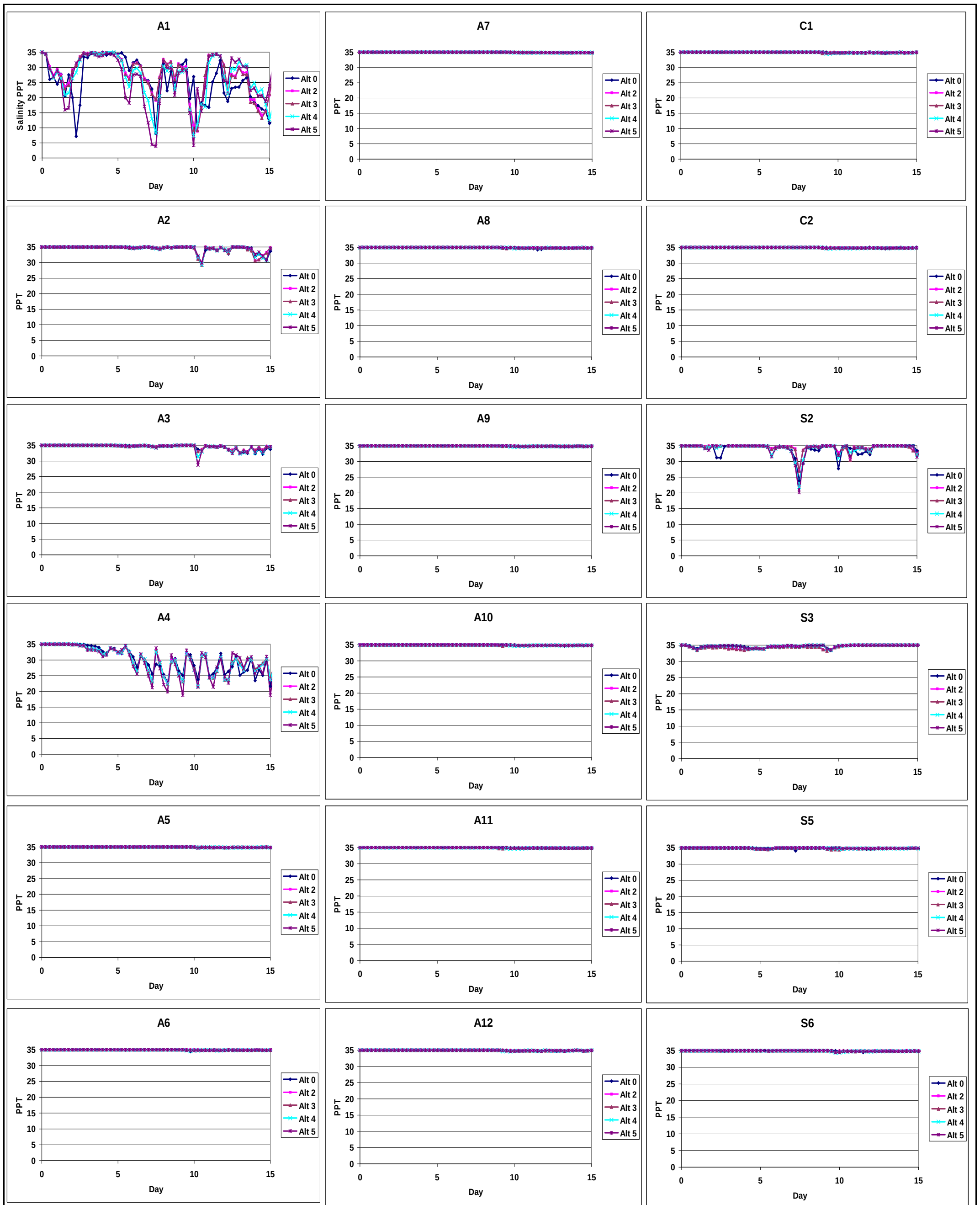

Figure 5-39. Alternative Salinities

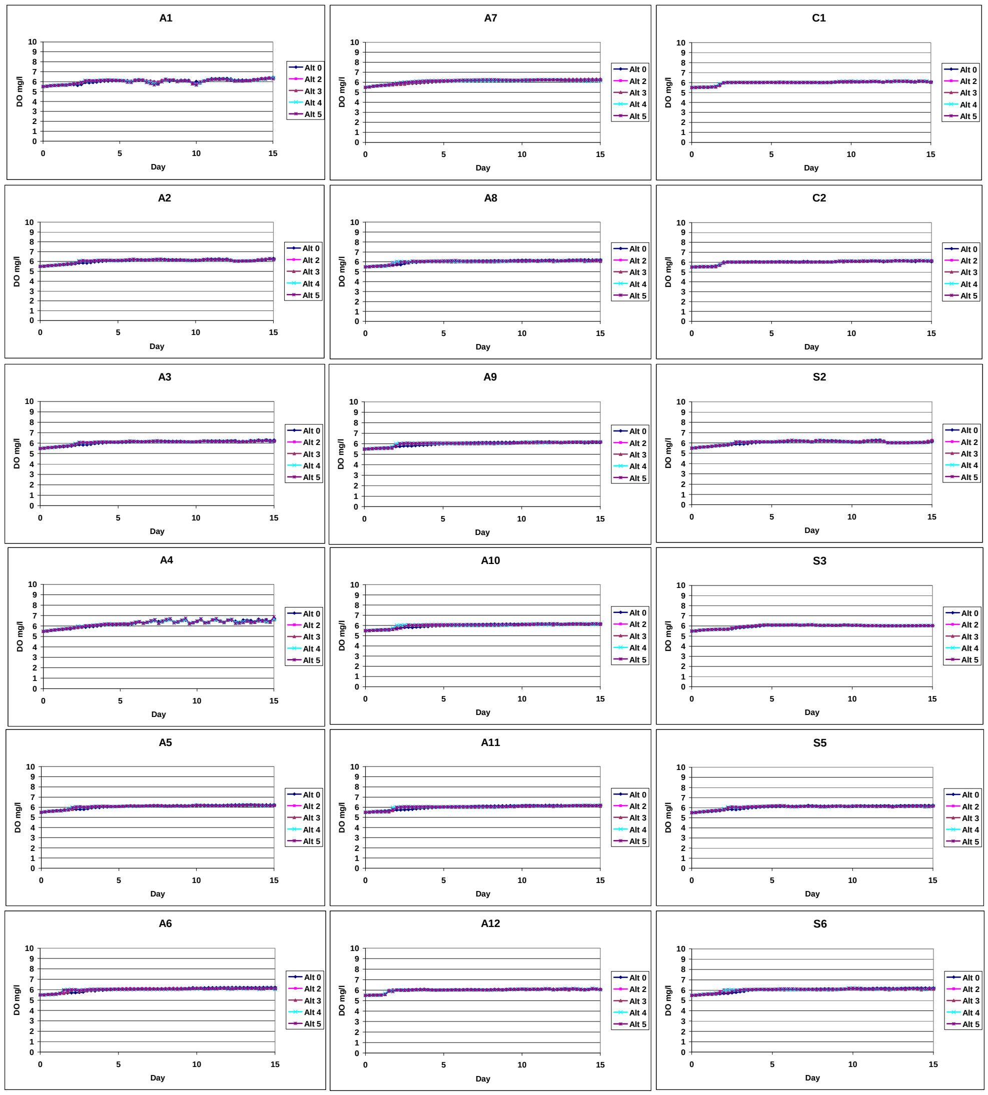

Figure 5-40. Alternative Dissolved Oxygen Concentrations

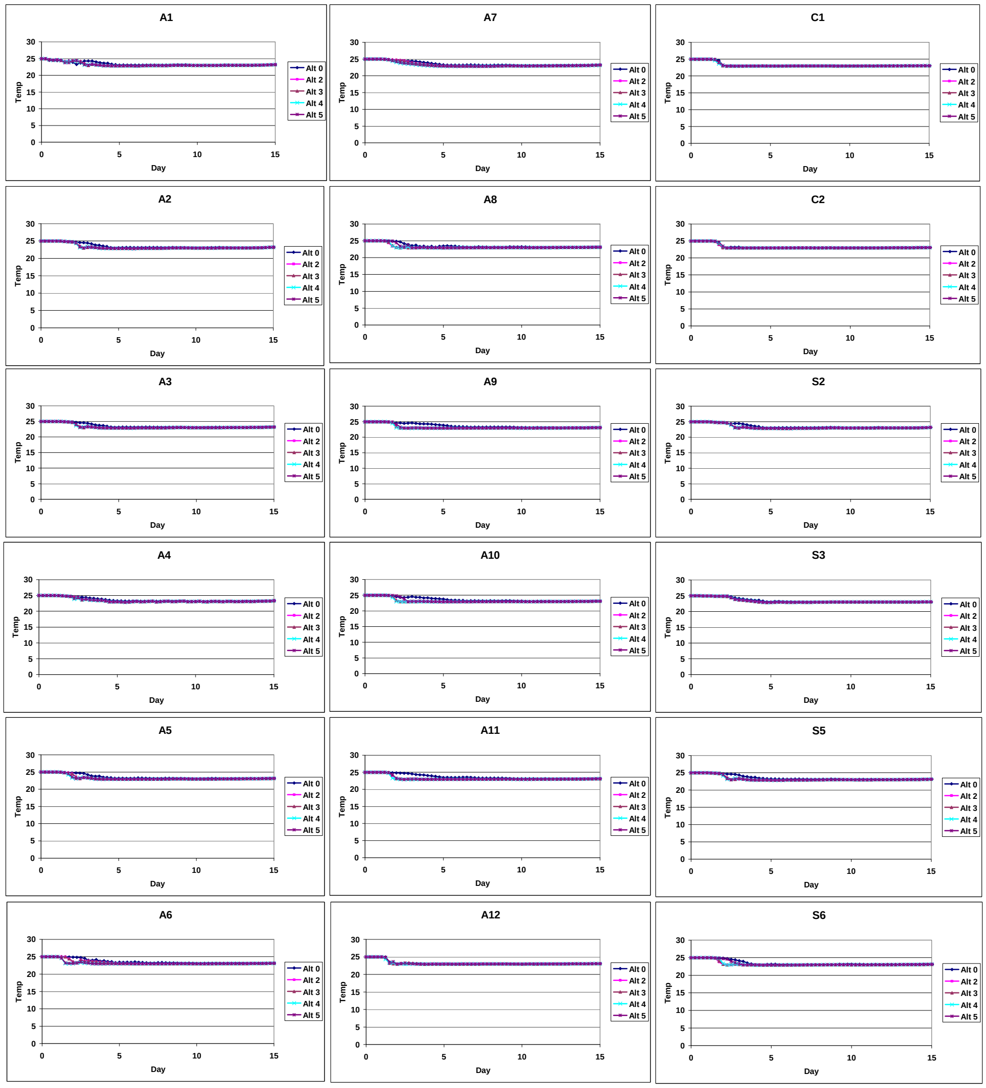

Figure 5-41. Alternative Temperatures

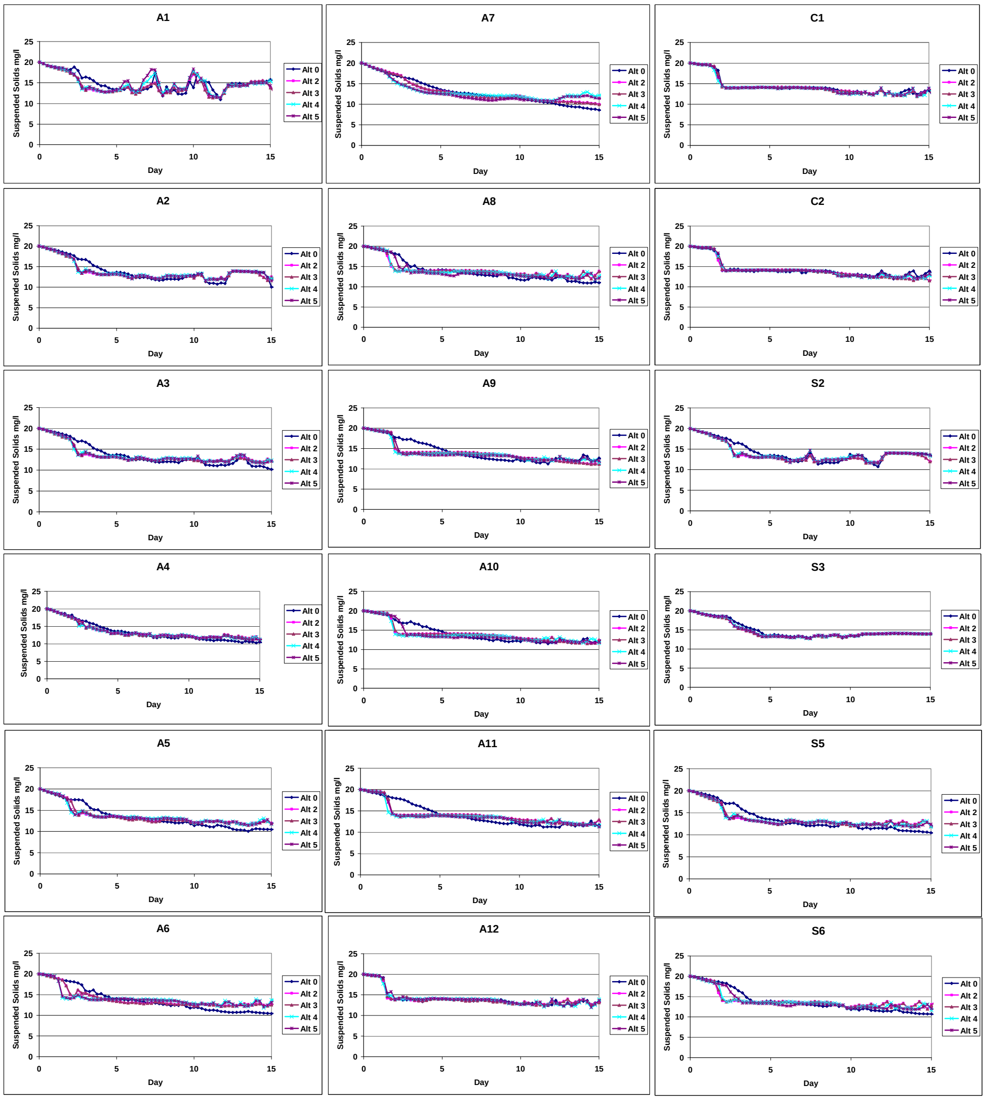

Figure 5-42. Alternative Suspended Solids

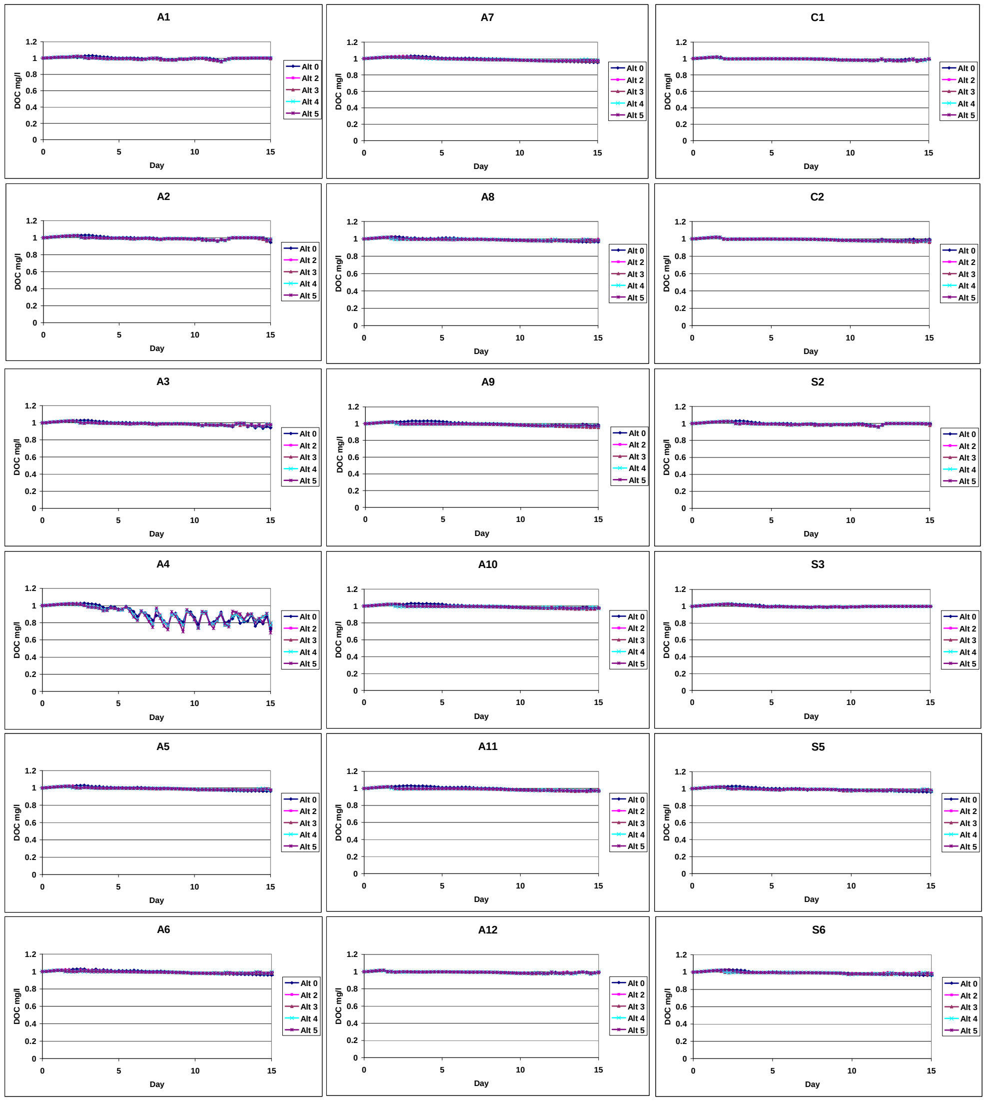

Figure 5-43. Alternative Dissolved Organic Carbon Concentrations

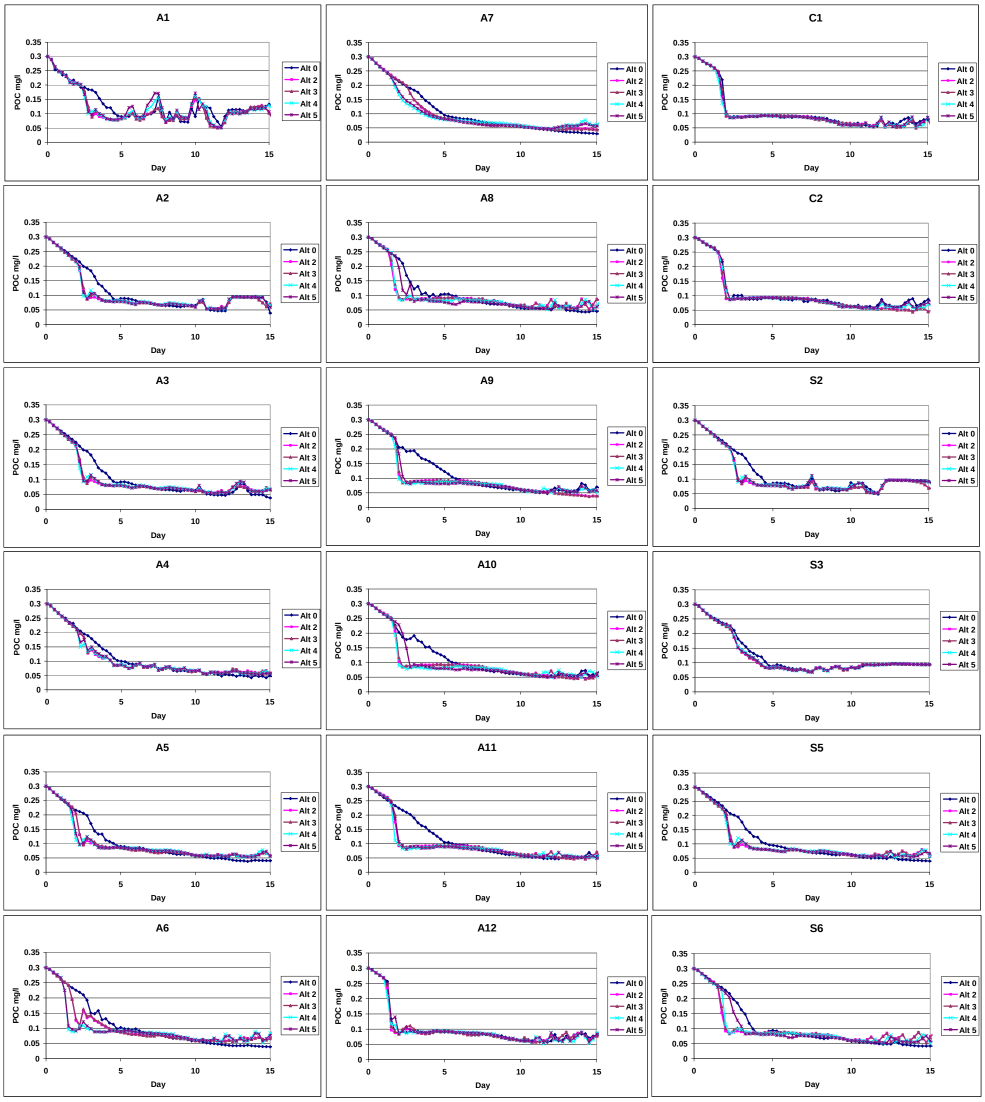

Figure 5-44. Alternative Particulate Organic Carbon Concentrations

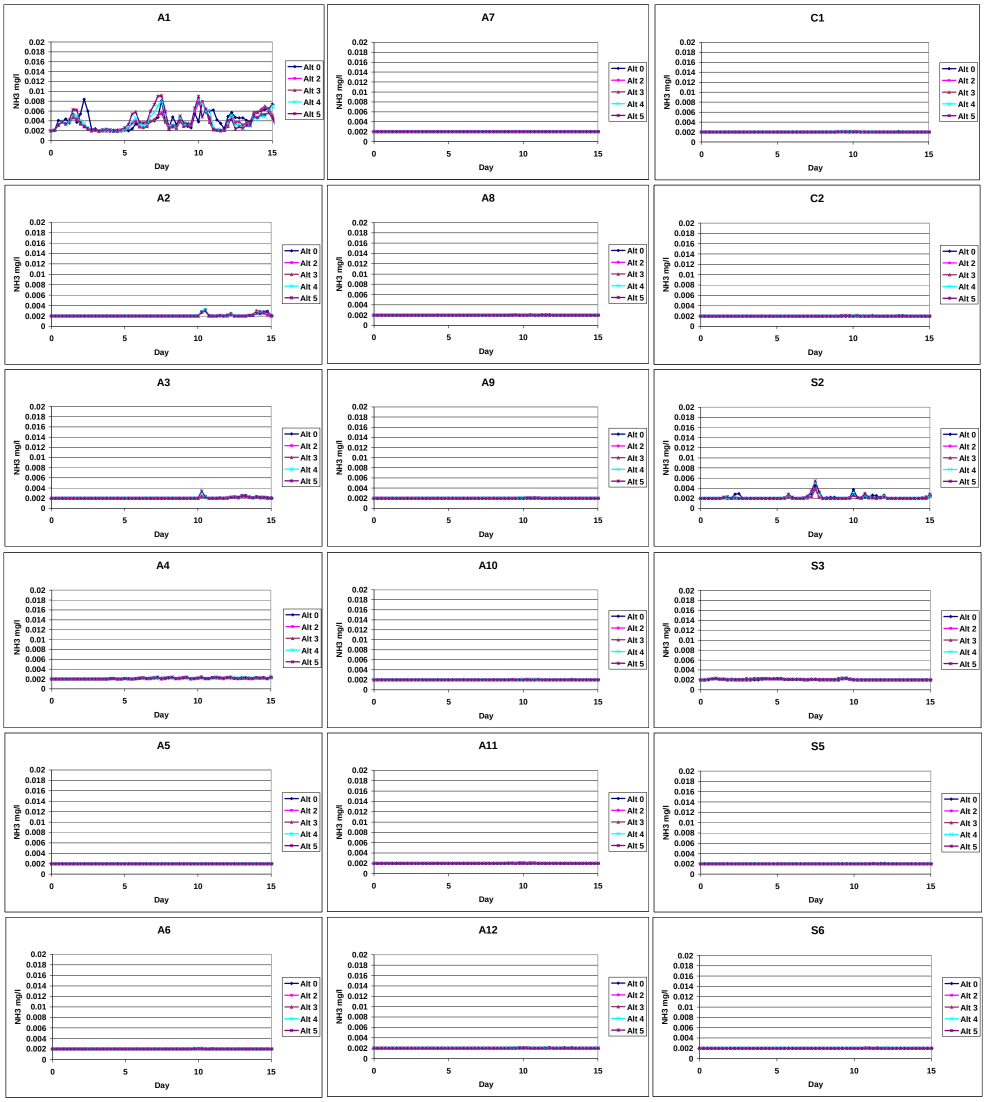

Figure 5-45. Alternative Ammonia Concentrations

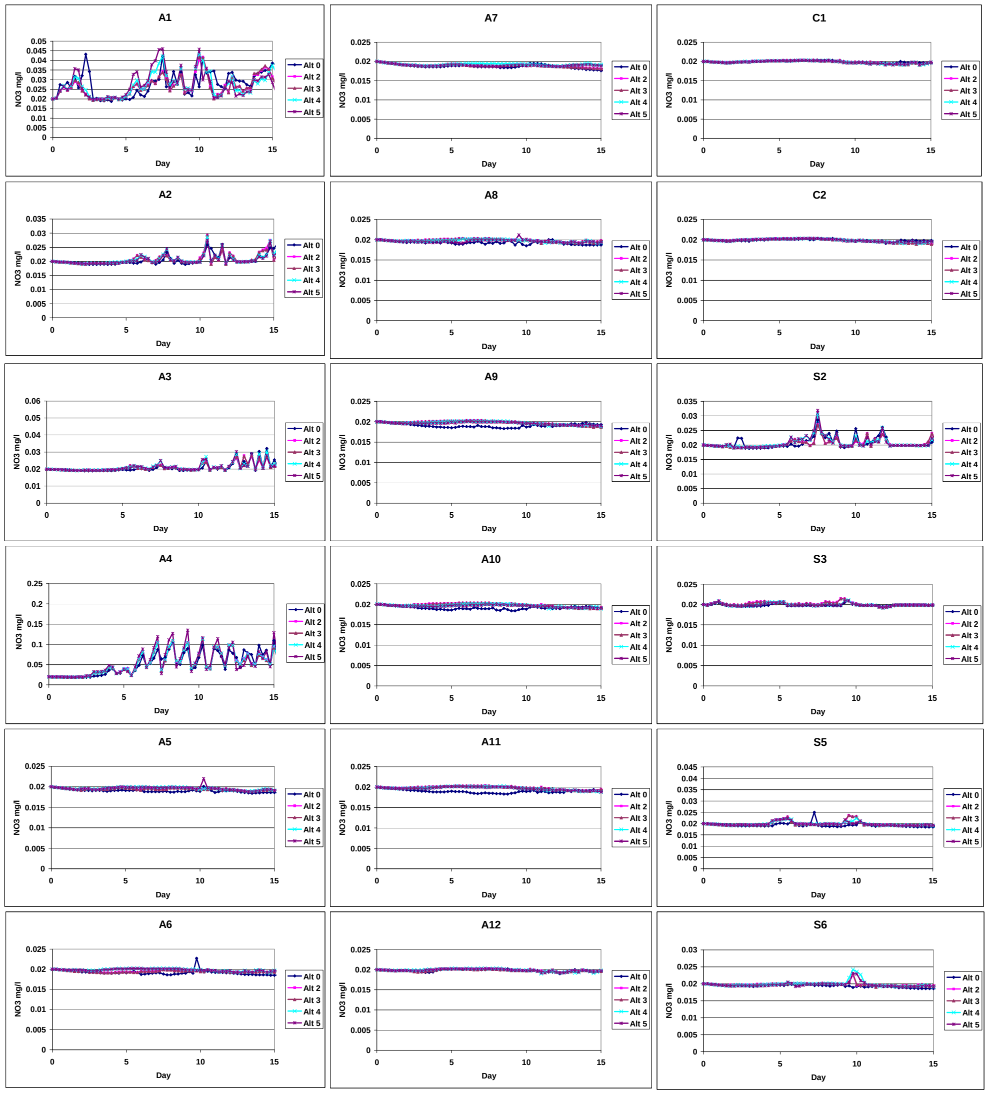

Figure 5-46. Alternative Nitrate Concentrations

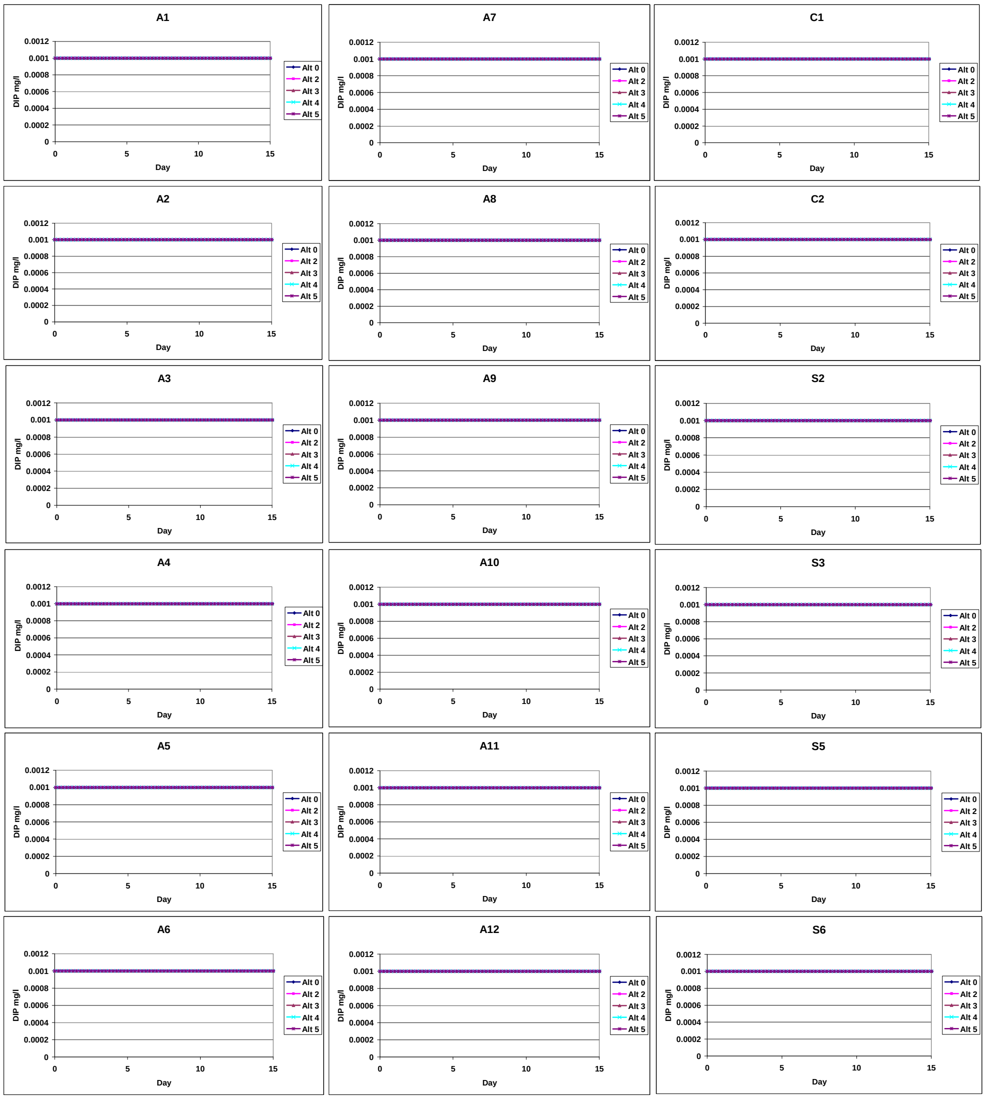

Figure 5-47. Alternative Dissolved Inorganic Phosphorus Concentrations

Salinity results, Figure 5-39, indicated that the conditions inside of the harbor are the same at all stations regardless of the harbor alternative chosen. There were some subtle differences at station A1, which is at the mouth of the Wailuku River. This is the most active station monitored in the model output as a result of its location in the Wailuku River. At this location, the results for the base case exhibited a drop in salinity around day 2.0. Similar decreases were seen in the salinity for the other alternatives but not to the degree observed in the base case. Salinity results for Station S2 indicate a similar dip in salinity around day 2.0. Station S2 is the nearest station to station A1. No dips are seen in the salinity concentrations at stations S2 for the proposed harbor alternative configurations. This should be taken as an indication of the added flushing in this portion of the system as a result of the openings in the breakwater. This flushing would aid in the dispersal of any materials in originating from the Wailuku River.

Results for dissolved oxygen were similar for the base and four harbor alternatives evaluated, Figure 5-40. This is somewhat expected. The dissolved oxygen conditions in the harbor are good. The two dimensional approach used in the model prevents creation of stratification and lower dissolved oxygen levels below the surface. Reaeration acts to counter any deficient between computed dissolved oxygen levels and saturation and will in the absence of significant oxygen demand result in a dissolved oxygen concentration near saturation.

Temperature results for the 18 stations were similar for all harbor alternatives and the base case, Figure 5-41. The only difference occurs in the first few days of the simulation when there is a slight decrease in temperature as the result of the waters from outside of the harbor replacing waters inside of the harbor. This is caused by the temperature boundary condition used on the outer boundary being slightly less than the initial temperature specified throughout the model. Of interest is that the temperature decrease at stations inside of the harbor is lagged in the base case when compared to all of the harbor alternatives. This is again an indication of the degree of flushing occurring as a result of the harbor breakwater breaches.

Suspended solids results indicated similar behavior for the four proposed harbor alternatives evaluated, Figure 5-42. There were some deviations during the initial flush period around day 2 between the multi-gap and single gap alternatives. After that they were near identical. The base case though exhibited higher concentrations as there was limited flushing. By day 10 suspended solids levels were similar for the four proposed alternatives and the base case.

Dissolved organic carbon results for the four harbor alternative configurations were similar to base results, Figure 5-43. There were subtle variations between the alternatives but nothing of significance. Ammonia exhibited similar behavior as did nitrate.

Particulate organic carbon results indicated more variation among the four alternatives (2, 3, 4, and 5), Figure 5-44. However, all were different than the base case. The greatest differences occurred at locations where the flushing in the base would be less than in the alternatives, stations S2 and

S5, and A8, A9, A10, A11. The reason for these differences is thought to be the role of settling. In more quiescent waters, settling will remove material more so than in waters where there is flushing and mixing. The fact that model predictions for particulate organic carbon are higher for the proposed harbor configurations than the base is indication of the relatively limited exchange in the current configuration. The difference is due to the POC settling out of the water column more so in the base than in the proposed harbor configurations.

Ammonia concentrations in the alternative evaluated were very similar. There was some variation at stations closest to the tributary sources, but elsewhere, differences were indistinguishable, Figure 5-45. This is mainly due to the very low levels of ammonia in the system.

Nitrate concentrations in the different alternatives showed slightly more variation than other constituents modeled, Figure 5-46. This is due to the differing boundary conditions on the two major tributaries. However, differences were minimal in the model and possibly not detectible in the actual system.

Dissolved inorganic phosphorus results for the proposed harbor alternatives were similar, Figure 5-47. There were some lags and deviations at some stations (A5, A6, and S5) early in the simulations during the period of the initial flush. However, after that point all proposed harbor configuration had near identical values. The base case results were different though. Much longer periods were required for concentrations to decrease at all stations. This can be taken as an indication of the limited level of flushing and mixing in the current system in comparison to the proposed alternatives evaluated.

6. ESTIMATED COSTS AND OTHER CONSIDERATIONS

6.1. Construction Costs

Cost estimates for the conceptual alternatives were prepared by the Honolulu District to enable comparison between the various conceptual features. A contingency of 20% was assumed for all cost estimate line items based on the uncertainty of the input data. Assumptions used in the preparation of the cost estimates included that the rock for new breakwater construction would come from the existing breakwater and that all excess rock and dredged material would be disposed of in an approved offshore disposal site.

6.1.1. Alternative 1

For Alternative 1, the approximate amount of material to be removed from the existing breakwater through demolition of 7,500 feet of the structure was assumed to be 620,000 tons. At a unit price for $42/ton, breakwater removal would cost about $31,248,000. Construction of approximately 2,000 feet of new breakwater would require placement of approximately 210,000 tons of material at $72/ton for a cost of $18,144,000. Mobilization and demobilization costs (including preparation of the work road and staging area) would be $2,400,000. Dredging requirements would be approximately 780,000 cubic yards at a unit price of $14 for a cost of $13,104,000. The total cost of Alternative 1 would therefore be $66,096,000.

6.1.2. <u>Alternative 2</u>

For Alternative 2, the approximate amount of material to be removed from the existing breakwater to create the six notches was assumed to be 125,000 tons. At a unit price for $42/ton, breakwater notching would cost about $6,300,000. Once the notches are made in the breakwater, each of the 12 ends would need to be reshaped at a unit price of $180,000 and a cost of $2,592,000. Mobilization and demobilization costs would be $2,400,000. Dredging requirements would be approximately 780,000 cubic yards at a unit price of $14 for a cost of $13,104,000. The total cost of Alternative 2 would therefore be $24,396,000.

6.1.3. <u>Alternative 3</u>

For Alternative 3, the approximate amount of material to be removed from the existing breakwater to create the six notches was assumed to be 125,000 tons. At a unit price for $42/ton, breakwater notching would cost about $6,300,000. Once the notches are made in the breakwater, each of the 12 ends would need to be reshaped at a unit price of $180,000 and a cost of $2,592,000. The six offset detached breakwaters would require placement of approximately 180,000 tons of material at $156/ton for a cost of $33,696,000. Mobilization and demobilization costs would be $2,400,000. Dredging requirements would be approximately 780,000 cubic yards at a unit price of $14 for a cost of $13,104,000. The total cost of Alternative 3 would therefore be $58,092,000.

6.1.4. <u>Alternative 4</u>

For Alternative 4, the approximate amount of material to be removed from the existing breakwater to create the 500-foot gap along the root of the structure was assumed to be 42,000 tons. At a unit price for $42/ton, breakwater notching would cost about $2,117,000. Once the gap is made in the breakwater, each of ends would need to be reshaped at a unit price of $180,000 and a cost with contingency of $432,000. Mobilization and demobilization costs would be $2,400,000. Dredging requirements would be approximately 780,000 cubic yards at a unit price of $14 for a cost of $13,104,000. The total cost of Alternative 4 would therefore be $18,053,000.

6.1.5. Alternative 5

For Alternative 5, the approximate amount of material to be removed from the existing breakwater to create the 500-foot gap along the root of the structure was assumed to be 42,000 tons. At a unit price for $42/ton, breakwater notching would cost about $2,117,000. Once the gap is made in the breakwater, each of newly exposed ends of the structure would need to be reshaped at a unit price of $180,000 and a cost with contingency of $432,000. The 500-foot offset detached breakwaters would require placement of approximately 60,000 tons of material at $156/ton for a cost of $11,232,000. Mobilization and demobilization costs would be $2,400,000. Dredging requirements would be approximately 780,000 cubic yards at a unit price of $14 for a cost of $13,104,000. The total cost of Alternative 5 would therefore be $29,285,000.

6.1.6. Cost Summary

Tables 6-1, 6-2 and 6-3 provide summaries of the estimated costs for each alternative investigated in this study. Table 6-1 displays costs for dredging approximately 750,000 cubic yards of material as described above for each of the alternatives. Mobilization and demobilization of dredging equipment is estimated at $1,000,000 with actual dredging and dredged material disposal costs of $10,920,000. With a contingency of 20%, the total cost of dredging is estimated at $14,304,000 for each alternative. Table 6-2 shows the cost of mobilization, demobilization, demolition of specific portions of the existing breakwater, reshaping of exposed breakwater ends and construction of detached breakwaters where applicable for each alternative. Mobilization and demobilization of breakwater construction equipment is estimated at $1,000,000. A contingency of 20% is assumed throughout. Breakwater costs for the five alternatives range from $3,749,000 for Alternative 4 to $51,792,000 for Alternative 1. Total estimated cost of dredging and breakwater work for each alternative is provided in Table 6-3.

Table 6-1. Estimated dredging cost for each alternative					
Alternative	**Mob/Demob**	**Dredging**	**Breakwater**	**Contingency (20%)**	**Total**
1	$1,000,000	$10,920,000	$0	$2,384,000	$14,304,000
2	$1,000,000	$10,920,000	$0	$2,384,000	$14,304,000
3	$1,000,000	$10,920,000	$0	$2,384,000	$14,304,000
4	$1,000,000	$10,920,000	$0	$2,384,000	$14,304,000
5	$1,000,000	$10,920,000	$0	$2,384,000	$14,304,000

Table 6-2. Estimated breakwater cost for each alternative					
Alternative	**Mob/Demob**	**Dredging**	**Breakwater**	**Contingency (20%)**	**Total**
1	$1,000,000	$0	$42,160,000	$8,632,000	$51,792,000
2	$1,000,000	$0	$7,410,000	$1,682,000	$10,092,000
3	$1,000,000	$0	$35,490,000	$7,298,000	$43,788,000
4	$1,000,000	$0	$2,124,000	$625,000	$3,749,000
5	$1,000,000	$0	$11,484,000	$2,497,000	$14,981,000

Table 6-3. Estimated total cost for each alternative					
Alternative	**Mob/Demob**	**Dredging**	**Breakwater**	**Contingency (20%)**	**Total**
1	$2,000,000	$10,920,000	$42,160,000	$11,016,000	$66,096,000
2	$2,000,000	$10,920,000	$7,410,000	$4,066,000	$24,396,000
3	$2,000,000	$10,920,000	$35,490,000	$9,682,000	$58,092,000
4	$2,000,000	$10,920,000	$2,124,000	$3,009,000	$18,053,000
5	$2,000,000	$10,920,000	$11,484,000	$4,881,000	$29,285,000

6.2. Other Considerations

Other considerations that should be evaluated prior to detailed planning of any breakwater modifications include the effect on the Hilo Bay shoreline, the changes to breakwater access, and the impact to Blonde Reef. The evaluation of these additional impacts was not included in the scope of this report.

The increase in wave energy inside Hilo Harbor that will occur with any of the proposed alternatives may result in increased wave height and/or current speed at the shoreline, depending on a simultaneous increase in water level. This could potentially increase existing rates of sediment transport and exacerbate any current erosion problems along the sandy shoreline and in the littoral zone. The magnitude of these effects will vary by alternative. A thorough review of existing sediment studies of the area as well as an evaluation of changes to sediment transport rates and patterns for proposed breakwater modification is suggested prior to implementation of any structural changes.

In addition, access to the breakwater will be affected by any alternative that places gaps in the structure (Alternatives 2, 3, 4, and 5). Access to the trunk and head of the breakwater for inspection, repair, or for recreational uses will not be feasible on foot or by vehicle following implementation of these alternatives. Access to these areas will be limited to an approach by boat. The impacts of this result on both the maintenance of the structure (USACE responsibility) as well as the ability of the public to use the structure for recreational purposes such as fishing should be considered and coordinated with the appropriate Federal and state agencies including USACE, and/or community groups.

Several of the proposed modifications also involve construction of new rubble-mound structures adjacent to the existing breakwater (Alternatives 1, 3, and 5). This new construction would result in adding to the structure "footprint", which may have impacts to Blonde Reef as well as generating other environmental concerns to plant/marine species, fish habitat, etc. Consultation with Federal, State and County environmental agencies as well as community groups should be undertaken early in the planning stages of any of these alternatives.

7. SUMMARY OF RESULTS AND RECOMMENDATIONS FOR FUTURE WORK

7.1. Effects on Waves in Hilo Harbor

The wave transformation modeling completed for all five proposed breakwater alternatives under various wave conditions indicates increases in wave energy within the harbor will occur to varying degrees following their implementation. Alternative 1 appears to have the most drastic effect including significant increases in wave energy within the navigation channel (from 1.0 to 1.65 meters) and at the shoreline, making it the least desirable option, regardless of the improvements it may make to water quality within the harbor.

Alternatives 2 and 4 involve placing unprotected gaps in the breakwater. These alternatives allow waves to propagate through the gaps into the harbor, with some energy dissipation due to depth-limited wave breaking across Blonde Reef before entering the gaps, and diffraction due to the sheltering effect of the adjacent breakwater structure. These alternatives result in a maximum wave increase of 0.34 and 0.30 meters in the navigation channel for the typical wave condition, respectively, which may be considered suitable for maintaining safe navigation. Due to the greater number of gaps in Alternative 2 and their location along the outer portion of the breakwater, this alternative allows more wave energy to advance to the bay shoreline than in Alternative 4, which could have long-term effects on this area. Based on the observed relative changes to waves within the harbor under typical conditions, these alternatives warrant further consideration in combination with their cost and minor increase in wave energy within the harbor.

Alternatives 3 and 5 include the excavation of gaps within the existing breakwater, in addition to supplemental wave protection with the construction of interior or exterior detached breakwaters. These additional structures provide added wave energy reduction due to their effect on direct wave breaking as well as diffraction of waves around the detached breakwaters. The result is a maximum wave height increase in the navigation channel of approximately 0.1 meters for both alternatives under typical wave conditions. This is likely an acceptable increase for maintaining safe navigation. Both alternatives appear to cause minimal increases to wave height at the shoreline. Based on the observed relative changes to waves within the harbor under typical conditions, these alternatives warrant further consideration in combination with their cost and minor increase in wave energy within the harbor.

7.2. Effects on Hilo Bay Flushing and Water Quality

Water quality data recently collected by Wiegner and Mead (2009) indicate that the water within the bay is not critically impaired. Nutrients tended to be low during the period sampled and modeled. At the same time dissolved oxygen levels were high, near saturation in many instances. There were occurrences of stratification in the observed data. It appears that this stratification is the result of the creation of a freshwater lens via tributary flow into the harbor. This is a three-dimensional process which was not captured with the two dimensional depth average water quality model used in the present study. All alternative configurations under consideration caused increased flushing which resulted in ocean waters entering the harbor at a much greater rate than is currently possible. Since the ocean waters are of a higher quality than the waters in the harbor, this results in improved water quality. Results for the four harbor configurations modeled (which excluded Alternative 1) indicate that they would result in significant positive impacts to the water quality of Hilo Harbor.

7.3. Summary Matrix

The following table summarizes the principal results of the wave, circulation, and water quality modeling completed, as well as the estimated costs for each conceptual alternative. This matrix is intended as a brief synopsis of the primary decision criteria that have been evaluated in this report, to facilitate selection of alternatives for further study. The areas shaded in red represent the least desirable results for each evaluation criterion, the yellow areas represent marginal results, and green areas show the most desirable results for that decision criterion. Navigation impacts are represented as the maximum wave height increase (in meters) observed in the navigation channel for the typical tradewind wave condition. Water quality improvements are shown as a qualitative evaluation of whether improvement would occur. Finally, breakwater costs are presented for each alternative as the estimated cost for the structural changes to the breakwater only (no dredging).

Table 7-1. Summary of Alternatives

Alternative	Navigation Impacts (meters)	Water Quality	Breakwater Costs
1	> 1.00	Improved	$51,792,000
2	0.34	Improved	$10,092,000
3	0.10	Improved	$43,788,000
4	0.30	Improved	$3,749,000
5	0.10	Improved	$14,981,000

Overall, water quality model predictions indicated little difference in the results for any of the proposed harbor alternatives. At some locations there were differences in some constituent values such as particulate organic carbon. However, these differences appear to be due to phasing in the model response to the circulation and were relatively small and short lived. As discussed in the following section, three-dimensional water quality modeling will be required to quantify proposed alternative performance variability.

7.4. Recommendations for Future Work

The next phase of study would include detailed three dimensional water quality modeling. The existing system exhibits three-dimensional behavior which is not captured in this modeling effort. A review of field measures of the temperature and salinity within Hilo Bay (M & E Pacific (1980), Dudley (1991), Wiegner and Mead (2009)) reveals that strong and persistent vertical and horizontal gradients exit. Although the use of a depth-averaged two dimensional hydrodynamic model is justified for comparing bay flushing characteristics for the five alternative breakwater configurations, the prediction of bay-wide circulation in support of a comprehensive water quality study will require three dimensional baroclinic hydrodynamic modeling.

The effects of changing the circulation in this system should be evaluated using a three-dimensional model so that the impacts upon the water column structure can be assessed. Water quality modeling results indicate that there are currently locations of poorer circulation, which may be depositional zones inside the harbor. If these truly are depositional zones, which accumulate organic matter over time, it is likely that they exert a localized impact upon water quality via increased sediment oxygen demand. These issues could be better addressed with a three dimensional water quality model utilizing sediment diagenesis.

An issue not addressed in this study is the issue of microbiological contamination. From this study it is evident that opening the breakwater will have a positive impact upon conditions in the harbor. Flushing should help address issues related to microbial contamination. To fully ascertain the degree to which this will occur, the source or sources of suspected contamination need to be identified. With this information it would be possible to discern the relative impacts of one harbor configuration over another in terms of microorganisms in the water.

Numerical modeling to evaluate the effects of breakwater modifications on sediment transport along the Hilo Bay shoreline is also recommended. Sediment transport modeling linked with the three-dimensional circulation model would allow a quantification of shoreline response from the proposed alternatives being considered. The modeling would provide predictions of erosion or accretion in addition to changes in sediment transport pathways and rates.

Water quality in Hilo Harbor and Hilo Bay is dependent on several interrelated environmental processes, which include the effects of the breakwater, as detailed in this report. Another major contributor to the water quality in Hilo Bay is the input of pollutants and organic materials from the Hilo Bay watershed via surface water, ground water, and storm water runoff. In order to comprehensively evaluate the bay's water quality and possible methods for improvement, these sources of contaminants must also be included in an overall watershed study that encompasses the ancient Hawaiian ahupua'a concept of "mountain to the sea" stewardship. This approach has been initiated and led by the Hilo Bay Watershed Advisory Group and Dr. Tracy Wiegner at UHH, and should be continued with a more detailed evaluation of breakwater modifications and their effect on water quality included as an integral component of the study.

8. REFERENCES

Bouws, E., Gunther, H., Rosenthal, W., and Vincent, C.L. (1985). “Similarity of the Wind Wave Spectrum in Finite Depth Water 1 Spectral Form,” *Journal of Geophysical Research* 1 (C1), 975 - 986.

Bunch, B. W., Channel, M., Corson, W. D., Ebersole, B. A., Lin, L., Mark, D. J., McKinney, J. P., Pranger, S. A., Schroeder, P. R., Smith, S. J., Tillman, D. H., Tracy, B. A., Tubman, M. W., and Welp, T. L. (2003). “Evaluation of Island and Nearshore Confined Disposal Facility Alternatives, Pascagoula River Harbor Dredged Material Management Plan,” Technical Report ERDC-03-3, U.S. Army Engineer Research and Development Center, Vicksburg, MS.

Bunch, B. W., Tillman D. H., and Mark, D. J. (in preparation). “Port of Los Angeles (POLA) Main Channel Deepening Water Quality and Hydrodynamic Modeling Study,” Technical Report EL-00-XXX, U.S. Army Engineer Research and Development Center, Vicksburg, MS.

Bunch, B., Cerco, C., Dortch, M., Johnson, B., and Kim, K. (2000). “Hydrodynamic and Water Quality Model Study of San Juan Bay and Estuary,” ERDC TR-00-1, U.S. Army Engineer Research and Development Center, Vicksburg MS.

Cerco, C. and Bunch, B, (1997). “Passaic River Tunnel Diversion Model Study, Report 5, Water Quality Modeling,” Technical Report HL-96-2, U.S. Army Engineer Waterways Experiment Station, Vicksburg, MS.

Cerco, C. and Cole, T. (1994). “Three-Dimensional Eutrophication Model of Chesapeake Bay,” Technical Report EL-94-4, U.S. Army Engineer Waterways Experiment Station, Vicksburg, MS.

Cerco, C., Bunch, B., Cialone, M., and Wang, H. (1994). “Hydrodynamic and Eutrophication Model,” Technical Report EL-94-4, U.S. Army Engineer Waterways Experiment Station, Vicksburg, MS.

Chapman, R. S., Johnson, B. H., and Vemulakonda, S.R. (1996). “Users Guide for the Sigma Stretched Version of CH3D-WES; A Three-Dimensional Numerical Hydrodynamic, Salinity and Temperature Model,” Technical Report HL-96-21, U.S. Army Engineer Waterways Experiment Station, Vicksburg, MS.

Cialone, M. A., Brown, M. E., Smith, J. M., and Hathaway, K.K. (2008). “Southeast Oahu Coastal Hydrodynamic Modeling with ADCIRC and STWAVE,” Technical Report TR-08-9, U.S. Army Engineer Research and Development Center, Vicksburg MS.

Cox, A.T., Greenwood, J.A., Cardone, V.J., and Swail, V.R. (1995). “An Interactive Objective Kinematic Analysis System,” 4th International Workshop on Wave Hindcasting and Forecasting. October 16-20, 1995, Bannf, Alberta, Canada.

Dudley, W.C. Jr and L. E. Hallacher. (1991). “Distribution and Dispersion of Sewerage Pollution in Hilo Bay and Contiguous Waters, Final report,” County of Hawai`i Department of Public Works.

Eiker, E. E. (1977). “Heat Exchange Programs, Thermal Simulation of Lakes, User’s Manual,” U. S. Army Engineer District, Baltimore, Baltimore, MD.

Gravens, M. B., Kraus, N. C., and Hanson, H. (1991). “GENESIS: Generalized Model for Simulating Shoreline Change. Report 2, Workbook and System User’s Manual,” Technical Report CERC-89-18, U.S. Army Engineer Waterways Experiment Station, Vicksburg, MS.

Johnson, B. H., Heath, R. E., Hsieh, B. B., Kim, K. W., and H. L. Butler. (1991). “Users Guide for a Three-dimensional Numerical Hydrodynamic, Salinity and Temperature Model of Chesapeake Bay,” Technical Report HL-91-20, U.S. Army Engineer Waterways Experiment Station, Vicksburg, MS.

LeProvost, C. M., L. Genco, F. Lyard, P. Vincent, and P. Canceil. (1994). Spectroscopy of the World Ocean Tides from a Finite Element Hydrodynamical Model. *Journal of Geophysical Research* 99(C12):24777–24797.

Luettich, R. A., Jr., Westerink, J. J., and N. W. Scheffner. (1992). “ADCIRC: An Advanced Three-Dimensional Circulation Model for Shelves, Coasts, and Estuaries,” Technical Report DRP-92-6, U.S. Army Engineer Waterways Experiment Station, Vicksburg, MS.

M&E Pacific, Inc. (1977). “Hilo Harbor First Spring Season Environmental Study.” Prepared for the USACE, Honolulu District.

M&E Pacific, Inc. (1980). “Geological, Biological, and Water Quality Investigations of Hilo Bay.” Prepared for the USACE, Honolulu District.

Neighbor Island Consultants (1973). “Baseline Environmental Investigations of Hilo Harbor.” Prepared for the USACE, Honolulu District.

Public Health Service (1963). “A Study of Dispersion in Hilo Bay, Hawaii.”

Sea Engineering, Inc. (1981). “Circulation and Sediment Transport Study, Hilo Bayfront Beach, Hilo, Hawaii.” Prepared for the USACE, Honolulu District.

Sheng, P. Y. (1986). “A Three-Dimensional Mathematical Model of Coastal, Estuarine and Lake Currents Using Boundary Fitted Grid,” Report No. 585, A.R.A.P. Group of Titan Systems, New Jersey, Princeton, NJ, 22.

Smith, J. M., Resio, D. T., and Zundel, A. K. (1999). “STWAVE: Steady-State Spectral Wave Model. Report 1, User’s Manual for STWAVE Version 2.0,” Instructional Report CHL-99-1, U.S. Army Engineer Waterways Experiment Station, Vicksburg, MS.

Thompson, E. F. and Scheffner, N. W. (2004). “Typhoon-Induced Stage-Frequency Relationships for the Island of Rota, Commonwealth of the Northern Mariana Islands,” Technical Report TR-04-1, U.S. Army Engineer Research and Development Center, Vicksburg MS.

Wiegner, T. and Mead, L., (2009). “Water Quality in Hilo Bay Hawai’I under Baseflow and Storm Conditions,” Project Report Preliminary Analysis, Marine Science Department, University of Hawai’i at Hilo.